

ESL-TR-84-28

Composition and Photochemical
Reactivity of Turbine
Engine Exhaust

C.W. SPICER, M.W. HOLDREN,
T.F. LYON, and R.M. RIGGIN

BATTELLE.COLUMBUS LABORATORIES
505 KING AVENUE
COLUMBUS, OH 43201

SEPTEMBER 1984

FINAL REPORT
JANUARY 1982 - MARCH 1984

DTIC
ELECTE
FEB 26 1985
S A D

APPROVED FOR PUBLIC RELEASE; DISTRIBUTION UNLIMITED

AD-A150 559



AFEGSC

ENGINEERING AND SERVICES LABORATORY
AIR FORCE ENGINEERING AND SERVICES CENTER
TYNDALL AIR FORCE BASE, FLORIDA 32403

85 02 05 106

DTIC 1 210

UNCLASSIFIED

SECURITY CLASSIFICATION OF

5 PAGE (When Data Entered)

REPORT DOCUMENTATION PAGE		READ INSTRUCTIONS BEFORE COMPLETING FORM
1. REPORT NUMBER	2. GOVT ACCESSION NO. <i>A15-055-9</i>	RECIPIENT'S CATALOG NUMBER
4. TITLE (and Subtitle) Composition and Photochemical Reactivity of Turbine Engine Exhaust		5. TYPE OF REPORT & PERIOD COVERED Final Report January, 1982 - March, 1984
		6. PERFORMING ORG. REPORT NUMBER
7. AUTHOR(s) C. W. Spicer, M. W. Holdren, T. F. Lyon, and R. M. Riffin		8. CONTRACT OR GRANT NUMBER(s) F-98635-82-C-0131 ↑ 0
9. PERFORMING ORGANIZATION NAME AND ADDRESS Battelle, Columbus Laboratories 505 King Avenue Columbus, OH 43201		10. PROGRAM ELEMENT, PROJECT, TASK AREA & WORK UNIT NUMBERS JON: 19002032 PE: 62601F
11. CONTROLLING OFFICE NAME AND ADDRESS Air Force Engineering and Services Center (RDVS) Tyndall AFB, FL 32403		12. REPORT DATE September 1984
		13. NUMBER OF PAGES 183
14. MONITORING AGENCY NAME & ADDRESS (if different from Controlling Office)		15. SECURITY CLASS. (of this report) Unclassified
		15a. DECLASSIFICATION/DOWNGRADING SCHEDULE
16. DISTRIBUTION STATEMENT (of this Report) Approved for public release; distribution unlimited.		
17. DISTRIBUTION STATEMENT (of the abstract entered in Block 20, if different from Report)		
18. SUPPLEMENTARY NOTES Availability of this report is specified on the reverse of front cover.		
19. KEY WORDS (Continue on reverse side if necessary and identify by block number) Turbine Engines; Organic Emissions; Environmental Analysis; Photochemistry.		
20. ABSTRACT (Continue on reverse side if necessary and identify by block number) The environmental impact of organic compounds emitted from jet aircraft turbine engines has not been firmly established due to the lack of data regarding the emission rates and identities of the compounds. The objectives of this project were to identify and quantify the organic compounds present in gaseous emissions from jet engines and to study the photochemical reactivity of these compounds. These objectives were met through a five-task approach. Tasks 1 and 2 involved sampling and analysis methods development and validation.		

DD FORM 1473
1 JAN 73

UNCLASSIFIED

The efficiency and specificity of the methods were demonstrated in laboratory experiments with simulated turbine engine exhaust, and with actual exhaust from a full-scale 1/6th sector combustor rig. The results of Tasks 1 and 2 are available in a published Interim Report (ESL-TR-82-43).

This report reviews the Task 1 and 2 studies, and describes Tasks 3-5 in detail. Task 3 involved detailed exhaust organic composition studies with two full-scale turbine engines utilizing three fuels. Task 4 investigated the photochemical reactivity of the exhausts, and Task 5 involved analysis and interpretation of results. Originator furnished keywords include:

The organic composition and photochemical reactivity experiments were performed with exhausts from TF-39 and CFM-56 engines, the former representing first-generation high-thrust, high-bypass-ratio design, and the latter representing latest technology, fuel-efficient, advanced emission abatement design. Three fuels were investigated during the full-scale engine experiments, including JP-4, JP-5 and a shale-derived fuel meeting JP-8 specifications. Exhaust composition experiments were carried out with all three fuels at engine idle, and at 30 percent power and maximum continuous power with JP-5 fuel. The photochemical reactivity experiments were conducted with exhaust collected at engine idle using two 8.5 m³ outdoor Teflon[®] smog chambers.

Results of the turbine engine exhaust study are interpreted in terms of organic compound distribution, carbon balance, relative emissions of toxic compounds, comparability of full scale engine and combustor rig exhausts, relative photochemical reactivity of the exhausts among engines and fuels, comparability of measured and composition-predicted reactivity, and relative contribution of turbine engines to photochemical air pollution.

Distribution For	
ASST (2041)	<input checked="" type="checkbox"/>
ASST (2041)	<input type="checkbox"/>
ASST (2041)	<input type="checkbox"/>
Distribution/	
Availability Codes	
(Inst)	(Avail and/or Special)
A-1	



PREFACE

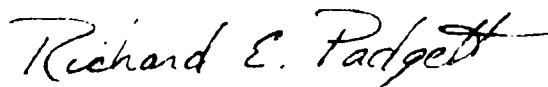
This report was prepared by Battelle, Columbus Laboratories, Columbus, Ohio 43201, under Contract Number F08635-82-C-0131 for the Air Force Engineering and Services Center, Engineering and Services Laboratory (AFESC/RDV), Tyndall Air Force Base, Florida 32403. Co-sponsors of the study include the Naval Air Propulsion Center of the U.S. Navy, and the Federal Aviation Administration.

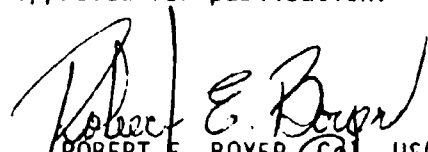
This final report describes the experimental aspects of the program and presents the results and interpretive analysis of the composition and photochemical reactivity of turbine engine exhaust (Tasks 3-5). An earlier interim report (ESL-TR-82-43) described preliminary studies (Tasks 1 and 2) leading to full-scale engine testing. This work was performed between January, 1982 and March, 1984. AFESC(RDVS) project officer was Major Richard E. Padgett.

Principal research staff at Battelle included Mr. M. W. Holdren, Dr. R. M. Riggan, and Dr. C. W. Spicer. Assistance in conducting the program was provided by Mrs. D. L. Smith, Mr. R. N. Smith, Mr. G. F. Ward, Mr. J. R. Koetz, Dr. M. R. Kuhlman, Mr. C. Bridges, Mr. L. W. Miga, and Mrs. M. A. Roberts. Engine and combustor testing were conducted with assistance from personnel at the GE Evendale Combustion Laboratory and the GE Peebles Test Operation. Mr. T. F. Lyon and Mr. E. Rogala provided technical direction and program management for the General Electric subcontract. Battelle Program Manager was Dr. C. W. Spicer.

This report has been reviewed by the Public Affairs Officer (PA) and is releasable to the National Technical Information Service (NTIS). At NTIS, it will be available to the general public, including foreign nationals.

This report has been reviewed and is approved for publication.


RICHARD E. PADGETT, Maj, USAF, BSC
Project Officer


ROBERT E. BOYER, Col, USAF
Director, Engineering and Services
Laboratory

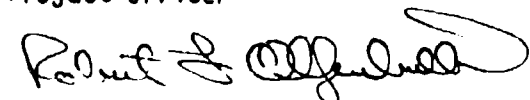

ROBERT F. OLFENBUTTEL, Lt Col, USAF, BSC
Chief, Environics Division

TABLE OF CONTENTS

Section	Title	Page
I	INTRODUCTION.	1
II	SUMMARY OF TASKS 1 AND 2.	3
	A. METHOD VALIDATION AND COMBUSTOR RIG STUDIES (Tasks 1 and 2).	3
III	EXPERIMENTAL METHODS.	5
	A. TASK 3 EMISSIONS TESTING	5
	1. Engine Descriptions	5
	2. Engine Test Facility and Engine Instrumentation	9
	3. Engine Emissions Measurements	10
	B. TASK 4 PHOTOCHEMICAL REACTIVITY.	25
	1. Photochemical Chamber Characteristics	25
	2. Analytical Methods.	28
	3. Chamber Operation	32
IV	RESULTS	36
	A. TASK 3 ENGINE EXHAUST MEASUREMENTS	36
	1. Engine Operation.	36
	2. Hydrocarbon Emissions and Fuels Analysis.	36
	3. Aldehyde Determinations	47
	4. PNA Analysis.	61
	B. Task 4 PHOTOCHEMISTRY EXPERIMENTS.	61
	1. Chamber Characterization and Validation	61
	2. TF-39 Engine Exhaust Reactivity Experiments	74
	3. CFM-56 Engine Exhaust Reactivity Experiments	80
V	DISCUSSION.	86
	A. TASK 3 ENGINE EXHAUST MEASUREMENTS	86
	1. Carbon Balance.	86
	2. Individual Hydrocarbon Species.	88
	3. Distribution of Emissions By Compound Class.	89



TABLE OF CONTENTS (CONCLUDED)

Section	Title	Page
	4. Distribution of Emissions By Carbon Number. .	89
	5. Ratio of Selected Aromatic and Aliphatic Compound Pairs.	96
	6. Comparison of TF-39 Combustor Rig and Full-Scale Engine	96
	7. Carbonyl Compounds--Method Performance. . . .	100
	8. Comparison of Jet Turbine Engine Emission Rates to Other Mobile Sources	101
B.	TASK 4 PHOTOCHEMISTRY EXPERIMENTS.	109
	1. Introduction.	109
	2. TF-39 Photochemistry Experiments.	111
	3. CFM-56 Photochemistry Experiments.	122
	4. Comparison of TF-39 and CFM-56 Exhaust Reactivities.	131
	5. Influence of Exhaust Composition on Photochemical Reactivity.	133
	6. Comparison of Observed and Calculated Photochemical Reactivities.	140
	7. Comparison of Turbine Engine Exhaust Reactivity With Other Emission Sources. . . .	142
VI	CONCLUSIONS	147
	A. ENGINE EMISSION TESTING.	147
	B. PHOTOCHEMICAL REACTIVITY	148
	C. RECOMMENDATIONS FOR FUTURE RESEARCH.	149
	REFERENCES.	151
APPENDIX		
	A. SMOG CHAMBER PROFILES	154

LIST OF FIGURES

Figure	Title	Page
1	TF-39 Engine and Sampling Rake During Emission Measurement Studies	6
2	CFM-56 Engine and Sampling Rake During Emission Measurement Studies	8
3	Engine Exhaust Sampling Rake	11
4	Closeup of Sampling Rake Mounted Behind Engine	12
5	Overall Sampling System	13
6	Schematic Diagram of Sampling Manifold	16
7	Photochemical Chambers During CFM-56 Engine Experiments	27
8	Schematic Diagram of Instrument Manifold for Smog Chamber Sampling	30
9	GC/FID Chromatogram for JP-4 Fuel	53
10	GC/FID Chromatogram of C ₂ to C ₁₁ Organics in the Exhaust of TF-39 Engine	54
11	GC/FID Chromatogram of C ₂ to C ₁₁ Organics in the Exhaust of the TF-39 Engine	55
12	Chromatogram for JP-5 Fuel and XAD Sample Exhaust from TF-39 Engine Operated on JP-5 Fuel at Idle	56
13	Chromatogram for JP-8 Shale Fuel	57
14	Chromatogram for XAD Sample of Exhaust from TF-39 Engine Operating on JP-8 Fuel at Idle	58
15	HPLC Chromatogram of Aldehyde Emissions from CFM-56 Engine Operating at Idle on JP-5 Fuel	59
16	HPLC Chromatogram of Aldehyde Emissions from CFM-56 Engine Operating on JP-8 Shale Fuel	60
	Plot of K ₁ Measurements vs UV Radiometer Signal	69

LIST OF FIGURES (CONTINUED)

Figure	Title	Page
18	Comparison of Actionmetry Results from This Study With Data of Zafonte et al.	71
19	Temperature and UV Intensity for Chamber Experiment on June 9, 1983	72
20	Dual-Chamber Experiment, Butane/Propene Hydrocarbon Mix, June 9, 1983	73
21	Profiles from AF-1 Chamber A, July 18, 1983	75
22	Profiles from AF-1 Chambers A and B, July 18, 1983	76
23	Aldehyde Formation in Chamber A During System Demonstration Experiment	77
24	Aldehyde Formation in Chamber B During System Demonstration Experiment	78
25	Plots of O ₃ Concentration from Chamber A and Chamber B During System Demonstration, July 18, 1983	79
26	Compound Class Distributions for Emissions Using JP-5 Fuel and Ground Idle Test Point	93
27	Comparison of Distributions of Organic Emissions from TF-39 Combustor Rig and Full-Scale Engine	98
28	Percentage of Aldehydes in Exhaust from Three Combustion Sources	108
29	Smog Chamber Profiles from AF-3 Using TF-39 Engine and JP-4 Fuel	112
30	Smog Chamber Profiles from AF-3 Using TF-39 Engine and JP-4 Fuel	113
31	Smog Chamber Profiles from AF-3 Using TF-39 Engine and JP-4 Fuel	114
32	Maximum O ₃ from TF-39 Experiments	119
33	Maximum O ₃ from CFM-56 Experiments	126

LIST OF FIGURES (CONTINUED)

Figure	Title	Page
A-1	Smog Chamber Profiles from AF-2 Using TF-39 Engine and JP-5 Fuel	155
A-2	Smog Chamber Profiles from AF-2 Using TF-39 Engine and JP-5 Fuel	156
A-3	Smog Chamber Profiles from AF-2 Using TF-39 Engine and JP-5 Fuel	157
A-4	Smog Chamber Profiles from AF-3 Using TF-39 Engine and JP-4 Fuel	158
A-5	Smog Chamber Profiles from AF-3 Using TF-39 Engine and JP-4 Fuel	159
A-6	Smog Chamber Profiles from AF-3 Using TF-39 Engine and JP-4 Fuel	160
A-7	Smog Chamber Profiles from AF-4 Using TF-39 Engine and JP-4 Fuel	161
A-8	Smog Chamber Profiles from AF-4 Using TF-39 Engine and JP-4 Fuel	162
A-9	Smog Chamber Profiles from AF-4 Using TF-39 Engine and JP-4 Fuel	163
A-10	Smog Chamber Profiles from AF-5 Using TF-39 Engine and JP-8 Shale-Derived Fuel	164
A-11	Smog Chamber Profiles from AF-5 Using TF-39 Engine and JP-8 Shale-Derived Fuel	165
A-12	Smog Chamber Profiles from AF-5 Using TF-39 Engine and JP-8 Shale-Derived Fuel	166
A-13	Profiles from AF-6 Using CFM-56 Engine and JP-5 Fuel, October 19, 1983	167
A-14	Smog Chamber Profiles from AF-6	168
A-15	Smog Chamber Profiles from AF-6	169
A-16	Smog Chamber Profiles from AF-6	170

LIST OF FIGURES (CONCLUDED)

Figure	Title	Page
A-17	Profiles from AF-8 Using CFM-56 Engine and JP-4 Fuel, October 25, 1983	171
A-18	Smog Chamber Profiles from AF-8	172
A-19	Profiles from AF-9 Using CFM-56 Engine and JP-4 Fuel, October 26, 1983	173
A-20	Profiles from AF-9 Reference Chamber, October 26, 1983	174
A-21	Smog Chamber Profiles from AF-9	175
A-22	Smog Chamber Profiles from AF-9	176
A-23	Profiles from AF-10 Using CFM-56 Engine and JP-5 Fuel, November 3, 1983	177
A-24	Smog Chamber Profiles from AF-10	178
A-25	Smog Chamber Profiles from AF-10	179
A-26	Smog Chamber Profiles from AF-10	180
A-27	Profiles from AF-11 Using CFM-56 Engine and JP-8 Fuel, November 7, 1983	181
A-28	Smog Chamber Profiles from AF-11	182
A-29	Smog Chamber Profiles from AF-11	183
A-30	Smog Chamber Profiles from AF-11	184

LIST OF TABLES

Table	Title	Page
1	VARIABLES MEASURED DURING THE EMISSION EXPERIMENTS	15
2	SAMPLING PERIOD OF EACH METHOD DURING A TEST RUN	24
3	SCHEDULE OF ENGINE EMISSIONS EXPERIMENTS	26
4	VARIABLES MEASURED DURING THE CHAMBER EXPERIMENTS	29
5	ENGINE OPERATING CONDITIONS AND STANDARD EMISSIONS DATA . .	37
6	MAJOR ORGANIC SPECIES IN EXHAUST OF JET ENGINE OPERATING WITH JP-4 FUEL	39
7	MAJOR ORGANIC SPECIES IN EXHAUST OF JET ENGINE OPERATING WITH JP-5 FUEL	42
8	MAJOR ORGANIC SPECIES IN EXHAUST OF JET ENGINE OPERATING WITH JP-8 FUEL	44
9	PERCENT COMPOSITION OF MAJOR ORGANIC SPECIES IN JP-4 FUEL . .	48
10	PERCENT COMPOSITION OF MAJOR ORGANIC SPECIES IN JP-5 FUEL . .	49
11	PERCENT COMPOSITION OF MAJOR ORGANIC SPECIES IN JP-8 FUEL . .	50
12	RESULTS FOR STANDARD FUEL ANALYSIS	51
13	PNA ANALYSIS DATA	62
14	CHAMBER DILUTION RATES DURING CHARACTERIZATION EXPERIMENTS .	64
15	OZONE DECAY RATE IN OUTDOOR SMOG CHAMBERS.	66
16	SCHEDULE OF TF-39 ENGINE PHOTOCHEMISTRY EXPERIMENTS	81
17	OZONE AND b_{scat} RESULTS FOR TF-39 ENGINE EXHAUST PHOTO- CHEMISTRY EXPERIMENTS	82
18	SCHEDULE OF CFM-56 ENGINE EXHAUST PHOTOCHEMISTRY EXPERIMENTS.	84
19	OZONE AND b_{scat} RESULTS FOR CFM-56 ENGINE EXHAUST PHOTO- CHEMISTRY EXPERIMENTS	85

LIST OF TABLES (CONTINUED)

Table	Title	Page
20	COMPARISON OF TOTAL ORGANICS BY CONTINUOUS FID VERSUS SPECIATION METHODS	87
21	MAJOR ORGANIC SPECIES SUMMARIZED BY COMPOUND CLASS IN EXHAUST OF JET ENGINES OPERATING WITH JP-4 FUEL	90
22	MAJOR ORGANIC SPECIES SUMMARIZED BY COMPOUND CLASS IN EXHAUST OF JET ENGINES OPERATING WITH JP-5 FUEL	91
23	MAJOR ORGANIC SPECIES SUMMARIZED BY COMPOUND CLASS IN EXHAUST OF JET ENGINES OPERATING WITH JP-8 FUEL	92
24	TOTAL ORGANIC SPECIES IN EXHAUST OF SELECTED TEST RUNS, DISTRIBUTION BY CARBON NUMBER	94
25	HYDROCARBON DISTRIBUTION BY CARBON NUMBER IN VARIOUS FUELS	95
26	SELECTED AROMATIC/ALIPHATIC RATIOS FOR EMISSIONS USING JP-5 FUEL	97
27	COMPARISON OF EMISSION LEVELS OF SELECTED COMPOUNDS FROM TF-39 COMBUSTOR RIG AND FULL-SCALE ENGINE OPERATING ON JP-5 FUEL AT GROUND IDLE	99
28	COMPARISON OF AQUEOUS AND ACETONITRILE (ACCN) DNHP PROCEDURES FOR ALDEHYDES.	102
29	COMPARISON OF BENZENE EMISSIONS FROM VARIOUS MOBILE SOURCES.	104
30	COMPARISON OF BENZO(a)PYRENE EMISSIONS FROM VARIOUS SOURCES.	105
31	FORMALDEHYDE EMISSIONS FROM A VARIETY OF MOBILE SOURCES.	107
32	COMPOSITION OF TF-39 EXHAUST USED IN PHOTOCHEMISTRY EXPERIMENTS	115
33	MAXIMUM REACTION PRODUCT CONCENTRATIONS OBSERVED IN TF-39 SMOG CHAMBER EXPERIMENTS	117
34	TF-39 EXHAUST REACTIVITY RELATIVE TO REFERENCE MIXTURE	121
35	COMPOSITION OF CFM-56 EXHAUST USED IN PHOTOCHEMISTRY EXPERIMENTS	124
36	MAXIMUM REACTION PRODUCT CONCENTRATIONS OBSERVED IN THE CFM-56 SMOG CHAMBER EXPERIMENTS	125

LIST OF TABLES (CONCLUDED)

Table	Title	Page
37	INTEGRATED UV INTENSITIES	128
38	CFM-56 EXHAUST REACTIVITY RELATIVE TO REFERENCE MIXTURE . . .	130
39	COMPARISON OF NORMALIZED PHOTOCHEMICAL REACTIVITIES ACROSS ENGINES AND FUELS	132
40	MOLAR DISTRIBUTION OF EXHAUST ORGANIC COMPOUNDS	135
41	FIVE CLASS REACTIVITY CATEGORIZATION OF ORGANIC COMPOUNDS . .	136
42	MOLAR CONCENTRATIONS AND TOTAL REACTIVITY	137
43	CONTRIBUTION OF COMPOUND CLASSES TO PHOTOCHEMICAL REACTIVITY	138
44	MEASURED AND CALCULATED EXHAUST REACTIVITIES NORMALIZED TO REFERENCE MIXTURE REACTIVITY	141
45	MOLAR REACTIVITIES CALCULATED FROM EXHAUST COMPOSITION . . .	143
46	MOLAR REACTIVITIES OF ORGANIC EMISSIONS CALCULATED FROM COMPOSITION DATA	145

SECTION I

INTRODUCTION

The environmental significance of organic emissions from aircraft turbine engines has not been established, in spite of the completion of numerous studies in the area. Specifically, the contribution of aircraft exhaust organic emissions to photochemical pollutant formation is poorly understood since complete data concerning the qualitative and quantitative chemical composition of these emissions are not available.

Several studies have been conducted to determine the organic chemical composition of jet turbine engines. One study employed subtractive gas chromatography to determine compound classes and selected individual paraffins in jet aircraft emissions under various operating conditions (Reference 1). Other studies determined total aldehyde and hydrocarbon emissions under a variety of conditions (References 2,3). Another study employed a liquid chromatographic technique to separately determine unreactive and reactive hydrocarbons (Reference 4). Unfortunately, none of the above studies determined individual organic compounds.

Two studies have been reported in which a large number of individual organic compounds were determined in gas turbine exhaust (References 5,6). One study (Reference 5) qualitatively determined 273 individual organic compounds, but did not attempt to quantify these materials. A second study attempted to perform a quantitative mass balance of the hydrocarbon emissions (Reference 6). While relatively good mass balance (85 percent) was obtained by comparing individual species and total hydrocarbons at high thrust, poor mass balance (32 percent) was obtained under idle operating conditions. Another study demonstrated that particle-bound organic emissions are a very small fraction of the total organic composition of the exhaust and from a mass balance standpoint can be ignored (Reference 7).

In view of the sparse data available concerning individual organic components in jet turbine exhaust, any estimate of the environmental significance of these emissions, including photochemical pollutant formation, is likely to be highly inaccurate. Consequently, the

Enviroics Division, Air Force Engineering and Services Laboratory, Air Force Engineering and Services Center, Tyndall AFB, Florida, contracted with Battelle, Columbus Laboratories (BCL) to perform a comprehensive study of organic emissions from jet aircraft turbine engines.

The specific objectives of this study were as follows:

- (1) to obtain a detailed analysis of the composition of the gaseous hydrocarbon species emitted in gas turbine engine exhaust and
- (2) to determine the effect of these hydrocarbons on atmospheric photochemical processes, using an outdoor smog chamber.

This program was completed in five separate tasks as follows:

- Task 1 -- Development and validation of sampling and analysis procedures for selected organic compounds representative of gas turbine engine emissions.
- Task 2 -- Evaluation of the procedures developed in Task 1 using a laboratory combustor rig.
- Task 3 -- Identification and quantification of individual organic compounds emitted from two commercial jet engines operated at various thrust settings and burning three different fuels.
- Task 4 -- Concurrently, with Task 3, investigation of the photochemical behavior of the emissions (at the idle thrust setting) using a Teflon[®] smog chamber.
- Task 5 -- Evaluation of the data from Tasks 3 and 4 in terms of environmental impact of jet aircraft operations.

An earlier report (Reference 8) presents the results obtained in the first two Tasks. This report includes a brief summary of the first two Tasks and presents a detailed description of the procedures employed and results obtained in Tasks 3 through 5. The results for the overall program are discussed in terms of the environmental significance of turbine engine emissions.

SECTION II

SUMMARY OF TASKS 1 AND 2

A. METHOD VALIDATION AND COMBUSTOR RIG STUDIES (Tasks 1 and 2)

The results for these two tasks are presented in detail in a publicly available interim report (Reference 8) and are briefly summarized below.

Methods developed during Task 1 included the following:

- (1) an on-line cryogenic trapping/gas chromatography method for C₂-C₁₂ hydrocarbons,
- (2) a resin-adsorption (XAD-2) technique for C₉-C₁₈ hydrocarbons,
- (3) a gas chromatography/mass spectrometry procedure for polynuclear aromatic hydrocarbons (PNAs),
- (4) a high-performance liquid chromatography procedure for aldehydes, and
- (5) a direct-injection gas chromatography/photoionization detection (GC/PID) method for alcohols.

The precision and recovery of the various methods were evaluated by introducing known concentrations of relevant test compounds into a Teflon[®]-lined 17.3 m³ chamber and withdrawing air from the chamber in a manner closely simulating the engine sampling procedure. Recoveries were approximately 90 percent for cryogenic trapping, 85-90 percent for resin adsorption, and 60-100 percent for aldehydes. Precision ranged from \pm 5 percent for cryogenic trapping to \pm 25 percent for selected aldehydes.

Task 2 involved sampling and analysis of emissions from a 60-degree sector TF-39 combustor rig operated at ground idle thrust setting using the techniques developed in Task 1. A total of 16 tests, all using JP-5 fuel, were conducted over a 4-day period. The Task 2 data were very encouraging in that: (1) 88 percent carbon balance was obtained by comparing the total hydrocarbon concentration to the summation of individual hydrocarbon species, (2) a significant portion (60 percent) of the total hydrocarbon content was attributable to specific compounds

determined by GC/MS, and (3) good method performance in terms of precision and recovery (comparable to or better than Task 1 in all cases) was obtained.

If further details of the Task 1 and 2 results are desired, the reader should consult the interim report (Reference 8). A comparison of the Task 2 TF-39 combustor rig data with the Task 3 TF-39 full-scale engine data is presented in Section V of this report.

SECTION III
EXPERIMENTAL METHODS

A. TASK 3 EMISSIONS TESTING

The two engines selected for testing in Tasks 3 and 4 were the TF-39 and CFM-56. Both are large turbofan engines of a design currently used in operational military or commercial aircraft. The TF-39 represents first-generation, high-thrust, high-bypass-ratio engines used to power early wide-body transports. Since control of gaseous emissions was not a significant factor in the design of these early engines, the TF-39 has somewhat higher hydrocarbon emission levels than the newer engines. Because the CFM-56 represents the latest technology (fuel efficient engines with advanced emissions control features), it has a very low total hydrocarbon emission level.

1. Engine Descriptions

a. TF-39 Engine

The General Electric TF-39 engine used in this study is shown in Figure 1. This engine is a dual-rotor, high-bypass turbofan engine, currently in service on the U.S. Air Force Lockheed C-5 aircraft. It has a takeoff thrust rating of 41,100 pounds, and a dry weight of 7311 pounds. A one-and-one-half-stage front fan is driven by a six-stage, low-speed, low-pressure, turbine through a shaft concentric with the core engine rotor. The fan and fan turbine are each supported by two bearings and, together, form the low-pressure system. The core engine is the high-pressure system and consists of a 16-stage compressor with variable inlet guide vanes and first six stator stages; an annular combustor; a two-stage, air-cooled turbine; and an accessory gearbox with controls and accessories. The core engine rotor system is supported by three bearings.

The military TF-39 has essentially the same core engine as the commercial CF6-6 which powers the McDonnell Douglas DC-10 Series 10 tri-jet aircraft. In addition, General Electric has adapted this

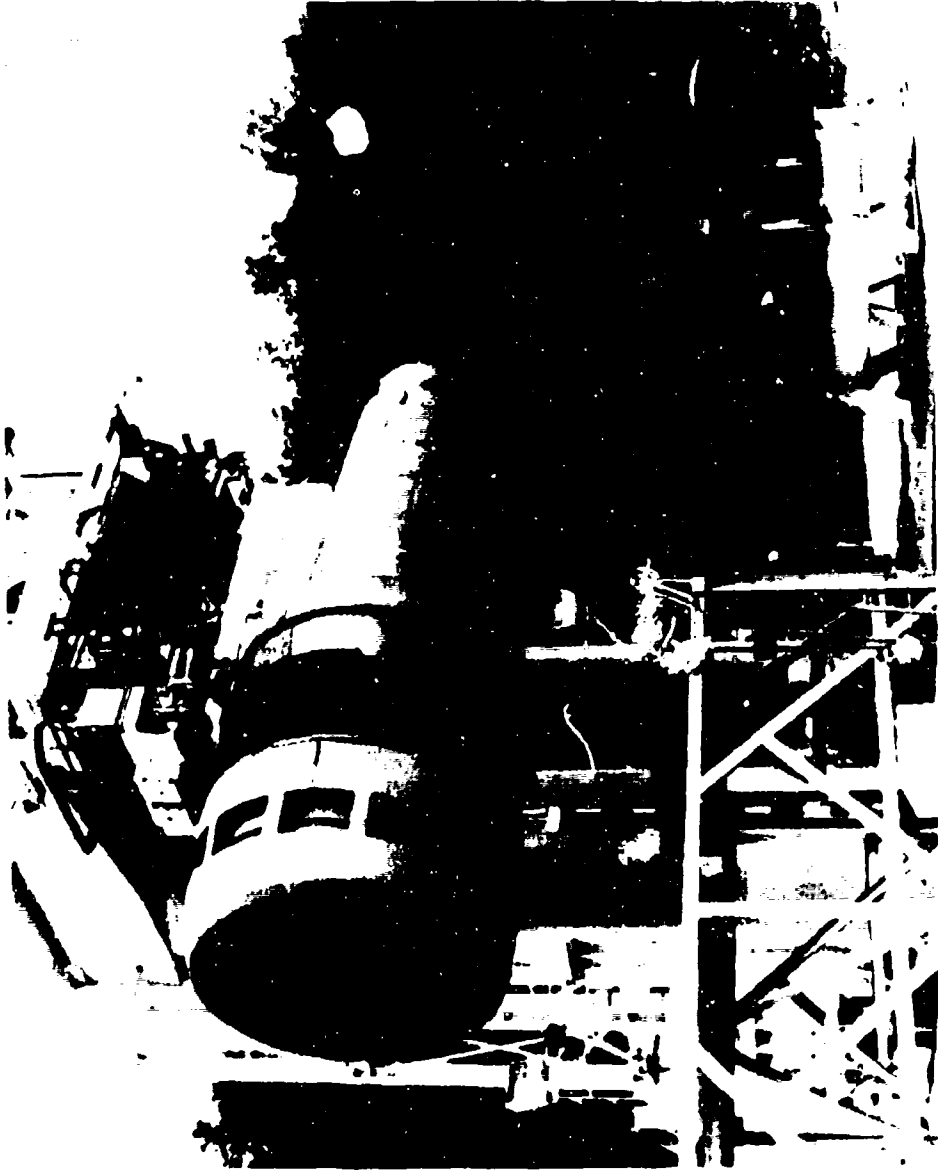


Figure 1. TF-30 engine and Sampling Rake During Emission Measurement Studies

same basic core engine to industrial and marine applications, where it is known as the LM2500. The LM2500 powers gas transmission line compressors and electrical generators. In marine applications, the LM2500 powers the U.S. Navy Spruance Class (DD963) destroyers and a number of other surface ships.

The TF-39 engine combustion system consists of 30 pressure atomizing, duplex-type fuel nozzles and an annular combustor. Axial swirlers in the combustor dome provide the intense mixing of fuel and air required for good combustion stability and low-smoke emissions. Except for the low-smoke features, the TF-39 combustion system is not equipped with emission abatement features. Thus, it does not meet the EPA or ICAO standards for gaseous emissions, and, being a military engine, it is not required to.

The engine tested was a Model TF-39-1C, Serial Number 441-024/20. The tests were run at Peebles Test Operation Site IIIC in between 18-22 July 1983. For these tests, all exhaust analysis equipment was located in the underground control room within about 75 feet of the sampling rake.

b. CFM-56 Engine

The CFM-56 engine used in this study is shown in Figure 2. This engine is a product of CFM International, a company jointly owned by General Electric and SNECMA (France). In addition to its high-bypass ratio, major features are high component efficiencies and low weight, aimed at combining good performance with low noise and emission levels, low operating costs, and high productivity. The engine is fully modular in construction. The CFM-56 is a dual-rotor engine with single-stage fan, three-stage compressor, and four-stage low-pressure turbine on the low-pressure rotor. The high-pressure section consists of a nine-stage compressor, annular combustor, and single-stage turbine.

Two versions of the CFM-56 are currently in production. The CFM-56-2 engine is rated at 24,000 pounds thrust and applications include re-engining of the Air Force KC135 tankers and McDonnell Douglas DC-8 Series 70 commercial transports. The CFM-56-3 engine is rated at 20,000 pounds thrust and is scheduled for service on the Boeing 737-300.

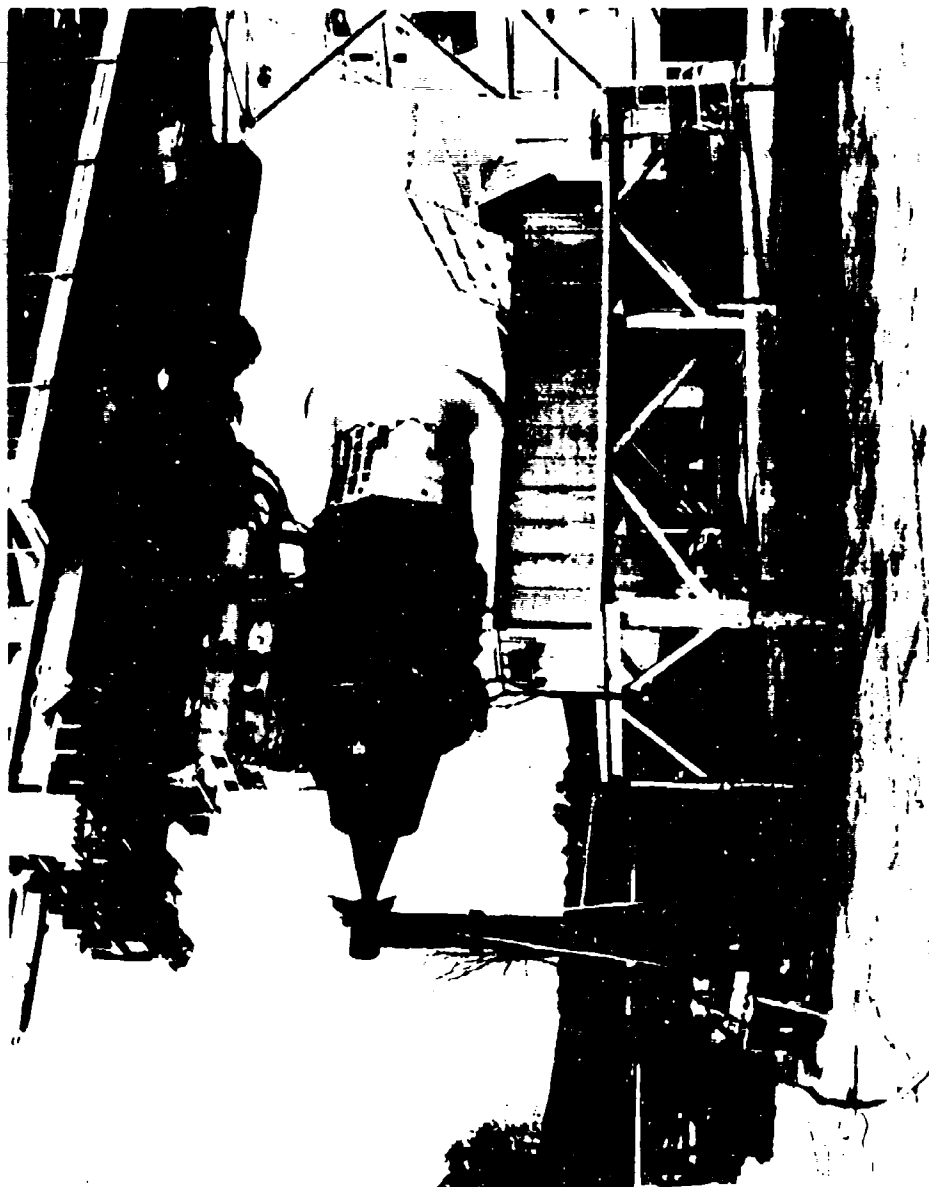


Figure 2. CFM-56 Engine and Sampling Rake During
Emission Measurement Studies

The core engine of the CFM-56 is essentially the same as that of the U.S. Air Force F101 engine for the B-1B bomber.

The CFM-56 combustor is extremely compact with a very high combustion space rate at takeoff operating conditions. The fuel injection system consists of 20 pressure atomizing, duplex-type fuel nozzles in an annular combustor. Low emission has been a key design consideration throughout the combustor development. This has resulted in a combustion system which yields emissions meeting all EPA and ICAO standards by a wide margin.

The CFM-56 engine tested was a Model CFM-56-3, Serial Number 700-001/3. The tests were run at Peebles Test Operation Site IVA between October 19 and November 7, 1983. For these tests, all exhaust analysis equipment was located in trailers parked on the test pad adjacent to the engine.

2. Engine Test Facility and Engine Instrumentation

The General Electric Peebles Test Operation is situated near Peebles, Ohio, in a remote location approximately 80 miles east of the main General Electric plant in Evendale, Ohio. Since all test sites at Peebles are outdoors, this isolated 6000-acre facility is ideally suited for running a variety of special engine tests which cannot be run in enclosed test cells. Included in the special test capabilities are cross-wind testing, acoustic and infrared measurements, thrust reverser testing, high-energy X-ray inspection, icing tests, and ingestion tests. The six test sites are equipped with the most modern data acquisition systems and with data transmission links directly to computers in Evendale.

The Peebles Test Facility was well-suited to the engine tests since it provides ready access to the engine by the fuel truck, smog chambers, and mobile laboratory. In addition, there was a large unobstructed area for smog chamber exposure near each test site.

Each engine was equipped with instrumentation to monitor temperatures and pressures at numerous locations throughout the engine, rotor speeds, thrust, fuel flow, and ambient conditions. At approximately 10-minute intervals during the tests, the automatic data acquisition system (DMS) would acquire a complete set of readings of the instruments and

perform calculations of desired values. Selected items from this complete tabulation are included in the data from the various tests in a later section of this report.

3. Engine Emissions Measurements

a. Sampling System

The sampling rake (GE P/N 4013262-600) used for the emissions tests had a cruciform-shaped head, mounted on a single pylon which was attached to a large base and anchored to the pad behind the engine. A sketch of the rake system is shown in Figure 3. A closeup photograph of the rake mounted behind the engine is shown in Figure 4. The rake head consisted of four equally spaced arms extending radially outward from the central hub. Each arm had individual sampling ports located at 1-inch intervals from 6 to 17 inches radius. This arrangement gave considerable flexibility in choosing sampling patterns to accommodate the different engine exhaust nozzle configurations. Three ports on each arm were selected (near centers of equal area) for the two engines being tested. These sampling ports were internally connected to a common manifold and a single sample was thus obtained. The sample lines in the rake head were stainless steel and the internal sample line passed down the center support pylon where it joined an electrically heated, flexible Teflon[®] line which led to the base of the rake platform. At this point the sample line was connected via a tee to a clean-air purge line and pumping station. The pumping station contained a 6-inch stainless steel (s.s.) filterholder (Pallfax quartz fiber filter) coupled to a s.s. metal bellows pump (Metal Bellows Corp. model MB-60JHT). The pump directed the exit flow to Battelle's manifold. A portion of the exit flow was also diverted to the GE manifold via a second smaller metal bellows pump. During normal emissions sampling operations a flow of 2.0 ft³/min passed through the Battelle manifold (Brooks rotameter R-8M-25-5); GE required 0.5 ft³/min for their instrumentation. Figure 5 is a schematic diagram of the overall sampling system. The entire sampling system was maintained at 300°F. Each component of the system was interconnected via heated Teflon[®] lines (Technical Heaters, Inc.). The s.s. ball valves (Whitey SS-63SW8T), tees, and manifolds were wrapped with heating tape. Heat to these items

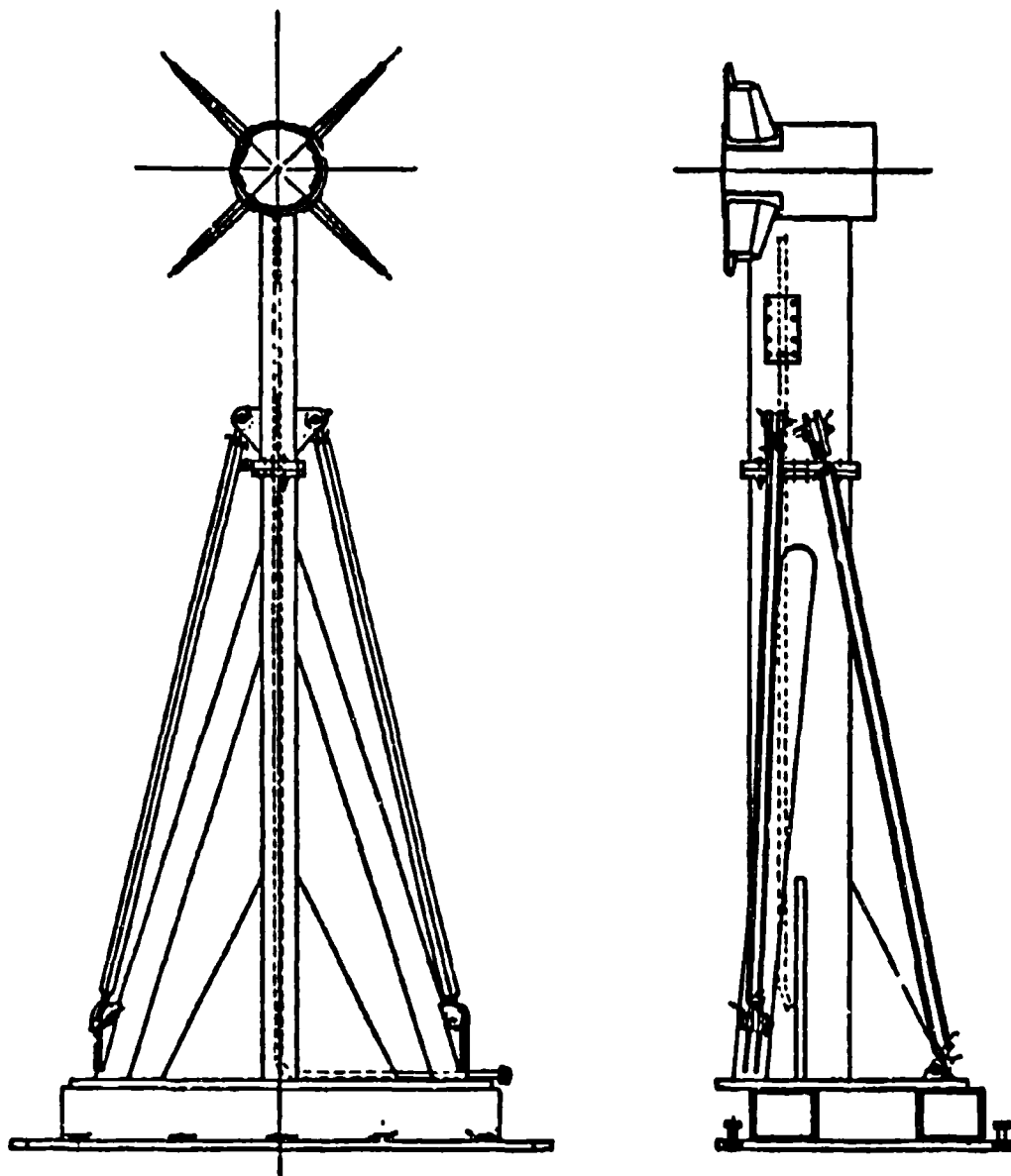


Figure 3. Engine Exhaust Sampling Rake

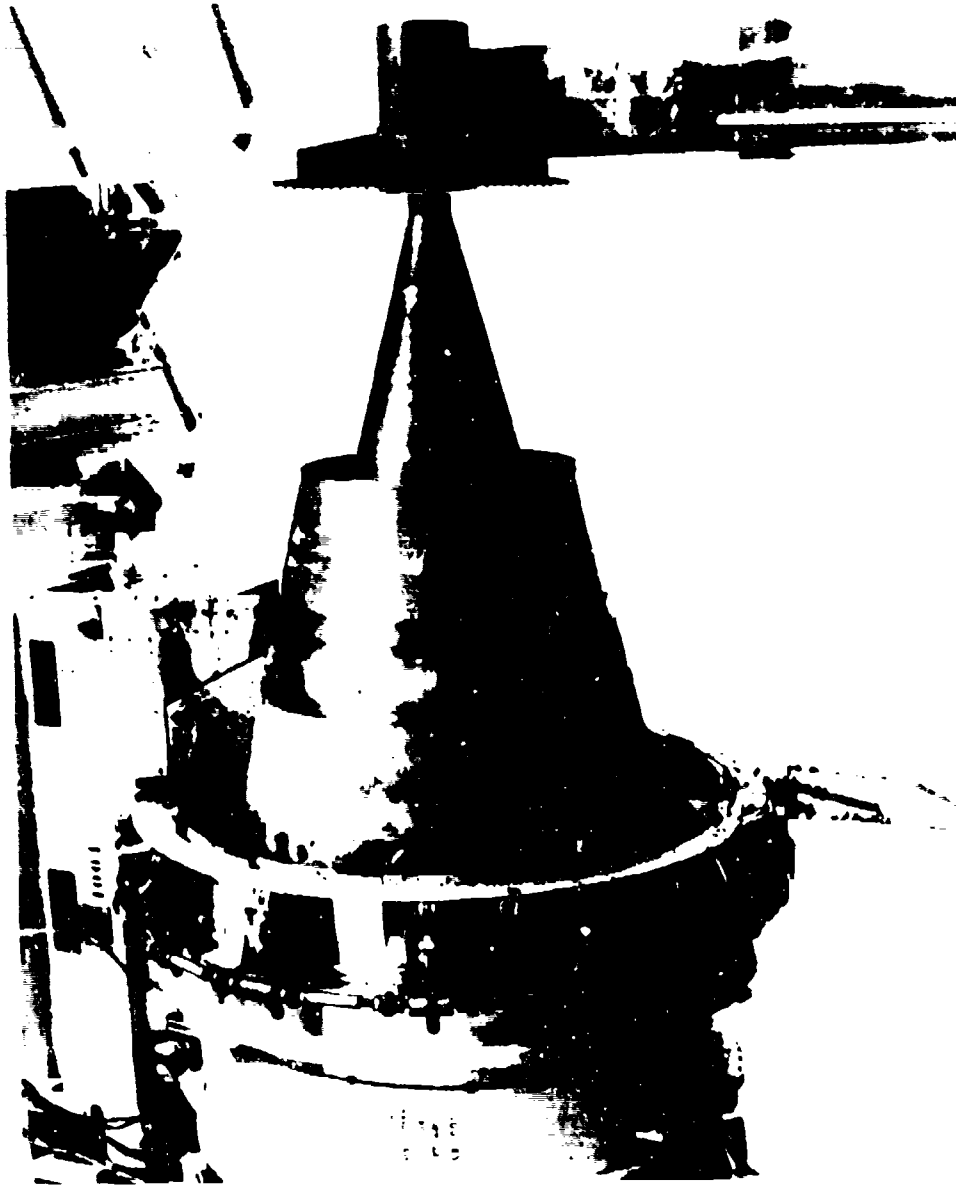


Figure 4. Closeup of Sampling Rake Mounted Behind Engine

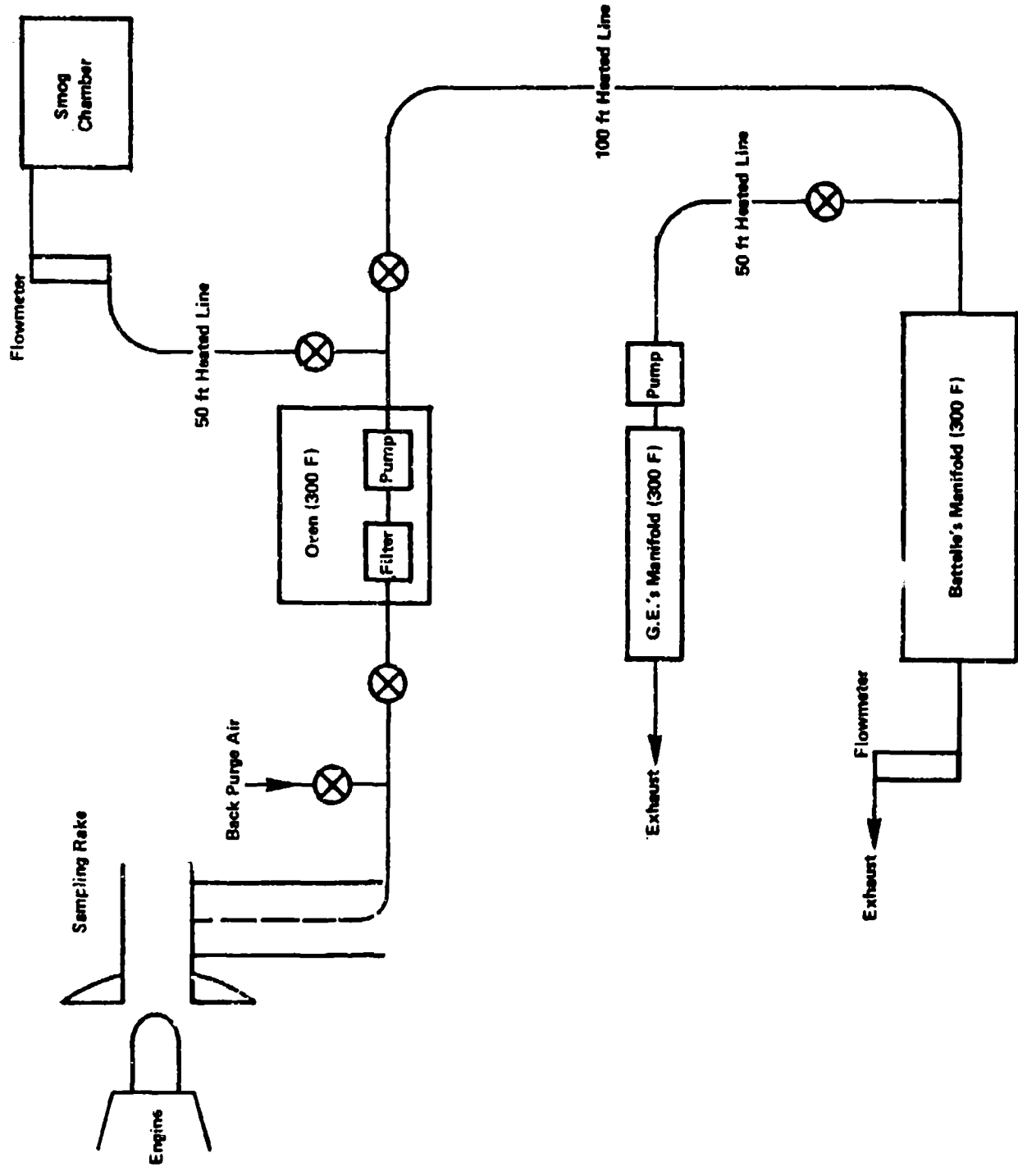


Figure 5. Overall Sampling System

was supplied via temperature controllers or variacs. Thermocouples were positioned throughout the system to check actual temperatures.

b. Sampling and Analysis Procedures

General Electric emissions analysis package consisted of four gas analyzers. The four analyzers are manufactured by Beckman Instruments, Inc. The CO (Model 865) and CO₂ (Model 864) analyzers are nondispersive infrared instruments. The NO/NO₂ analyzer is a Model 951 heated chemiluminescence instrument. The total hydrocarbon analyzer is a Model 402 flame-ionization instrument. The output from each instrument is continuously monitored on a dual-channel recorder. Data reduction is performed by a dedicated Apple II microcomputer.

The gaseous emissions analyzers were calibrated daily with certified mixtures of propane in air, CO and CO₂ in nitrogen, and NO in nitrogen. Each analyzer was calibrated with four separate dilute mixtures to cover the range of concentrations of the exhaust samples. Each calibration gas was certified by the vendor to an accuracy of ± 2 percent. In addition, the calibration gases were compared with Standard Reference Materials (SRM) from the National Bureau of Standards. During the field study General Electric and Battelle personnel cross-compared the various propane standards.

The variables measured by Battelle during the emissions experiments are listed in Table 1. The position of each sampling method within the manifold is illustrated in Figure 6.

(1) XAD-2 Samples. XAD-2 samples were used to quantify C₁₀ through C₁₇ hydrocarbons and polycyclic aromatic hydrocarbons (PNA). A 22-gram portion of XAD resin (prepurified by methylene chloride extraction) was placed in a glass-sampling module thermostated at 130°F using a constant-temperature circulating water bath. The exhaust samples were collected at a rate of 1 cfm for 35 minutes to collect a total volume of 1 m³. After collection the trap/condenser assembly was capped with glass connectors and transported to the laboratory for analysis.

The XAD-2 resin cartridges were extracted within 24 hours after collection. The resin was extracted (Soxhlet) for 16 hours with methylene chloride. The extract was spiked with 100 µg of

TABLE 1. VARIABLES MEASURED DURING THE EMISSION EXPERIMENTS

Variable	Technique	Instrument
<u>General Electric</u>		
NO/NO _x	Chemiluminescence	Beckman 951
CO	Nondispersive Infrared	Beckman 865
CO ₂	Nondispersive Infrared	Beckman 864
THC	Flame Ionization	Beckman 402
<u>Battelle</u>		
Methane	Canister Samples/Flame Ionization GC	Beckman 6800
CO	Canister Samples/Flame Ionization GC	Beckman 6800
C ₂ to C ₁₀ Organics	On-Line Flame Ionization GC	Hewlett-Packard 5880
C ₁₀ to C ₁₇ Organics	XAD-2/Flame Ionization GC	Hewlett-Packard 5730
PNA Compounds	XAD-2/Gas Chromatography/Mass Spectrometry	Finnigan 4000
Aldehydes	DNPH Derivatization/HPLC	Altex 110A HPLC System With LDC Spectro Monitor III UV Detector
THC	Flame Ionization	Beckman 402

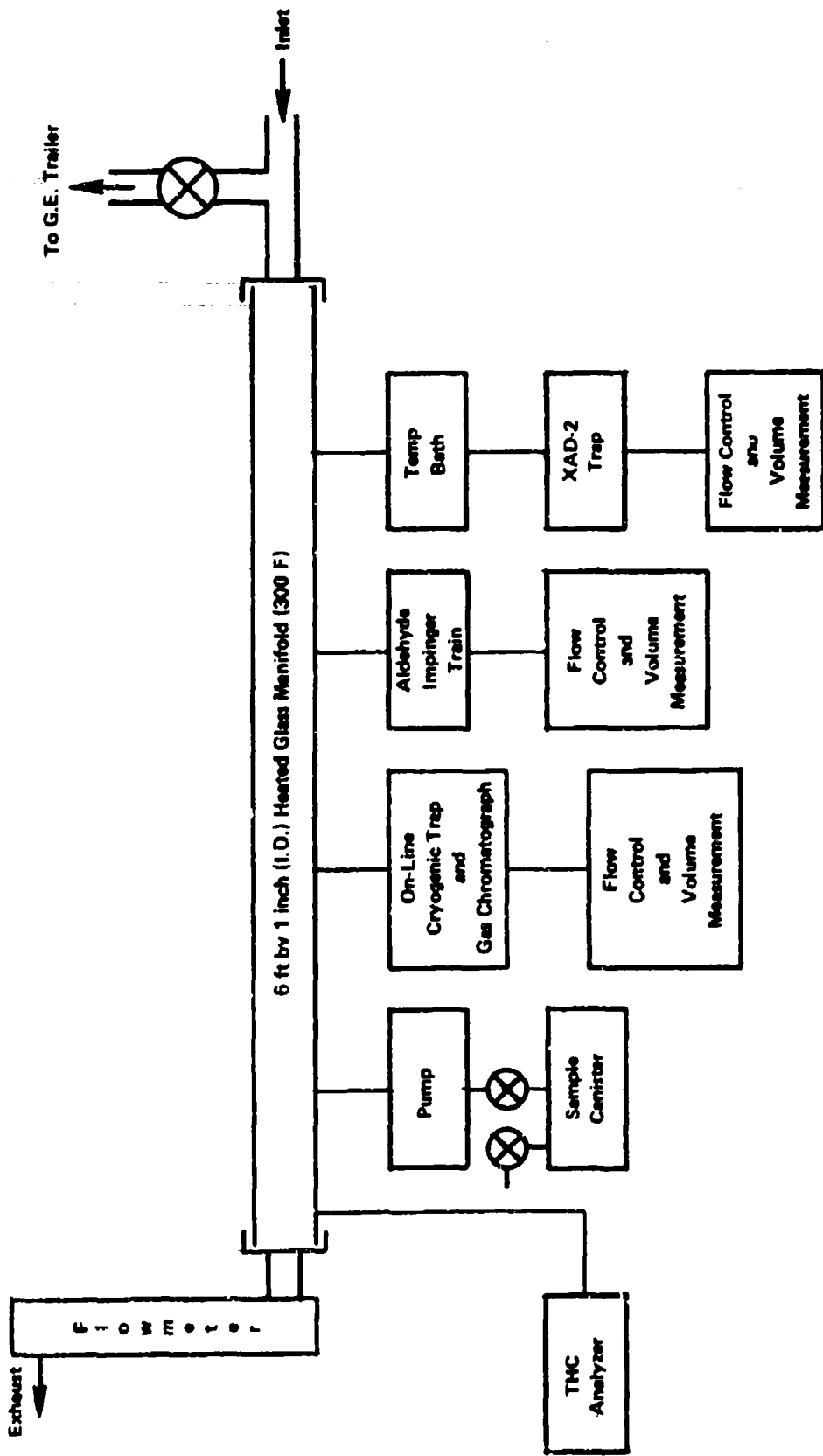


Figure 6. Schematic Diagram of Sampling Manifold

hexaethylbenzene (HEB) and 10 μg of each of the following deuterated PNAs; D₈-naphthalene, D₁₀-phenanthrene, D₁₂-chrysene, and D₁₂-benzo(a)pyrene (BAP). HEB was used as an internal standard for GC/FID quantification of hydrocarbons whereas the deuterated PNAs were used as internal standards for GC/MS quantification of PNAs.

The solvent extract was then concentrated to 1-10 ml using a Kuderna-Danish (K-D) concentrator and analyzed by GC/FID. The larger final volume (10 mL) was employed for idle runs because of the large quantity of hydrocarbons present in the exhaust, while the smaller volume (1 ml) was employed for 30 percent and 80 percent thrust experiments.

The GC/FID analysis conditions employed were as follows:

GC - Carlo Erba Model 2160

Column - 50-meter SE-54 cross-linked wide bore, thick film-fused silica capillary, Hewlett-Packard

Carrier Flow - H₂ @ 50 cm/sec

Injector/Detector Temperature - 275°C

Temperature Program - Inject at room temperature and increase to 50°C after 1 minute; hold isothermal at 50°C for 1 minute; then 50-250 at 6 degrees/minute

Injection - 2 μl splitless, split on at 45 seconds.

Data were acquired and processed on a Computer Inquiry Systems chromatographic data system and all raw data were archived on nine-track magnetic tape. The GC system was calibrated using a calibration standard containing 63 $\mu\text{g}/\text{ml}$ of each normal paraffin from n-C₉ to n-C₁₆ and 50 $\mu\text{g}/\text{ml}$ of HEB. All data were reported as ppmC, using the response factor of HEB for all components except the normal paraffins for which specific response factors were determined.

Selected XAD-2 extracts and fuel samples were analyzed by GC/MS in the full spectrum scan mode (40-500 amu) using the same conditions as for GC/FID. Helium, rather than hydrogen carrier gas, was used since the GC/MS system could not accept hydrogen. An Extranuclear EI/CI mass spectrometer interfaced to a Hewlett-Packard Model 5730 gas chromatograph was used for this work.

One XAD extract from each test was analyzed for PNAs, using a GC/MS isotope dilution procedure. The extract was concentrated, exchanged into cyclohexane (final volume, 1 ml), and subjected to silica gel cleanup. Davidson Grade 923 (100-200 mesh) silica gel was rinsed with methanol and activated in an oven at 130°C for 24 hours. Ten grams of activated silica gel was placed in 40 ml of methylene chloride and the suspension poured into a 1 cm x 25 cm chromatographic column. The column was eluted with 40 ml of hexane. The cyclohexane solution (XAD extract) was placed on the silica gel column, rinsing the sample container with an additional 2 ml of cyclohexane. The column was then sequentially eluted with 25 ml of hexane (Fraction 1), benzene (Fraction 2), and methanol (Fraction 3). These fractions contain aliphatic/olefinic hydrocarbons, aromatic hydrocarbons, and polar-substituted compounds, respectively.

The benzene fraction was concentrated to 1 ml and analyzed for PNAs using GC/MS in the multiple-ion detection (MID) mode. A Finnigan 4000 GC/MS system, operating with an INCOS data system, was used. A 30-meter DB-5 fused silica capillary column (J & W Scientific) and helium carrier gas were used. The temperature program was from 50° to 300°C at 6 degrees/minute and the column was held at 300°C until no more material eluted (approximately 15 minutes).

Ions monitored were as follows: m/e 128 (naphthalene), m/e 136 (D₈-naphthalene), m/e 142 (methyl naphthalenes), m/e 156 (dimethyl naphthalenes), m/e 178 (phenanthrene/anthracene), m/e 188 (D₁₀ phenanthrene), m/e 202 (pyrene/fluoranthene), m/e 212 (D₁₀ pyrene), m/e 228 (chrysene/benzanthracene), m/e 240 (D₁₂-chrysene), m/e 252 (benzopyrenes/benzofluoranthenes/perylene), and m/e 264 (D₁₂-benzo(a)pyrene). The methyl and dimethylnaphthalenes were quantified with the response factor for D₈-naphthalene, whereas all other compounds were quantified with the corresponding deuterated PNA.

The GC/MS system was calibrated each day with a standard containing 1 µg/ml of each native PNA, and 10 µg/ml of each deuterated PNA. Fuel samples were also analyzed for PNAs by processing 250 µl of fuel dissolved in 1 ml of cyclohexane through the silica gel cleanup procedure described for XAD samples.

(2) Carbonyl Compounds. Carbonyl compounds in the exhaust stream were collected in liquid impingers containing 2,4-dinitrophenylhydrazine (DNPH) wherein the DNPH derivatives were formed. The derivatives were then returned to the Battelle laboratory, extracted into an organic solvent, concentrated, and analyzed by high-performance liquid chromatography (HPLC) using a UV detector.

The DNPH reagent (0.05 percent DNPH in 2 N HCl) was purified by extraction with hexane/methylene chloride 70/30 within 24 hours before sampling. Two midget impingers, connected in series, were loaded with 10 ml of DNPH reagent and 10 ml of isooctane (maintained at 0°C) and the sample was collected at a rate of 1 liter per minute for 20 minutes. The impinger contents, along with isooctane washes, were placed in 50 ml screw-capped vials and delivered to the laboratory for workup.

In the laboratory the isooctane layer was transferred to a conical centrifuge tube and extracted by shaking for 15 minutes with 10 ml of hexane/methylene chloride, 70/30. The organic extract was then combined in a centrifuge tube and concentrated to dryness on a vortex evaporator at 30°C. The residue was dissolved in 5-25 ml of methanol and analyzed by HPLC with UV detection at 370 nm. The amount of each aldehyde was determined from response factors for pure DNPH derivatives. A Zorbax ODS (4.6 x 25 cm) column and 80/20 methanol/water mobile phase were used for the HPLC separation. A 25 ml extract final volume was employed for the engine idle experiments whereas a 5 ml final volume was employed for the 30 percent and 80 percent thrust experiments. The instrument was calibrated daily by injecting a standard containing 2 mg/l of each DNPH derivative of interest.

Because of the large number of aldehyde analyses to be performed during the smog chamber studies, a recently reported (Reference 9) simplified DNPH procedure was used for Task 4 (smog chamber) analyses. This procedure used an impinger solution consisting of 250 mg of 2,4-dinitrophenylhydrazine and 0.2 ml of 98 percent sulfuric acid dissolved in 1 liter of acetonitrile (ACCN). This reagent was prepared within 72 hours of sampling and was stored in a sealed 1-gallon metal can containing a layer of charcoal. The collected samples (for both

DNPH procedures) were also placed in a charcoal-containing sealed can until analyzed.

A 10 ml volume of the ACCN/DNPH reagent was used in the Task 4 studies. Samples were collected from the smog chamber at 1 liter/minute for 15-20 minutes. The impinger contents were transferred to a 10 ml graduated cylinder and the impinger rinsed with 1-2 ml of ACCN, which was then delivered into the graduated cylinder. The final volume was adjusted to 10 ml with ACCN and the sample was placed in a 20-ml glass vial having a Teflon[®]-lined screw cap. The vial was labeled, sealed with Teflon[®] tape, and placed in a charcoal-containing metal can until analyzed.

To compare the two DNPH procedures, ACCN/DNPH samples were collected for some of the engine emission tests (primarily for the CFM-56 engine). During emissions testing, two impingers, each containing 10 ml of the ACCN/DNPH reagent, were placed in series in an ice bath (because of the elevated temperature of the exhaust stream) and samples were collected for 10-20 minutes at 1 liter/minute. The contents of both impingers were placed in a 40 ml screw capped glass vial having a Teflon[®]-lined screw cap. Each impinger was rinsed with 1-2 ml of ACCN which was added to the vial. The vials were sealed with Teflon[®] tape, placed in a sealed metal can and sent to the laboratory for analysis. The sample volume was adjusted to 25 ml in the laboratory prior to HPLC analysis.

The ACCN/DNPH samples were analyzed by HPLC, as described above, for the aqueous DNPH samples. In addition, the samples were analyzed for dicarbonyl compounds (glyoxal, biacetyl, and methyl glyoxal) by a modified procedure (Reference 9). This procedure involved heating the sealed vial at 65-70°C for 1 hour, using a aluminum heating block, evaporating the sample to dryness, using a stream of high purity nitrogen gas at 65-70°C, and dissolving the residue in 2 ml of acetonitrile. This solution was analyzed for glyoxal, methyl glyoxal, and biacetyl, using the same HPLC conditions as described above, except that a UV detector operating at 254 nm and a 75/25 ACCN/water mobile phase were employed.

(3) On-Line Cryogenic Trap/Gas Chromatograph. A Hewlett-Packard Model 5880 gas chromatograph with microprocessor control and integration capabilities provided on-line data collection for C₂ to C₁₀ hydrocarbons during the engine emission experiments. The sampling procedure involved the passage of a specific volume of air (usually 30 cc) through a freeze-out sample trap (15 cm long by 0.2 cm i.d. stainless steel tubing) filled with 60/80 mesh silanized glass beads. Two traps were used in this study for separate analyses of C₂ to C₅ and C₄ to C₁₀ hydrocarbons, with samples collected sequentially. Sampling was initiated by immersing each trap into a dewar of liquid argon (-186° C) and collecting a known volume of air. Injections were accomplished by transferring the collected sample from each trap through a heated (150°C) six-port valve (Carle Instruments Model 5621) and onto the analytical column. The components in each trap were then flash-evaporated into the gas chromatograph by rapidly heating a thermocouple wire which was wound around the sampling trap (a hot water dewar was used to heat the trap collecting the C₂ to C₅ organics). During normal operations the trap system was heated from liquid argon temperature to 150°C within 20 seconds. The sample line for the C₄ through C₁₀ organics was maintained at 150°C; the sample line for the C₂ to C₅ organics was unheated. The sample lines and traps were back-flushed with zero-grade N₂ after each test run.

The GC was equipped with two flame-ionization detectors. The C₂ through C₅ hydrocarbons were resolved with a 6-meter by 0.2-centimeter i.d. column packed with phenylisocyanate on 80/100-mesh Porasil[®] Q. The column was housed in an oven external to the GC. Isothermal operation at 45°C provided adequate resolution of these species. A 50-meter OV-1 wide-bore fused-silica column (Hewlett-Packard) was used to separate the C₄ through C₁₀ organics. Optimum results in component resolution were achieved by temperature programming from -50° to 150°C at 8 degrees/minute. This two-column analytical approach was necessary to adequately resolve the major C₂ to C₁₀ organic species. The overlap in peak detection capabilities (C₄ through C₅ hydrocarbons), when using this two-column approach, provided a good internal check of the system.

Calibration of the gas chromatographic systems was accomplished by injecting an external standard mixture into each GC. A

ppbC response was determined and the value obtained was assigned to all identified and unidentified compounds (i.e., 1 ppbC propane responds the same as 1 ppbC hexane, etc.). The standard mixtures are cross-checked with several NBS propane and benzene in air standards.

(4) Canister Samples. Specially passivated aluminum cylinders were used to collect integrated can samples. Canisters were initially purged with sample air for 5 minutes and then filled to 15 psig. The canisters were returned to the Battelle laboratory for methane and carbon monoxide determination, using a Beckman 6800 GC. A portion of each sample was also analyzed by gas chromatography/mass spectrometry procedures. Cryogenic trapping and GC conditions identical to the field studies were employed during the GC/MS analyses. Analyses were carried out with a Hewlett-Packard 5700 GC interfaced to an ExtraNuclear SpectrEL mass spectrometer operating with an INCOS data system. The GC/MS analyses were used to verify the peak identities assigned to the exhaust components with the on-line field GC/FID system.

(5) Total Hydrocarbon Analyzer. A Beckman 402 total hydrocarbon analyzer (flame ionization detection), containing a heated (150°C) Teflon[®] sampling line and stainless steel analysis zone, was used for measuring the total hydrocarbons. Daily span (125 ppmC and 9.0 ppmC propane) and zero checks were performed. Multipoint calibrations (5-500 ppmC, propane) were completed prior to the field study.

c. Emissions Test Sequence

Emissions testing was carried out as follows. Several hours prior to starting the test engine, the sampling apparatus was positioned, as shown in Figure 5, and heated to 150°C. The purge air line was opened and the rake was back-flushed to prevent unburnt fuel from entering the sampling system during engine startup. Once a successful engine start had been accomplished, the purge air valve was closed, the inlet and outlet ball valves to the pump were opened and the pump was turned on. Total flow to the two manifolds was 2 ft³/min. During chamber-filling operations, 1.5 cfm was diverted to the smog chamber by adjusting the two valves at the pump exit. The remaining flow (~0.5 cfm) passed

only through the Battelle manifold (GE's manifold was closed). This excess flow provided adequate sample for the total hydrocarbon analyzer on-line at the manifold. Once a stable THC reading was obtained (usually within 10 minutes), chamber filling was initiated as described in Section III.B.3. After the chamber loading was completed, the chamber line was closed and flow was directed to the two sampling manifolds in preparation for exhaust sampling.

Each test run required 35 minutes to complete. Three sequential test runs were performed at each engine set point (idle, 30 percent, 80 percent). The sampling period of each method during a test run is shown in Table 2. The XAD-2 sampling method was operational throughout the sampling period, as were the continuous monitoring analyzers. The sampling duration of the remaining methods was less than 35 minutes.

A 1-gallon fuel sample was collected at the beginning and end of each test. A portion of each fuel sample was returned to the Battelle laboratory and analyzed by GC/FID. The JP-5 and JP-8 fuel samples were analyzed in the same fashion as described previously for the XAD-2 samples. JP-4 fuel samples were analyzed after injecting measured amounts of fuel into a heated 2-liter flask. A known volume of air was removed from the flask and analyzed with the cryogenic GC system described earlier.

Fuel samples were also shipped to the Fuels Analysis Laboratory at Wright-Patterson AFB for ASTM characterization tests. These standard procedures include the following:

- Simulated distillation (ASTM D2887)
- Hydrocarbon type analysis (ASTM D-2789-71)
- Average carbon number (ASTM D-2887)
- Density at 30°, 32°, 70° and 100°F
- Freezing point (ASTM D2386)
- Smoke point (ASTM D1322)
- Viscosity (ASTM D445) at -30°, 32°, 70° and 100°F
- Total sulphur, weight percent (ASTM D1266)
- Aromatics, volume percent (ASTM D319)

TABLE 2. SAMPLING PERIOD OF EACH METHOD DURING A TEST RUN

Method	Sampling Rate, μpm	Sampling Duration, min	Total Sample Volume, Liters
<u>Battelle</u>			
XAD-2	28	35	980
Cryogenic Trapping	0.03	1	0.03
DNPH/Impingers	1	10-20	10-20
Canister/Pump	15	\sim 5	(a)
THC Analyzer	← Continuous →		
<u>General Electric</u>			
THC Analyzer			
NO/NO _x Analyzer			
CO Analyzer			
CO ₂ Analyzer			

^aCanisters (\sim 3 liters) were filled to 15 psig after purging for \sim 5 minutes.

- Olefins, volume percent (ASTM D1319)
- Distillation (ASTM D86)
- Hydrogen, weight percent (ASTM D3701).

d. Emission Test Schedule

A schedule of the engine emissions experiments is shown in Table 3. The TF-39 emissions experiments were completed within a 3-day sampling period beginning July 20, 1983, and ending July 22, 1983. Seventeen test runs were completed during this period. The CFM-56 experiments were initiated on October 19, 1983 and ended on November 3, 1983. During the 3-week sampling period, 18 test runs were carried out.

B. TASK 4 PHOTOCHEMICAL REACTIVITY

The photochemistry experiments used two outdoor smog chambers, an exhaust transfer system, and a mobile analytical facility. The design and operation of these facilities are described below.

1. Photochemical Chamber Characteristics

Two chambers were employed for the photochemistry experiments. One chamber was loaded with engine exhaust and the other with a reference hydrocarbon/NO_x/CO mixture. The two chambers were constructed onsite at the engine test facility in Peebles, OH. A modified A-frame design was used. A picture of the chambers onsite during the CFM-56 experiments is included in Figure 7. Each chamber is built on a separate wooden platform with heavy-duty metal base and axles, inflatable tires and trailer hitch. The floor dimensions are 3.7 meters by 2.0 meters. The wooden floor is covered with reflective aluminum foil and then Teflon[®]. At the apex, each chamber is 3.8 cm wide. The Teflon[®] sidewalls crop 1.88 meters in an "A" shape, then 0.29 meters vertically to the floor. The calculated volume of each chamber is 8.5 m³. The surface area is approximately 28 m², for a surface to volume ratio of 3.3 m⁻¹. The chambers are supplied with ultrahigh-purity air via an Aadco clean air generator. Each chamber has an independent stirring fan, and several stainless steel inlets and sampling tubes which extend into the chamber through the floor. One 5 cm diameter stainless steel sampling tube was

TABLE 3. SCHEDULE OF ENGINE EMISSIONS EXPERIMENTS

Engine	Date	Test Run No.	Power	Fuel
TF-39	7/20/83	1, 2	Idle	JP-4
	7/20/83	3, 4, 5	30%	JP-5
	7/20/83	6, 7, 8	Idle	JP-5
	7/21/83	9, 10, 11	Idle	JP-4
	7/21/83	12, 13, 14	80%	JP-5
	7/22/83	15, 16, 17	Idle	JP-8
CFM-56	10/19/83	1, 2, 3	Idle	JP-5
	10/19/83	4, 5, 6	30%	JP-5
	10/19/83	7, 8, 9	80%	JP-5
	10/20/83	10, 11, 12	Idle	JP-4
	10/20/83	13, 14, 15	Idle	JP-8
	11/3/83	16, 17, 18	Idle	JP-5

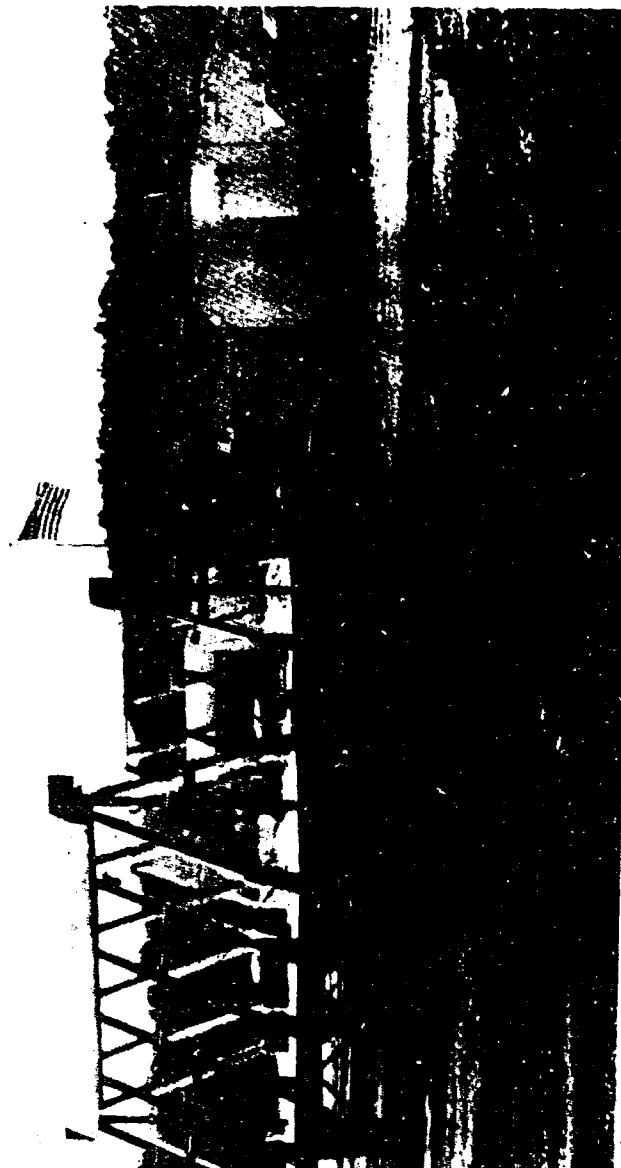


Figure 7. Photochemical Chambers During CFM-56 Engine Experiments

used as a shield for the temperature-measuring thermocouple, and also for sampling with an integrating nephelometer at the conclusion of each experiment. This tube also served as an exhaust port during chamber purging. A 1.3 cm diameter stainless steel tube was used for the majority of the sampling requirements, and was connected to the sampling manifold in the mobile laboratory via heated Teflon[®] tubing (1.3 cm dia.). Sampling for carbonyl compounds was performed at the side of each chamber, using a 0.64 cm diameter Teflon[®] tube connected to a 0.64 cm diameter stainless steel tube which extended into the chamber through the floor. The chambers were connected to the sampling manifold in the mobile laboratory by heated 1.3 cm diameter Teflon[®] tubing. The sampling tube from each chamber was connected to a large-bore, computer-actuated stainless steel valve. A single heat-traced Teflon[®] line connected the valves to the sampling manifold. An Apple II computer sequentially actuated the valves to sample each chamber for 5 minutes, then ambient air for 5 minutes. The first 2 minutes of each 5-minute sampling period were used to purge the sampling lines and manifold. The computer then acquired data for 3 minutes, converted the data to the proper units and calculated the average for the 3-minute period.

2. Analytical Methods

The variables measured during the chamber experiments are listed in Table 4. The instruments were housed in an air-conditioned mobile laboratory located alongside of the chambers. A heated Teflon[®] sample line transported the sample air to the mobile laboratory, where it passed through a Pyrex[®] moisture drop-out jar and into a Pyrex[®] manifold. A Metal Bellows pump (MB41) connected to the rear of the manifold was used to draw sample air from the chambers through the manifold. A schematic diagram of the manifold and instrument layout is shown in Figure 8. The residence time of air in the sampling system was ~3 seconds. The total hydrocarbon instrument sampled from the location where the heat-traced Teflon[®] line entered the mobile laboratory. Air was transported to the instrument through a heated Teflon[®] line and a heated pump. This arrangement bypassed the manifold and minimized loss of low volatility organics by maintaining the sample at high temperature

TABLE 4. VARIABLES MEASURED DURING THE CHAMBER EXPERIMENTS

Variable	Technique	Instrument
Ultraviolet light intensity	Radiometer	Eppley TUVR
Temperature	Thermocouple	EG&G 911
Dew-Point Temperature	Controlled Condensation	EG&G 911
Relative Humidity	Calculated from T and DPT	EG&G 911
O ₃	Chemiluminescence	Bendix 8101
NO	Chemiluminescence	CSI 1600
NO ₂	Chemiluminescence	CSI 1600
NO _x	Chemiluminescence	CSI 1600
Total Hydrocarbon	Flame Ionization	Beckman 402
CO	Nondispersive Infrared	Beckman 415
SF ₆ (tracer)	Electron Capture GC	Varian 1200
Aldehydes	DNPH Derivatization/HPLC	Altex 110A HPLC With LDC Spec- tro Monitor III UV Detector
Light-Scattering Aerosol	Integrating Nephelometry	MRI 1550

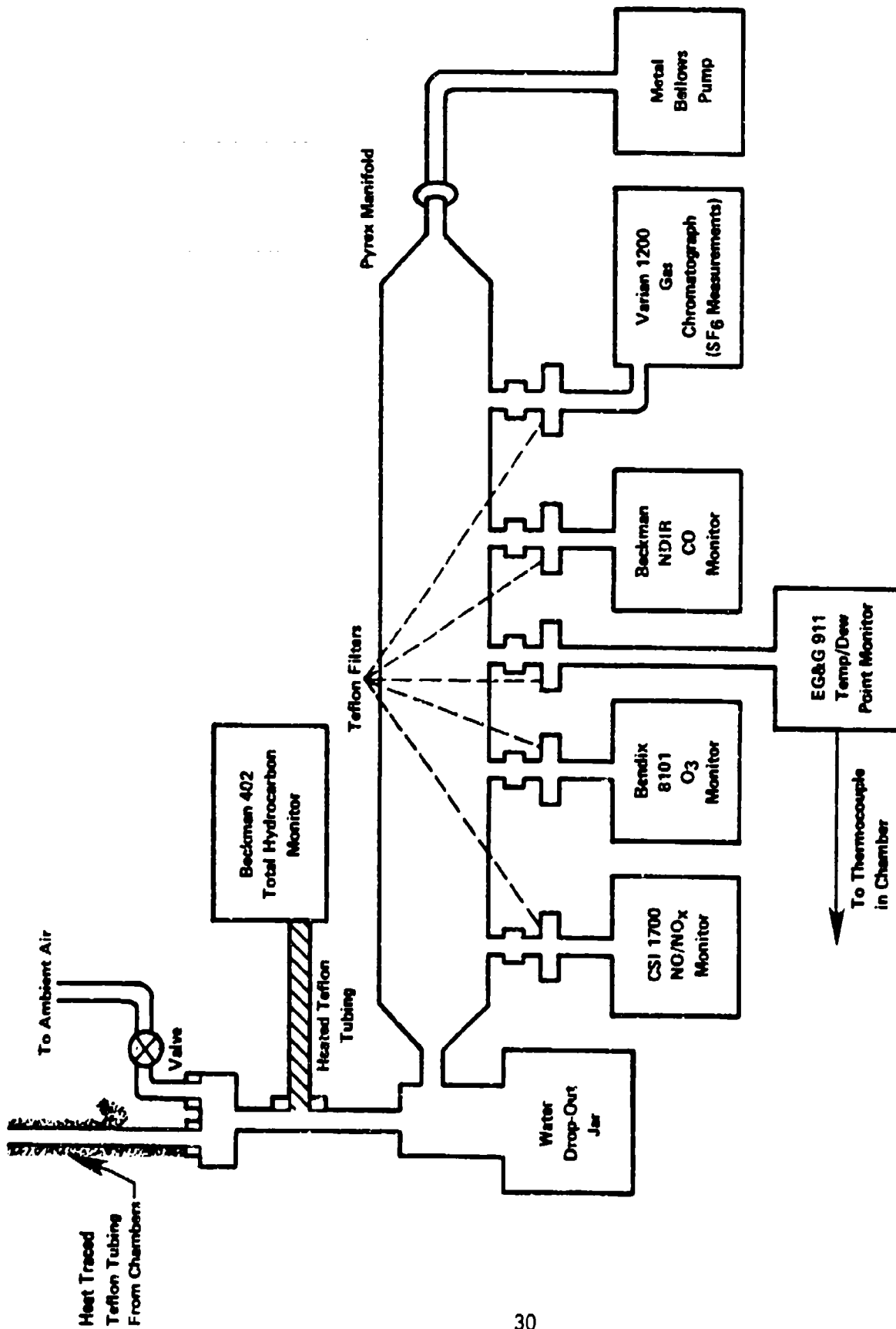


Figure 8. Schematic Diagram of Instrument Manifold for Smog Chamber Sampling

from chambers to analyzer. The other instruments were connected to the sampling manifold by Teflon[®] tubing. For protection of the instruments, the sample air passed through a 47 mm Teflon[®] filter in a Teflon[®] filter holder before entering each instrument. Data from the first 10 variables in Table 4 were acquired by an Apple II microprocessor-based data acquisition system. The results were printed every 5 minutes and stored on disc for later processing and plotting.

Sulfur hexafluoride was injected into the chambers at the start of each experiment and monitored by electron capture GC. The GC signal was plotted and the peaks integrated by a Hewlett Packard 3380 integrator.

Carbonyl compounds were determined from samples collected at 1.0 lpm for 10 minutes in acetonitrile solutions containing 250 mg/l of dinitrophenyl hydrazine (DNPH) and 200 μ l/l of H₂SO₄. The samples were analyzed by high-performance liquid chromatography. A more detailed description of the sampling and analytical procedures employed for carbonyl compounds may be found in Section III.A.3.

Light-scattering aerosol coefficient (b_{scat}) was measured at the conclusion of each experiment. The integrating nephelometer was assembled on a cart and positioned next to each chamber in turn. The nephelometer was connected to the 5 cm diameter sampling port of the chamber by a short length of 5 cm diameter flexible tubing. The data were read directly from the instrument's meter and entered in the Lab Book.

The instruments used to monitor UV intensity, temperature and dew-point temperature were calibrated at the factory. Operational checks were performed on these instruments before each experiment. The instruments used to monitor O₃, NO, NO₂, NO_x, CO and total hydrocarbons were calibrated with a CSI 1700 dynamic diluter. Ultrahigh-purity air (Matheson) was used to zero the instruments and to quantitatively dilute high concentration standards to the concentration range of interest. The standards employed for NO, CO and total hydrocarbons (propane) were referenced to primary standard cylinders obtained from the National Bureau of Standards. Ozone standards were generated in ultrazero air using the photolytic generator in the CSI 1700 calibrator. The ozone output of the CSI 1700 was calibrated against a Dasibi Model 1008 PC

photometer. These monitors were zeroed and spanned before each experiment. Multipoint calibrations were performed at the beginning and end of each engine test series, and after any interruption of more than 3 days in the experimental program.

Sulfur hexafluoride was used to monitor the chamber dilution rate. Only relative concentration data were required for this purpose, so absolute calibrations were not performed.

The HPLC instrument was calibrated for aldehyde response by injecting known concentrations of the DNPH derivatives of the individual aldehydes and generating a response curve.

The integrating nephelometer was calibrated at the start of each engine test series using fluorocarbon 12, as recommended by the manufacturer. The instrument zero and electronic span were checked before each photochemistry experiment.

3. Chamber Operation

For all of the engine exhaust irradiations, one chamber was loaded with engine exhaust and the other chamber with a reference hydrocarbon/NO_x/CO mixture. The chambers used for exhaust and reference were switched for each experiment to minimize memory effects from the previous experiment. The composition of the reference hydrocarbon mixture was 25 percent by volume propylene and 75 percent butane. This composition is known as the EKMA (Empirical Kinetic Modeling Approach) mixture, and was selected because of the wealth of experimental and modeling information available on its photochemical reactivity. The nominal loading for both reference and exhaust chambers was 10 ppmC of total hydrocarbons. The concentrations of NO, NO₂ and CO loaded into the reference chamber were held constant throughout all engine experiments, so that the results from the reference chamber could be used to account for the effects of daily variations in meteorological conditions on the exhaust chamber results. The reference chamber composition was chosen to match the hydrocarbon/CO/NO/NO₂ distribution of actual exhaust as observed during the System Demonstration experiment discussed in Section IV. The nominal composition of the reference mixture is shown below:

Nominal Concentrations in Reference Chamber

Total hydrocarbons	10 ppmC propylene/butane mix
CO	18 ppm
NO	0.08 ppm
NO ₂	0.34 ppm

During engine exhaust experiments, the reference chamber and the exhaust chamber were loaded simultaneously before sunrise. The reference chamber was loaded by injecting SF₆, the propylene/butane mixture, CO (8 percent in N₂), NO (1000 ppm in N₂) and NO₂ (1000 ppm in N₂) into the pure air inlet of the appropriate chamber. Carbon monoxide, NO and NO₂ were injected from compressed gas cylinders through a calibrated orifice. The hydrocarbon mix and SF₆ were injected by syringe through a septum in the pure air inlet line. During chamber loading, the mixing fans were operated and the pure air flow was adjusted to its maximum (150 lpm) to promote rapid mixing within the chambers.

Loading of the exhaust chamber required transporting the chamber to the engine test stand. Before the appropriate chamber was moved, background measurements were taken to ensure the cleanliness of the chamber. All sample and inlet tubes were then capped off, electrical lines were disconnected, and the chamber was rolled to the test pad. The engine was started and operated at idle until stable emissions were observed in the emissions laboratory (Section III.A.3). After a stable THC reading was obtained, a large fraction of the flow from the heated Metal Bellows exhaust sampling pump was switched to the chamber fill line. The fill line was a 50-foot by 3/8-inch i.d. section of heat-traced Teflon[®] tubing held at a constant temperature of 150°C. Thus the sample was maintained at 150°C from the sampling rake to the chamber. Flow from the pump was adjusted to provide 1.5 cfm through the chamber fill line. Flow was determined before loading the chamber with a Brooks rotameter (R-8M-25-5). Once the flow was set, the rotameter was disconnected and the sample line was connected to the chamber. The chamber was loaded by timed injection, knowing the exhaust hydrocarbon concentration and the flow rate. Throughout the chamber-filling process, the emissions measurements continued so

that the chamber loading time could be adjusted for small changes in THC emissions. After loading, the chamber was returned to the site of the photochemistry experiments (~100 m away), reconnected to the sampling system, the dilution tracer (SF_6) was injected, and the experiment was initiated. If the chamber THC concentration was significantly less than the design value of 10 ppmC, the chamber was returned to the test pad and additional exhaust injected. If the chamber was found to be overloaded, it was diluted down to 10 ppmC, using the output from the ultrapure air generator. Due to the difference in exhaust organic levels between the TF-39 and CFM-56 engines, it required 8-12 minutes to load the chamber with TF-39 exhaust and 25-40 minutes to load with CFM-56 exhaust.

The goal was to load both the exhaust and reference chambers and reconnect them to the sampling system before sunrise. While this schedule was met for most experiments, sometimes delays in engine startup delayed the chamber loading process until after sunrise. Because the chambers were loaded simultaneously, the chemical reactions were initiated at the same time, and the delayed loading should not have a significant effect on comparison of the relative reactivity of the exhaust and reference mixture.

The chamber experiments were continued until both chambers reached a peak in ozone concentration or until sundown. During irradiations, data were acquired from the continuous analyzers (THC, NO, NO_2 , NO_x , CO, UV, Temp, DPTemp, Relative Humidity) from each chamber and ambient air every 15 minutes. SF_6 tracer measurements were made on one chamber or the other every 15 minutes. Samples for carbonyl compound determination were obtained from each chamber approximately once each hour. At the conclusion of the experiment, a light-scattering aerosol (bscat) reading was obtained from each chamber.

After the final measurements were made, the large diameter exhaust ports were opened and the chambers were purged overnight with the full flow from the clean air generator. A screen was placed over the exhaust ports to prevent insects from entering the chambers during the purge cycle.

Once the chambers were loaded in the morning, flow from the clean air generator was discontinued. There was sufficient leakage of ambient air into the chamber to make up for the air withdrawn for sampling. The chamber dilution rate was determined from the SF₆ and CO concentration profiles, since both of these species are essentially inert over the reaction times involved in these experiments. The dilution rates were generally less than 0.05 hr⁻¹, although high and/or gusty winds tended to "pump" the sides of the chambers and caused higher dilution rates on a few days.

SECTION IV

RESULTS

A. TASK 3 ENGINE EXHAUST MEASUREMENTS

Emissions measurements were conducted over the May to November, 1983 time period, as indicated in Table 2. This section of the report presents the data obtained from these tests. The data are discussed in detail in Section V.

1. Engine Operation

The engine operating conditions and standard emissions data are summarized in Table 5. These data represent averages of numerous data points collected throughout each experimental test.

2. Hydrocarbon Emissions and Fuels Analysis

The major organic species identified and quantified by the various analytical techniques are listed in Tables 6, 7, and 8 for emissions, using JP-4, JP-5, and JP-8 (shale-derived) fuels, respectively. These compounds were selected for tabulation on the basis that their identities were confirmed by GC/MS or, in the case of aldehydes, by HPLC. Although numerous other aliphatic and aromatic hydrocarbons were detected by GC/MS the relative levels of such compounds were too low to allow accurate quantification.

In addition, a significant quantity (as much as 15-20 percent) of the total hydrocarbon emissions at idle were represented by a broad unresolved "hump" corresponding to a large number of aliphatic, cycloaliphatic, and aromatic structures. Although the total quantity of materials in the unresolved "hump" was accurately determined by GC/FID, further characterization was not possible. This unresolved material in each test is represented in Tables 6-8 by the difference between "resolved" and "total" species.

As shown in Tables 6-8, approximately 75 percent of the total hydrocarbon emissions were identified as specific compounds in each test.

TABLE 5. ENGINE OPERATING CONDITIONS AND STANDARD EMISSIONS DATA

TF-39 ENGINE

	7-20	7-20	7-20	7-20	7-20	7-20	7-20	7-20	7-20	7-20	7-21	7-21	7-21	7-21	7-21	7-21	7-21	7-21	7-21	7-21	7-22	7-22	7-22	7-22	7-22	7-22	7-22							
Gate (1983)	7-20	7-20	7-20	7-20	7-20	7-20	7-20	7-20	7-20	7-20	7-21	7-21	7-21	7-21	7-21	7-21	7-21	7-21	7-21	7-21	7-22	7-22	7-22	7-22	7-22	7-22	7-22	7-22						
Fuel	JP-4	JP-4	JP-5	JP-5	JP-5	JP-5	JP-5	JP-5	JP-5	JP-5	JP-4	JP-4	JP-4	JP-4	JP-5	JP-5	JP-5	JP-5	JP-5	JP-5	JP-8													
Power	Idle	Idle	30%	30%	Idle	Idle	Idle	Idle	Idle	Idle	Idle	Idle	Idle	Idle	80%	80%	80%	80%	80%	80%	Idle													
Test #	1	2	3	4	5	6	7	8	9	10	11	12	13	14	15	16	17				15	16	17											
Inlet Air Temp (°F)	75.1	75.1	81.5	84.0	87.7	89.9	90.7	--	79.0	80.4	81.9	92.2	93.3	94.0	73.6	73.5	73.5	73.6	73.6	73.6	73.6	73.5	73.5	73.6	73.5	73.5	76.3	76.3	76.3	76.3				
Atm Pressure (psia)	14.222	14.225	14.237	14.239	14.240	14.238	14.234	--	14.216	14.224	14.228	14.228	14.216	14.208	14.198	14.198	14.198	14.198	14.198	14.198	14.198	14.198	14.198	14.198	14.198	14.198	14.198	14.198	14.198	14.198	14.198	14.198		
Humidity (gr/lb)	119.9	122.6	126.3	128.6	125.1	116.5	117.5	--	122.9	123.0	125.1	136.0	129.3	129.8	98.7	103.4	105.4	105.4	105.4	105.4	105.4	105.4	105.4	105.4	105.4	105.4	105.4	105.4	105.4	105.4	105.4	105.4		
Fuel Flow (lb/hr.)	1207	1211	3793	3746	3670	1201	1201	--	1205	1196	1189	11952	11925	11882	1212	1214	1210	1210	1210	1210	1210	1210	1210	1210	1210	1210	1210	1210	1210	1210	1210	1210		
Air Flow (lb/sec.)	30.75	30.77	79.42	78.36	77.11	34.94	30.76	--	30.93	31.14	30.88	146.6	146.6	146.2	31.58	31.62	31.50	31.50	31.50	31.50	31.50	31.50	31.50	31.50	31.50	31.50	31.50	31.50	31.50	31.50	31.50	31.50		
Fuel/Air (Actual)	.00922	.00904	.01144	.01163	.01073	.01032	.01004	0.01031	0.01008	.01062	.01028	.01985	.01950	.02007	.01061	.00972	.01022	.01022	.01022	.01022	.01022	.01022	.01022	.01022	.01022	.01022	.01022	.01022	.01022	.01022	.01022	.01022	.01022	
Fuel/Air (Calc.)	.01090	.01093	.01327	.01328	.01322	.00955	.01085	--	.01082	.01067	.01070	.02265	.02260	.02258	.01066	.01066	.01067	.01067	.01067	.01067	.01067	.01067	.01067	.01067	.01067	.01067	.01067	.01067	.01067	.01067	.01067	.01067	.01067	.01067
Combustion Eff. (%)	96.47	96.29	99.75	99.75	99.74	97.06	97.04	97.21	96.78	97.03	96.91	99.96	99.97	99.96	97.13	96.85	97.01	97.01	97.01	97.01	97.01	97.01	97.01	97.01	97.01	97.01	97.01	97.01	97.01	97.01	97.01	97.01	97.01	97.01
NO _x (ppm)	17.3	16.8	61.4	60.8	60.6	19.6	19.9	20.2	17.1	17.3	17.0	313.4	325.4	319.4	19.4	18.3	18.9	18.9	18.9	18.9	18.9	18.9	18.9	18.9	18.9	18.9	18.9	18.9	18.9	18.9	18.9	18.9	18.9	
NO (ppm)	11.8	10.8	43.8	43.3	42.6	11.5	12.2	12.7	9.6	9.5	9.2	269.5	273.8	268.6	11.0	10.5	11.1	11.1	11.1	11.1	11.1	11.1	11.1	11.1	11.1	11.1	11.1	11.1	11.1	11.1	11.1	11.1	11.1	
CO (ppm)	555.3	551.5	95.5	96.2	93.0	551.9	537.0	535.5	543.0	539.6	544.6	24.2	20.4	24.4	548.5	542.9	541.1	541.1	541.1	541.1	541.1	541.1	541.1	541.1	541.1	541.1	541.1	541.1	541.1	541.1	541.1	541.1	541.1	541.1
CO ₂ (%)	1.85	1.80	2.41	2.45	2.26	2.09	2.04	2.10	2.02	2.14	2.07	4.22	4.14	4.44	2.16	1.97	2.07	2.07	2.07	2.07	2.07	2.07	2.07	2.07	2.07	2.07	2.07	2.07	2.07	2.07	2.07	2.07	2.07	2.07
THC (ppm)	401.9	421.6	15.0	14.7	14.5	359.0	354.1	335.3	404.2	388.5	390.2	4.0	4.5	4.2	361.8	369.9	368.5	368.5	368.5	368.5	368.5	368.5	368.5	368.5	368.5	368.5	368.5	368.5	368.5	368.5	368.5	368.5	368.5	368.5

TABLE 6. MAJOR ORGANIC SPECIES IN EXHAUST OF JET ENGINE OPERATING WITH JP-4 FUEL^a

	TF39 Engine			CFM56 Engine		
	Idle 7/20/83 \bar{x}	S.D.	Idle 7/21/83 \bar{x}	Idle 10/20/83 \bar{x}	S.D.	S.D.
<u>Whole Air Collection</u>	10.5	0.00	10.18	3.94	0.04	
<u>Methane</u>						
<u>Cryogenic Collection</u>						
Ethane	2.69	0.04	2.73	0.81	0.03	
Ethylene	69.35	1.42	68.92	23.68	0.77	
Propane	1.38	0.07	1.33	0.24	0.05	
Acetylene	18.32	0.23	16.71	4.29	0.73	
Propene	29.71	0.52	28.03	7.99	0.34	
1-Butene	11.21	0.62	11.11	3.05	0.32	
1,3-Butadiene	6.26	0.95	9.11	2.10	0.12	
1-Pentene	3.70	0.07	3.14	1.00	0.11	
C ₅ -ene	1.73	0.01	1.67	0.53	0.04	
n-Pentane	1.62	0.00	3.44	0.36	0.15	
C ₅ -ene	2.04	0.08	2.30	0.35	0.23	
C ₅ -ene	1.70	0.00	1.80	0.29	0.04	
2-Methylpentane	6.45	0.11	5.93	1.37	0.07	
3-Methylpentane	4.43	0.17	4.00	0.67	0.04	
1-Hexene	2.98	0.07	2.83	0.81	0.05	
n-Hexane	7.58	0.07	7.06	1.01	0.08	
Methylcyclopentane + Unknown	3.49	0.23	3.09	0.40	0.04	
Benzene	7.79	0.02	7.61	1.95	0.12	
2-Methylhexane	8.83	0.13	8.17	1.68	0.11	
3-Methylhexane	7.67	0.06	7.05	1.49	0.14	
n-Heptane	8.23	0.26	7.39	1.29	0.10	
Methylcyclohexane	3.25	0.01	2.87	0.24	0.02	

TABLE 6. MAJOR ORGANIC SPECIES IN EXHAUST OF JET ENGINE OPERATING WITH JP-4 FUEL^a (CONTINUED)

	TF39 Engine			CFM56 Engine		
	Idle 7/20/83 \bar{x}	S.D.	\bar{x}	Idle 7/21/83 \bar{x}	S.D.	Idle 10/20/83 \bar{x}
Toluene	5.36	0.40	5.01	0.48	1.26	0.09
2-Methylheptane	4.15	1.03	2.83	0.27	0.51	0.04
3-Methylheptane	4.73	0.13	4.18	0.40	0.76	0.07
n-Octane	4.46	0.21	3.74	0.33	0.53	0.05
Ethylbenzene	1.77	0.07	1.79	0.15	0.45	0.03
m,p-Xylene	5.61	0.12	5.31	0.43	1.25	0.09
Styrene	1.60	0.03	1.54	0.35	0.47	0.05
o-Xylene	2.40	0.03	2.39	0.20	0.54	0.04
n-Nonane	2.17	0.02	1.97	0.18	0.17	0.03
<u>XAD-2 Collection</u>						
C ₃ -Benzene	0.65	0.10	0.76	0.04	0.13	0.05
Phenol	0.60	0.11	0.68	0.06	0.25	0.01
C ₃ -Benzene	0.68	0.09	0.78	0.06	0.23	0.02
1-Decene	0.29	0.15	0.37	0.04	0.15	0.02
C ₃ -Benzene	3.75	0.56	4.36	0.20	0.85	0.07
n-Decane	1.95	0.16	1.89	0.13	0.27	0.03
C ₃ -Benzene	0.72	0.13	0.86	0.07	0.18	0.02
Methyl Styrene	0.46	0.09	0.47	0.03	0.12	0.008
C ₄ -Benzene	0.66	0.10	0.74	0.02	0.24	0.02
n-undecane	1.20	0.18	1.43	0.07	0.32	0.02
C ₄ -Benzene	0.40	0.07	0.46	0.02	0.12	0.05
Naphthalene	1.12	0.16	1.57	0.08	0.62	0.07
n-Dodecane	1.34	0.23	1.33	0.03	0.30	0.06
C ₁₃ -branched alkane	0.27	0.09	0.42	0.02	0.15	0.009

TABLE 6. MAJOR ORGANIC SPECIES IN EXHAUST OF JET ENGINE OPERATING WITH JP-4 FUEL^a (CONCLUDED)

	TF39 Engine			CFM56 Engine			
	Idle 7/20/83		S. D.	Idle 10/20/83		S. D.	
	\bar{x}			\bar{x}			
C ₁₄ -branched alkane	0.38	0.12		0.38	0.02	0.19	0.01
n-Tridecane	1.14	0.22		1.37	0.07	0.33	0.02
2-Methyl Naphthalene	0.45	0.10		0.57	0.03	0.25	0.02
1-Methyl Naphthalene	0.45	0.08		0.50	0.04	0.30	0.02
C ₁₄ -branched alkane	0.19	0.03		0.26	0.05	0.09	0.01
n-Tetradecane	0.68	0.10		0.85	0.05	0.22	0.01
n-Pentadecane	0.41	0.07		0.47	0.02	0.086	0.005
n-Hexadecane	0.10	0.013		0.12	0.008	0.027	0.001
n-Heptadecane	0.025	0.009		0.024	0.0008	0.004	0.0009
<u>DPMV/Impinger Collection</u>							
Formaldehyde	15.2	3.5		14.1	1.92	9.3	0.59
Acetaldehyde	9.2	1.5		7.2	0.12	2.1	0.17
Acrolein	6.7	1.1		5.6	0.21	2.4	0.08
Propenal	2.5	0.05		2.47	0.05	1.07	0.05
Acetone	1.4	0.45		1.08	0.17	0.65	0.11
Butanal/Crotonaldehyde	3.9	0.55		3.47	0.29	1.4	0.09
Benzaldehyde	1.9	0.11		1.63	0.58	0.60	0.05
Glyoxal	-	-		1.0	0.00	1.6	0.10
Methyl Glyoxal	-	-		3.7	0.00	1.1	0.30
<u>Total Identified Species</u>	312	17.4		306	36.0	91.1	6.3
<u>Total Resolved Species</u>	385	28.4		429	64.0	135	21.7
<u>Total Species</u>	410	34.4		453	67.8	141	23.1

^a \bar{x} = Average concentration of replicates in ppmc.
S. D. = Standard deviation of replicate measurements (3 replicates unless noted).

TABLE 7. MAJOR ORGANIC SPECIES IN EXHAUST OF JET ENGINE OPERATING WITH JP-5 FUEL^a

Compound (ppmC)	TF 39 Engine 30% Thrust		CFR 56 Engine 30% Thrust		CFR 56 Engine 30% Thrust	
	Date 7/20/83	S.D.	Date 7/20/83	S.D.	Date 10/19/83	S.D.
Whole Air Collection						
Methane	9.42	0.09	1.63	0.15	1.09	0.31
Cryogenic Collection						
Ethane	2.04	0.13	0.05	0.009	0.11	0.05
Ethylene	62.28	3.22	3.03	0.83	0.04	0.02
Propane	0.89	0.30	0.08	0.00	ND	ND
Acetylene	16.65	0.65	1.23	0.26	ND	ND
Propene	21.33	1.23	0.42	0.23	0.02	0.008
1-Butene	7.53	0.25	0.16	0.01	ND	ND
1,3-Butadiene	0.20	0.28	0.29	0.008	ND	ND
c-2-Butene	2.07	0.61	0.05	0.005	ND	ND
1-Pentene	2.95	0.10	0.07	0.003	ND	ND
n-Pentane	0.79	0.03	0.01	0.00	ND	ND
C ₅ -C ₆	1.81	0.38	0.05	0.005	ND	ND
2-Methyl-2-Butene	0.85	0.03	0.15	0.19	ND	ND
C ₅ -ene	1.92	0.09	0.03	0.009	ND	ND
2-Methylpentane	1.02	0.04	0.07	0.005	ND	ND
1-Hexene	3.15	0.12	0.04	0.005	ND	ND
Hexene	7.45	0.25	0.49	0.03	0.03	0.00
1-Heptene	1.97	0.09	0.02	0.00	ND	ND
n-Heptane	0.29	0.009	ND	ND	ND	ND
Toluene	2.71	0.08	0.11	0.005	0.04	0.00
Hexanal	0.55	0.05	0.01	0.00	ND	ND
1-Octene	1.25	0.07	0.01	0.005	0.03	0.019
n-Octane	0.34	0.05	0.01	0.00	0.04	0.014
Ethylbenzene	0.93	0.06	0.02	0.00	ND	ND
m-p-Tylene	1.38	0.10	0.06	0.005	ND	ND
Styrene	0.82	0.08	0.03	0.00	0.01	0.00
o-Tylene	1.16	0.10	0.04	0.00	ND	ND
1-Nonene	0.52	0.03	0.03	0.00	ND	ND
n-Nonane	ND	ND	0.10	0.01	1.63	0.32
C ₁₀ H ₁₈ S ₁₃	ND	ND	0.04	0.002	0.65	0.18
C ₁₀ H ₁₈ S ₁₄	ND	ND	0.04	0.002	0.65	0.18
Whole Air Collection						
Methane	9.42	0.09	1.63	0.15	1.09	0.31
Ethane	2.04	0.13	0.05	0.009	0.11	0.05
Ethylene	62.28	3.22	3.03	0.83	0.04	0.02
Propane	0.89	0.30	0.08	0.00	ND	ND
Acetylene	16.65	0.65	1.23	0.26	ND	ND
Propene	21.33	1.23	0.42	0.23	0.02	0.008
1-Butene	7.53	0.25	0.16	0.01	ND	ND
1,3-Butadiene	0.20	0.28	0.29	0.008	ND	ND
c-2-Butene	2.07	0.61	0.05	0.005	ND	ND
1-Pentene	2.95	0.10	0.07	0.003	ND	ND
n-Pentane	0.79	0.03	0.01	0.00	ND	ND
C ₅ -C ₆	1.81	0.38	0.05	0.005	ND	ND
2-Methyl-2-Butene	0.85	0.03	0.15	0.19	ND	ND
C ₅ -ene	1.92	0.09	0.03	0.009	ND	ND
2-Methylpentane	1.02	0.04	0.07	0.005	ND	ND
1-Hexene	3.15	0.12	0.04	0.005	ND	ND
Hexene	7.45	0.25	0.49	0.03	0.03	0.00
1-Heptene	1.97	0.09	0.02	0.00	ND	ND
n-Heptane	0.29	0.009	ND	ND	ND	ND
Toluene	2.71	0.08	0.11	0.005	0.04	0.00
Hexanal	0.55	0.05	0.01	0.00	ND	ND
1-Octene	1.25	0.07	0.01	0.005	0.03	0.019
n-Octane	0.34	0.05	0.01	0.00	0.04	0.014
Ethylbenzene	0.93	0.06	0.02	0.00	ND	ND
m-p-Tylene	1.38	0.10	0.06	0.005	ND	ND
Styrene	0.82	0.08	0.03	0.00	0.01	0.00
o-Tylene	1.16	0.10	0.04	0.00	ND	ND
1-Nonene	0.52	0.03	0.03	0.00	ND	ND
n-Nonane	ND	ND	0.10	0.01	1.63	0.32
C ₁₀ H ₁₈ S ₁₃	ND	ND	0.04	0.002	0.65	0.18
C ₁₀ H ₁₈ S ₁₄	ND	ND	0.04	0.002	0.65	0.18
Whole Air Collection						
Methane	9.42	0.09	1.63	0.15	1.09	0.31
Ethane	2.04	0.13	0.05	0.009	0.11	0.05
Ethylene	62.28	3.22	3.03	0.83	0.04	0.02
Propane	0.89	0.30	0.08	0.00	ND	ND
Acetylene	16.65	0.65	1.23	0.26	ND	ND
Propene	21.33	1.23	0.42	0.23	0.02	0.008
1-Butene	7.53	0.25	0.16	0.01	ND	ND
1,3-Butadiene	0.20	0.28	0.29	0.008	ND	ND
c-2-Butene	2.07	0.61	0.05	0.005	ND	ND
1-Pentene	2.95	0.10	0.07	0.003	ND	ND
n-Pentane	0.79	0.03	0.01	0.00	ND	ND
C ₅ -C ₆	1.81	0.38	0.05	0.005	ND	ND
2-Methyl-2-Butene	0.85	0.03	0.15	0.19	ND	ND
C ₅ -ene	1.92	0.09	0.03	0.009	ND	ND
2-Methylpentane	1.02	0.04	0.07	0.005	ND	ND
1-Hexene	3.15	0.12	0.04	0.005	ND	ND
Hexene	7.45	0.25	0.49	0.03	0.03	0.00
1-Heptene	1.97	0.09	0.02	0.00	ND	ND
n-Heptane	0.29	0.009	ND	ND	ND	ND
Toluene	2.71	0.08	0.11	0.005	0.04	0.00
Hexanal	0.55	0.05	0.01	0.00	ND	ND
1-Octene	1.25	0.07	0.01	0.005	0.03	0.019
n-Octane	0.34	0.05	0.01	0.00	0.04	0.014
Ethylbenzene	0.93	0.06	0.02	0.00	ND	ND
m-p-Tylene	1.38	0.10	0.06	0.005	ND	ND
Styrene	0.82	0.08	0.03	0.00	0.01	0.00
o-Tylene	1.16	0.10	0.04	0.00	ND	ND
1-Nonene	0.52	0.03	0.03	0.00	ND	ND
n-Nonane	ND	ND	0.10	0.01	1.63	0.32
C ₁₀ H ₁₈ S ₁₃	ND	ND	0.04	0.002	0.65	0.18
C ₁₀ H ₁₈ S ₁₄	ND	ND	0.04	0.002	0.65	0.18

TABLE 7. MAJOR ORGANIC SPECIES IN EXHAUST OF JET ENGINE OPERATING WITH JP-5 FUEL^a (CONCLUDED)

Compound	TF 39 Engine		TF 39 Engine		OTR 56 Engine		OTR 56 Engine	
	7/29/83 S.B.	7/29/83 S.B.	7/27/83 S.B.	7/27/83 S.B.	10/19/83 S.B.	11/13/83 S.B.	10/19/83 S.B.	10/19/83 S.B.
SD-2 Collection								
Propanol	0.64	0.03	0.00	0.00	0.40	0.35	0.00	0.00
1-Butene	0.57	0.63	0.00	0.00	0.42	0.15	0.07	0.00
n-Butane	1.50	0.05	0.00	0.00	0.72	0.06	0.32	0.01
C ₄ -Alkene	0.76	0.09	0.00	0.00	0.52	0.04	0.03	0.00
n-Butadiene	2.45	0.12	0.00	0.00	1.00	0.12	0.38	0.03
C ₅ -Cyclotriene	0.06	0.07	0.00	0.00	0.50	0.08	0.44	0.02
C ₅ -Alkene	0.80	0.05	0.00	0.00	0.50	0.06	0.21	0.06
1-Heptadiene	1.99	0.23	0.01	0.00	1.35	0.13	0.00	0.01
n-Heptane	2.04	0.09	0.00	0.00	1.04	0.24	0.31	0.05
C ₇ -branched alkane	0.6	0.12	0.00	0.00	0.42	0.09	0.19	0.04
C ₈ -branched alkane	6.92	0.26	0.00	0.00	0.42	0.09	0.23	0.05
n-Undecane	2.01	0.05	0.00	0.00	1.27	0.19	0.45	0.04
n-Tridecane	0.08	0.04	0.00	0.00	0.51	0.09	0.32	0.03
1-Methyl Naphthalene	0.08	0.06	0.00	0.00	0.61	0.09	0.30	0.04
C ₁₅ -branched alkane	0.49	0.03	0.00	0.00	0.40	0.16	0.20	0.02
n-Tetradecane	1.70	0.01	0.00	0.00	0.94	0.16	0.37	0.04
C ₁₆ -branched alkane	0.56	0.04	0.00	0.00	0.33	0.07	0.11	0.01
n-Pentadecane	0.92	0.02	0.00	0.00	0.39	0.06	0.16	0.00
n-Hexadecane	0.27	0.00	0.00	0.00	0.11	0.01	0.02	0.00
C ₁₆ -branched alkane	0.07	0.00	0.00	0.00	0.04	0.00	0.00	0.00
n-Heptadecane	0.07	0.00	0.00	0.00	0.02	0.00	0.00	0.00
SDM/Impinger Collection								
Formaldehyde	14.6	2.95	1.2	0.29	0.36	0.10	0.21	7.5
Acetaldehyde	7.5	0.23	0.51	0.11	0.09	0.06	0.14	2.8
Acrolein	6.17	1.08	0.35	0.07	0.03	0.02	4.2	0.05
Propenal	2.43	0.42	0.12	0.03	0.017	0.006	1.2	0.05
Acetone	0.78	0.38	0.20	0.16	0.17	0.10	0.61	0.10
Benzal/oxetane/aldehyde	3.17	0.39	0.13	0.06	0.015	0.007	1.7	0.08
Benzaldehyde	1.82	0.45	0.07	0.03	-0.01	0.00	0.99	0.02
Glyoxal	--	--	--	--	--	--	2.0	0.00
Heptyl Glyoxal	--	--	--	--	--	--	2.0	0.06
Total Identified Species	224	16.1	11.0	2.46	4.61	1.26	7.23	79.4
Total Resolved Species	294	31.3	14.8	4.50	5.71	1.30	182	15.9
Total Species	346	33.9	14.8	4.50	5.71	1.30	201	21.6

^a - Average concentration of replicates in ppm.
S.B. - Standard deviation of replicate measurements (3 replicates unless noted).

TABLE 8. MAJOR ORGANIC SPECIES IN EXHAUST OF JET ENGINE OPERATING WITH JP-8 FUEL^a

Compound	TF-39 Engine idle 7/22/83		CFM-56 Engine idle 10/20/83	
	\bar{x}	S.D.	\bar{x}	S.D.
<u>Whole Air Collection</u>				
Methane	9.25	0.00	6.31	0.10
<u>Cryogenic Collection</u>				
Ethane	2.02	0.04	1.55	0.31
Ethylene	60.22	2.40	36.79	3.09
Propane	0.78	0.26	0.65	0.19
Acetylene	15.20	0.69	9.99	1.30
Propene	19.96	0.53	10.83	0.21
1-Butene	8.27	0.59	4.39	0.21
1,3-Butadiene	9.21	0.49	3.91	0.14
c-2-Butene	1.80	0.17	1.12	0.12
1-Pentene	3.40	0.20	1.89	0.14
n-Pentane	0.68	0.04	0.38	0.008
C ₅ -ene	1.28	0.05	0.91	0.15
2-Methyl-2-Butene	0.79	0.25	0.39	0.05
C ₅ -ene	1.86	0.11	0.71	0.03
2-Methyl pentane	0.99	0.05	0.73	0.16
1-Hexene	3.02	0.60	1.72	0.08
Benzene	7.06	0.41	3.84	0.11
1-Heptene	2.40	0.15	1.20	0.03
n-Heptane	0.29	0.02	0.15	0.008
Toluene	2.61	0.15	1.44	0.07
Hexanal	0.63	0.03	0.40	0.05

TABLE 8. MAJOR ORGANIC SPECIES IN EXHAUST OF JET ENGINE OPERATING WITH JP-8 FUEL^a (CONTINUED)

Compound	TF-39 Engine		CFM-56 Engine	
	Idle 7/22/83 \bar{x}	S.D.	Idle 10/20/83 \bar{x}	S.D.
1-Octene	1.67	0.09	0.78	0.03
n-Octane	0.16	0.02	0.05	0.02
Ethylbenzene	0.86	0.06	0.44	0.02
m,p-Xylene	1.26	0.08	0.68	0.02
Styrene	1.56	0.10	0.69	0.06
o-Xylene	0.81	0.06	0.42	0.04
1-Hexene	1.36	0.09	0.59	0.04
n-Nonane	0.57	0.04	0.14	0.02
<u>IAO-2 Collection</u>				
C ₁₀ -ane	0.77	0.17	0.11	0.01
C ₁₀ -ene	1.02	0.09	0.46	0.04
C ₃ -Benzene	2.39	0.28	1.21	0.11
C ₉ -ene & Phenol	1.49	0.17	0.69	0.14
C ₉ -Diefin	1.11	0.13	0.49	0.09
n-Decane	8.04	0.68	2.85	0.16
C ₁₁ -branched alkane	1.16	0.26	0.51	0.05
C ₃ -Benzene	2.33	0.37	0.98	0.07
C ₄ -Benzene	2.19	0.33	0.94	0.18
C ₄ -Benzene	1.09	0.16	0.51	0.06
C ₄ -Benzene	1.20	0.16	0.80	0.11
n-Undecane	7.00	0.59	2.36	0.09
Naphthalene	3.01	0.17	1.95	0.24
n-Dodecane	4.12	0.22	0.90	0.08
C ₁₃ -branched alkane	1.87	0.44	0.85	0.13

TABLE 8. MAJOR ORGANIC SPECIES IN EXHAUST OF JET ENGINE OPERATING WITH JP-8 FUEL^a (CONCLUDED)

Compound (ppmC)	TF-39 Engine		CFM-56 Engine	
	Idle 7/22/83	S.D.	Idle 10/20/83	S.D.
n-Tridecane	2.72	0.31	1.07	0.08
2-Methyl Naphthalene	1.69	0.49	0.90	0.06
1-Methyl Naphthalene	1.62	0.50	0.81	0.07
C ₁₅ -branched alkane	0.49	0.12	0.38	0.05
n-Tetradecane	0.96	0.17	0.44	0.04
n-Pentadecane	0.36	0.08	0.16	0.03
n-Hexadecane	0.083	0.008	0.04	0.00
n-Heptadecane	0.017	0.004	0.009	0.002
<u>DPMH/Impinger Collection</u>				
Formaldehyde	14.2	0.92	13.3	0.25
Acetaldehyde	6.1	0.41	5.5	0.19
Acrolein	5.7	0.17	3.8	0.12
Propanal	2.3	0.05	1.3	0.08
Acetone	0.79	0.06	0.56	0.13
Butanal/Crotonaldehyde	3.1	0.22	1.9	0.05
Benzaldehyde	1.5	0.25	1.0	0.05
Glyoxal	-	-	1.7	0.45
Methyl Glyoxal	-	-	1.77	0.54
<u>Total Identified Species</u>	240	15.8	144	10.6
<u>Total Resolved Species</u>	340	42.5	195	19.6
<u>Total Species</u>	380	54.8	210	23.1

^a x̄ = Average concentration of replicates in ppmC.
 S.D. = Standard deviation of replicate measurements (3 replicates unless noted).

The corresponding analytical data for each raw fuel type are provided in Tables 9-11. The same analytical approach (i.e., quantification of the unresolved area and tabulation of specific compounds which can be accurately quantified) was employed as for the exhaust samples. The "apparent percent recovery" listed in these tables refers to the agreement between the known response for the internal standard (hexaethylbenzene) and the summation of peak areas (both resolved peaks and the unresolved "hump").

In general, apparent recoveries of 90-100 percent were achieved for the fuel analyses. Approximately 60 percent of the JP-4 fuel composition could be attributed to specific compounds, compared to only 25-30 percent for the JP-5 and JP-8 fuels. The composition of the JP-5 and JP-8 fuels is much more complex than the JP-4 fuel, as illustrated by the 40-60 percent unresolved "hump" contribution in Tables 10 and 11. Additional fuels analysis data were obtained using standardized ASTM procedures. These data are presented in Table 12.

Representative chromatograms for the various fuels and exhaust samples are provided in Figures 9-14. Features of these chromatograms are discussed more fully in Section V.

3. Aldehyde Determinations

The aldehyde composition data for the various exhaust samples are presented in Tables 6-8. Formaldehyde was the predominant aldehyde present in the exhaust for all tests, as was the case for the combustor rig data reported earlier (Reference 8). Interestingly, the use of an alternate DNPH technique (described in Section III) for selected runs allowed the detection of dicarbonyl compounds (e.g., glyoxal and methyl glyoxal). These compounds are significant from a photochemical viewpoint and their presence in combustion sources has not been previously recognized. Representative chromatograms for the aldehyde determinations are presented in Figures 15 and 16. The significance of these data is discussed more fully in Section V.

TABLE 9. PERCENT COMPOSITION OF MAJOR ORGANIC SPECIES IN JP-4 FUEL^a

Compound	TF-29 Engine		CFM-56 Engine	
	\bar{x}	S.D. (2 runs)	\bar{x}	S.D. (2 runs)
1-Pentane	0.90	0.03	0.75	0.05
i-Pentane	N.D.	N.D.	N.D.	N.D.
C ₅ -ene	N.D.	N.D.	N.D.	N.D.
n-Pentane	0.90	0.03	0.65	0.06
C ₅ -ene	N.D.	N.D.	N.D.	N.D.
C ₅ -ene	N.D.	N.D.	N.D.	N.D.
2-Methylpentane	3.05	0.05	2.50	0.15
3-Methylpentane	2.45	0.05	2.15	0.10
1-Hexane	N.D.	N.D.	N.D.	N.D.
n-Hexane	4.75	0.10	3.80	0.15
Methylcyclopentane (Unknown)	2.00	0.03	1.25	0.05
Benzene	0.40	0.00	0.20	0.03
2-Methylhexane	5.50	0.15	5.75	0.10
3-Methylhexane	4.85	0.15	5.35	0.08
n-Heptane	5.35	0.15	5.45	0.00
Methylcyclohexane	2.15	0.05	0.80	0.00
Toluene	1.05	0.05	0.85	0.00
2-Methylheptane	3.55	0.15	4.10	0.30
3-Methylheptane	3.50	0.20	3.85	0.30
n-Octane	3.40	0.15	2.95	0.25
Ethylbenzene	0.60	0.03	0.60	0.05
m & p-Xylene	2.15	0.10	2.25	0.25
Styrene	N.D.	N.D.	N.D.	N.D.
o-Xylene	0.90	0.08	0.75	0.08
n-Nonane	2.00	0.23	1.30	0.20
Benzaldehyde	N.D.	N.D.	N.D.	N.D.
C ₉ -Benzene	0.75	0.08	0.60	0.08
Phenol	N.D.	N.D.	N.D.	N.D.
C ₉ -Benzene	0.95	0.10	0.95	0.10
1-Decane	0.20	0.03	0.15	0.00
C ₁₀ /C ₉ -Benzene	2.00	0.20	1.75	0.00
n-Decane	1.85	0.15	1.35	0.08
C ₉ -Benzene	0.70	0.03	0.55	0.03
Methyl Styrene	0.95	0.03	0.65	0.03
C ₈ -Benzene	0.55	0.00	0.50	0.00
n-Undecane	1.60	0.03	2.15	0.03
C ₈ -Benzene	0.35	0.03	0.40	0.00
Naphthalene	0.45	0.00	0.45	0.00
n-Dodecane	1.35	0.00	2.25	0.08
C ₁₂ (Branched Alkane)	0.50	0.03	0.75	0.05
C ₁₄ (Branched Alkane)	0.30	0.08	0.45	0.05
n-Tridecane	1.10	0.03	1.55	0.15
2-Methyl Naphthalene	0.35	0.00	0.35	0.00
1-Methyl Naphthalene	0.30	0.00	0.30	0.00
C ₁₄ -(Branched Alkane)	0.25	0.03	0.25	0.05
n-Tetradecane	0.65	0.03	0.70	0.08
n-Pentadecane	0.25	0.00	0.20	0.00
n-Hexadecane	0.10	0.00	0.05	0.00
n-Heptadecane	0.05	0.00	N.D.	N.D.
Percent Identified	65.00	2.68	61.65	3.00
Percent Resolved	87	4.7	108	5.6
Apparent Percent Recovery	87	4.7	108	5.6

^a \bar{x} = Average percentage for replicates.
S.D. = Standard deviation of replicate measurements (three replicates unless noted).

TABLE 10. PERCENT COMPOSITION OF MAJOR ORGANIC SPECIES IN JP-5 FUEL^a

	TF-39 Engine		CFM-56 Engine	
	\bar{x}	S.D. (6 runs)	\bar{x}	S.D. (2 runs)
n-Nonane	-	-	0.63	0.03
Benzaldehyde	N.D.	N.D.	N.D.	N.D.
Phenol	N.D.	N.D.	N.D.	N.D.
1-Decene	0.065	0.05	0.11	0.01
n-Decane	1.61	0.06	1.70	0.00
C ₄ -Benzene	0.19	0.013	0.22	0.02
n-Undecane	3.88	0.16	4.80	0.30
C ₅ -Cyclohexane	0.61	0.15	0.78	0.02
C ₅ -Benzene	0.40	0.09	0.71	0.11
Naphthalene	0.085	0.081	0.30	0.06
n-Dodecane	5.39	0.31	6.80	0.50
C ₁₃ (Branched Alkane)	1.17	0.07	1.60	0.20
C ₁₄ (Branched Alkane)	1.08	0.06	1.03	0.02
n-Tridecane	5.26	0.22	6.05	0.15
2-Methyl Naphthalene	0.32	0.02	0.38	0.07
1-Methyl Naphthalene	0.18	0.03	0.18	0.04
C ₁₅ (Branched Alkane)	0.78	0.04	0.53	0.17
n-Tetradecane	3.44	0.19	3.50	0.10
C ₁₆ (Branched Alkane)	0.68	0.03	0.59	0.11
n-Pentadecane	1.61	0.08	1.10	0.36
n-Hexadecane	0.44	0.02	0.45	0.02
C ₁₆ (Branched Alkane)	0.009	0.014	N.D.	N.D.
n-Heptadecane	0.08	0.006	0.07	0.006
Percent Identified	27.2	1.69	31.5	2.30
Percent Resolved ($\geq C_{10}$)	44.2	2.07	69.0	2.2
Apparent Percent Recovery ($\geq C_{10}$)	99.8	4.11	116.5	2.5

^a \bar{x} Average percentage for replicates.
 S.D. = Standard deviation of replicate measurements
 (three replicates less noted).

TABLE 11. PERCENT COMPOSITION OF MAJOR ORGANIC SPECIES IN JP-8 FUEL^a

	TF-39 Engine		CFM-56 Engine	
	\bar{x}	S.D. (2 runs)	\bar{x}	S.D. (2 runs)
n-Nonane	-	-	0.40	0.00
C ₁₀ (Branched Alkane)	-	-	0.20	0.00
C ₁₀ (Branched Alkane)	-	-	1.25	0.05
Benzaldehyde/C ₃ Benzene	-	-	0.35	0.05
C ₉ Olefin/Phenol	0.35	0.03	0.45	0.15
C ₉ Olefin	0.34	0.015	0.35	0.15
n-Decane	8.04	0.21	7.65	0.15
C ₁₁ (Branched Alkane)	1.22	0.04	1.6	0.10
C ₃ Benzene	1.44	0.07	1.25	0.45
C ₄ Benzene	0.49	0.06	0.90	0.00
C ₄ Benzene	0.92	0.06	0.70	0.20
C ₄ Benzene	0.32	0.005	0.35	0.05
n-Undecane	8.88	0.21	8.70	0.20
Naphthalene	0.58	0.005	0.35	0.05
n-Dodecane	6.73	0.13	7.25	0.15
C ₁₃ (Branched Alkane)	1.78	0.02	2.05	0.05
n-Tridecane	3.61	0.065	3.65	0.05
2-Methyl Naphthalene	0.21	0.00	0.20	0.20
1-Methyl Naphthalene	0.16	0.005	0.10	0.10
C ₁₅ (Branched Alkane)	0.49	0.03	0.75	0.05
n-Tetradecane	1.19	0.03	1.20	0.00
n-Pentadecane	0.31	0.00	0.30	0.00
n-Hexadecane	0.049	0.004	0.10	0.00
n-Heptadecane	N.D.	N.D.	N.D.	N.D.
Percent Identified	37.1	0.99	40.1	2.2
Percent Resolved ($\geq C_{10}$)	56.8	0.40	77.8	2.0
Apparent Percent Recovery ($\geq C_{10}$)	93.4	2.05	104	1.0

^a \bar{x} = Average percentage for replicates.
 S.D. = Standard deviation of replicate measurements
 (three replicates unless noted).

TABLE 12. RESULTS FOR STANDARD FUEL ANALYSES

Parameter	Test	JP-4 Fuel			JP-5 Fuel			JP-8 Shale Fuel		
		Specification	TF-39 Fuel	CFM-56 Fuel	Specification	TF-39 Fuel	CFM-56 Fuel	Specification	TF-39 Fuel	CFM-56 Fuel
Existent Gum, mg/100ml	D381	7.0 Max	0.0	1.6	7.0 Max	0.4	4.8	7.0 Max	1.2	1.2
Aromatics, Vol. %	D1319	25 Max	14.8	14.0	25 Max	16.0	15.5	25.0 Max	21.3	22.0
Olefins, Vol. %	D1319	5 Max	1.0	1.0	5 Max	0.7	1.1	5.0 Max	1.4	1.4
Smoke Point, mm	D1322	20 Min	25	25	19 Min	21	21	19 Min	17.0	19.0
Freezing Point, °C	D2386	-58 Max	-72	-59	-46 Max	-42	-42	-50 Max	-50	-52
Mercaptan Sulfur, Mt. %	D3227	0.001 Max	0.000	0.000	0.001 Max	0.000	0.000	0.001 Max	0.000	0.000
Total Sulfur, Mt. %	D2622	0.040 Max	0.000	0.010	0.040 Max	0.00	0.00	0.3 Max	0.01	0.01
Hydrogen, Mt. %	D3343	13.6 Min	14.4	14.4	13.5 Min	13.9	13.9	13.5 Min	13.7	13.7
Distillation, °C	D86									
Initial Boiling Point		--	--	--	--	17.8	176	--	176	174
10%		--	--	--	205 Max	199	199	205 Max	184	186
20%		--	--	--	--	207	207	--	189	189
50%		--	--	--	--	222	221	--	199	199
90%		--	--	--	--	249	247	--	227	227
Endpoint		--	--	--	290 Max	268	269	300 Max	254	246
Residue		--	--	--	1.5 Max	1.0	1.0	1.5 Max	1.0	1.0
Loss		--	--	--	1.5 Max	1.0	1.0	1.5 Max	1.0	1.0
Simulated Distillation, °C	D2887									
Initial Boiling Point		--	23	26	--	37	108	--	130	146
10%		--	69	72	185 Max	178	182	186 Max	172	170
20%		145 Max	91	93	--	196	197	--	180	177
50%		185 Max	144	146	--	226	224	--	208	202
90%		250 Max	240	243	--	266	260	--	247	239
Endpoint		320 Max	293	293	320 Max	302	302	330 Max	288	283

TABLE 12. RESULTS FOR STANDARD FUEL ANALYSES (CONCLUDED)

Parameter	Test	JP-4 Fuel		JP-5		JP-8 Shale Fuel	
		Specification	Fuel	Specification	Fuel	Specification	Fuel
Hydrocarbon Type, Wt. %	D2789						
Paraffins		--	60.3	--	45.4	--	44.2
Monocycloparaffins		--	20.8	--	35.8	--	33.1
Dicycloparaffins		--	3.2	--	1.4	--	0
Total Cycloparaffins		--	24.0	--	37.2	--	33.1
Alkyl Benzenes		--	12.3	--	8.5	--	11.5
Indans and Tetralins		--	2.6	--	7.6	--	10.1
Naphthalenes		--	0.8	--	1.3	--	1.1
Specific Gravity, g/cm ³	D287						
-30°F		--	0.7970	--	0.8445	--	0.8385
32°F		--	0.7706	--	0.8204	--	0.8149
59°F		--	0.7593	--	0.8103	--	0.8036
70°F		--	0.7544	--	0.8058	--	0.7990
100°F		--	0.7411	--	0.7938	--	0.7868
Kinematic Viscosity, CS	U445						
-30°F		--	2.274	--	10.203	--	6.156
70°F		--	0.930	--	2.223	--	1.700
32°F		--	1.235	--	3.533	--	2.546
100°F		--	0.772	--	1.667	--	1.322
Average Carbon Number (50% Point)	D2887						
		--	8.7	--	12.5	--	11.4

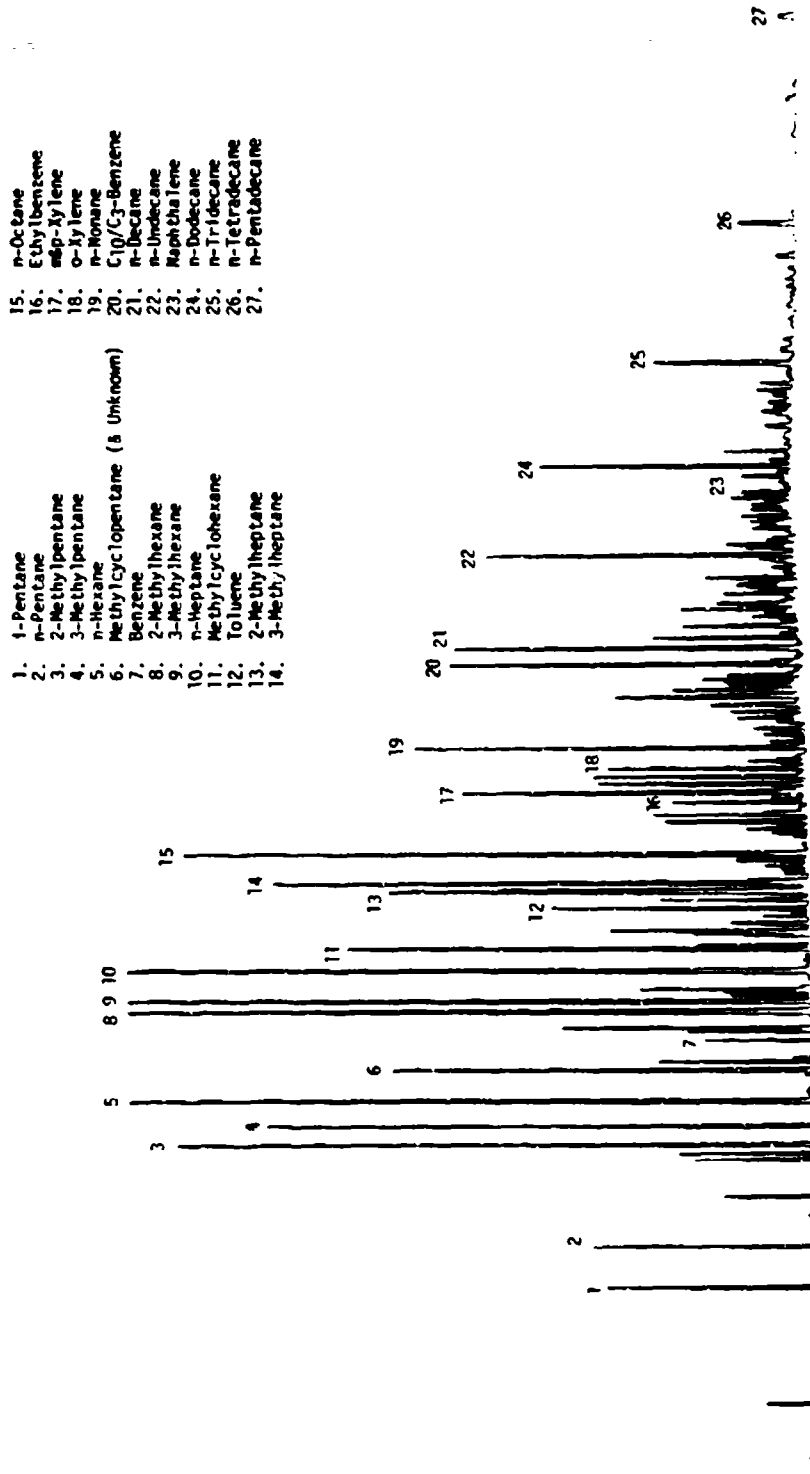


Figure 9. GC/FID Chromatogram for JP-4 Fuel

- | | |
|----------------------------------|--------------------------------|
| 1. Ethane | 23. Benzene |
| 2. Ethylene | 24. 2-Methylhexane |
| 3. Propane | 25. n-Heptane |
| 4. Acetylene | 26. Methylcyclohexane |
| 5. Propene | 27. Toluene |
| 6. Acetaldehyde | 28. 2-Methylheptane |
| 7. 1-Butene | 29. 3-Methylheptane |
| 8. 1,3-Butadiene | 30. n-Octane |
| 9. 2-Propenal (Acrolein) | 31. Ethylbenzene |
| 10. Acetone | 32. prop-1-yne |
| 11. 1-Pentene | 33. Styrene |
| 12. Cis-ene | 34. o-1,5-Diene |
| 13. n-2-Pentane | 35. n-Nonane |
| 14. Cis-ene | 36. Benzaldehyde |
| 15. Cis-ene | 37. p-1-Ethylhexane |
| 16. 2-Methyl-2-Propenal | 38. 1,2,8-Trimethylhexane |
| 17. 2-Methylpentane | 39. n-Decane |
| 18. 3-Methylpentane | 40. Methylbenzaldehyde + Ethyl |
| 19. 1-Hexene | 41. n-Dodecane |
| 20. n-Hexane | 42. Methylcyclohexane |
| 21. Methylcyclopentane + Unknown | |

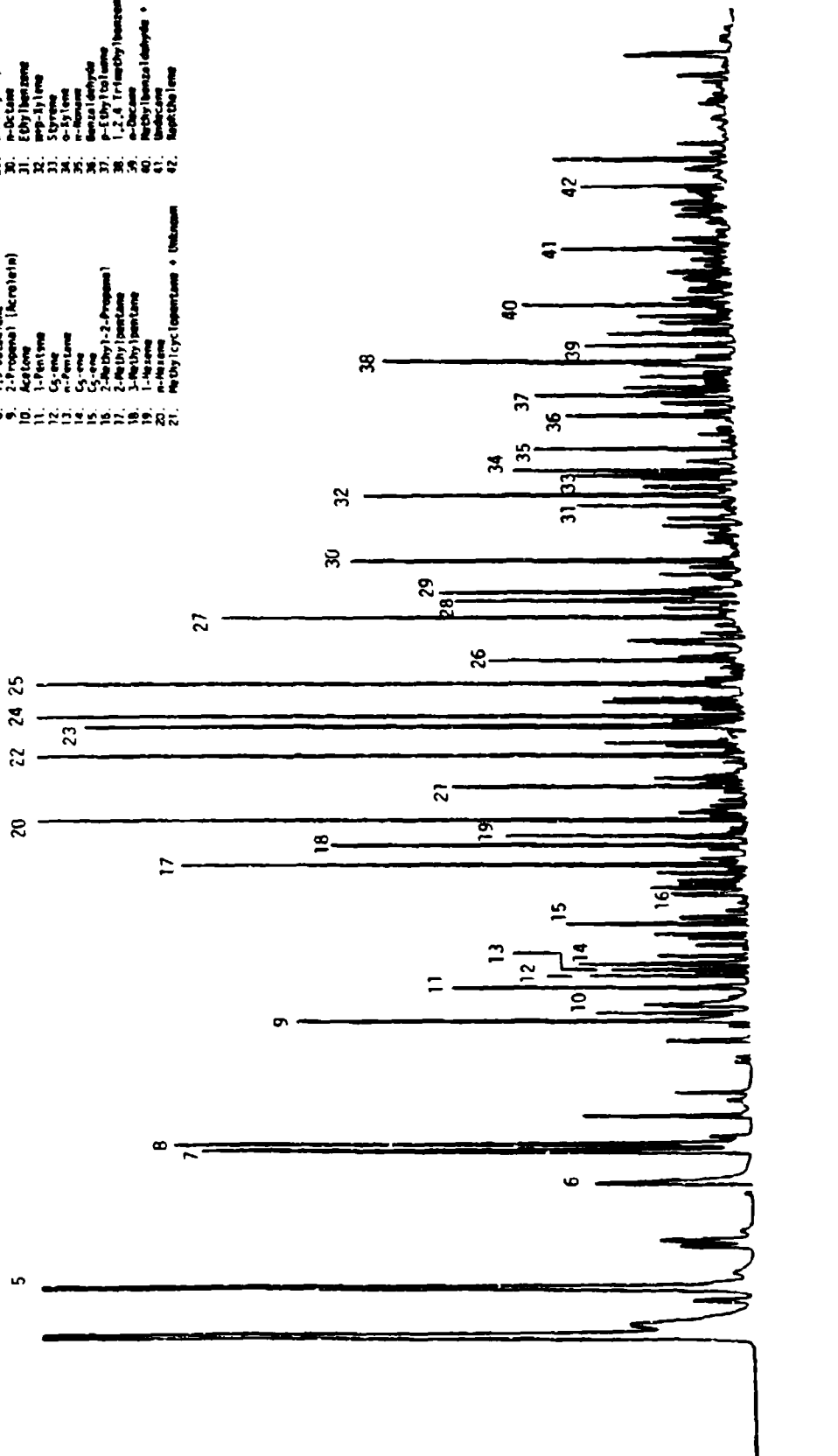


Figure 10. GC/FID Chromatogram of C2 to C11 Organics in the Exhaust of TF-39 Engine (Idle-JP-4 Fuel)

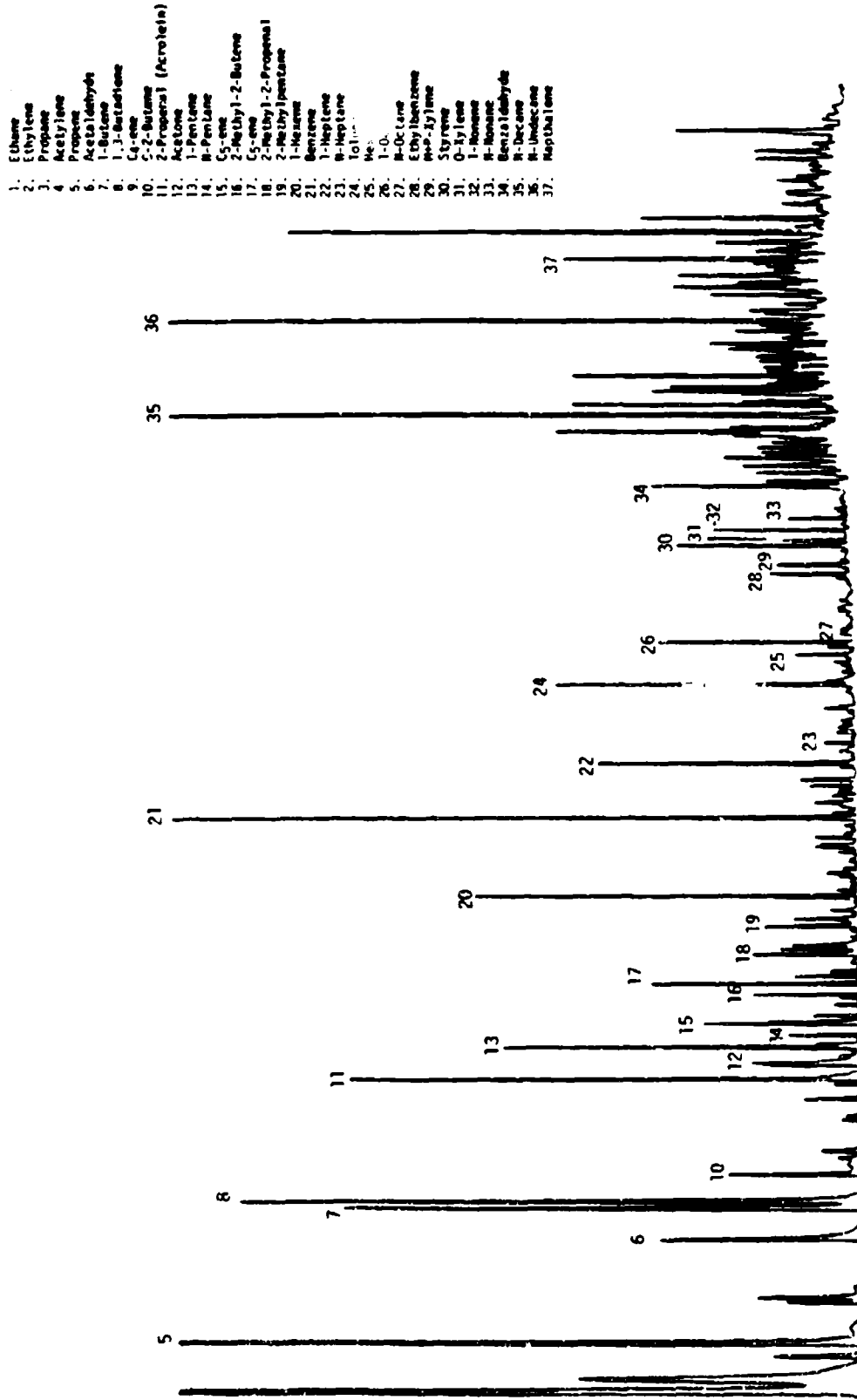


Figure 11. GC/FID Chromatogram of C2 to C11 Organics in the Exhaust of the TF-39 Engine (Idle-JP-5 Fuel)

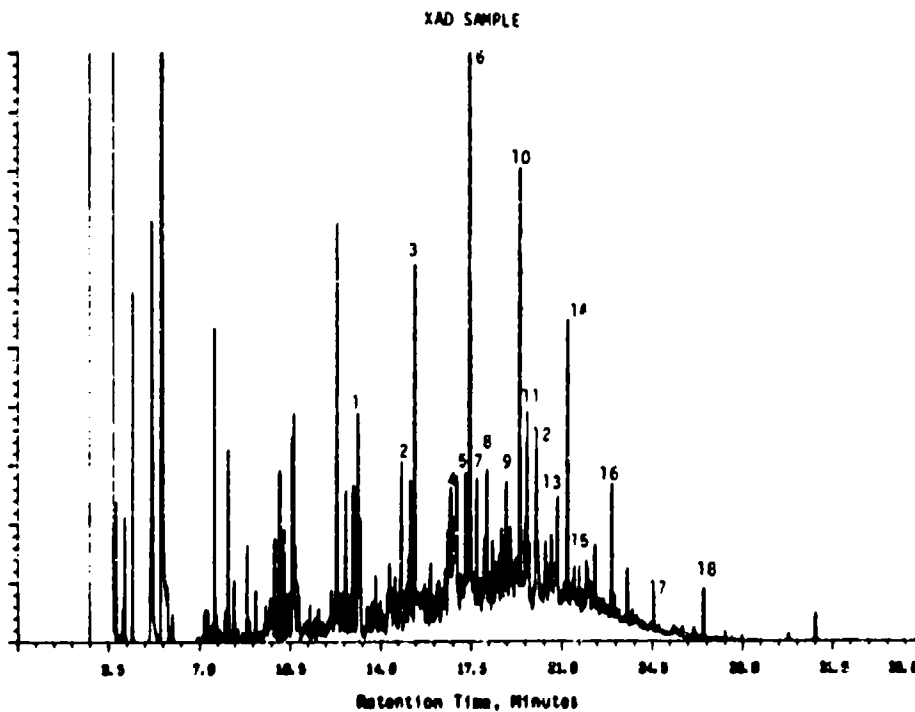
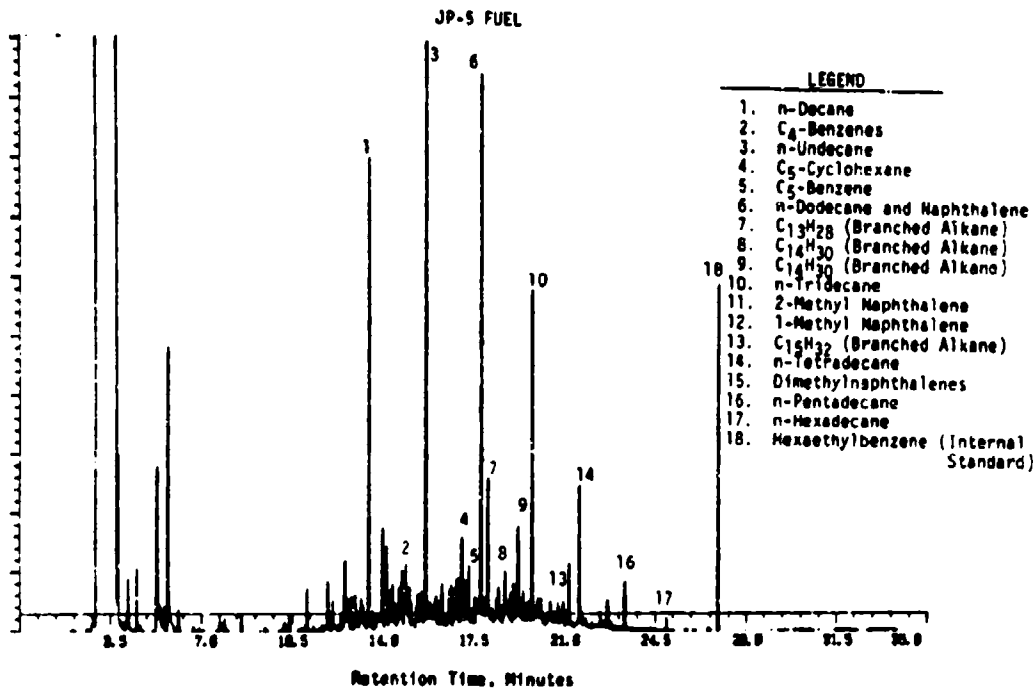


Figure 12. Chromatogram for JP-5 Fuel and XAD Sample of Exhaust from TF-39 Engine Operated on JP-5 Fuel at Idle

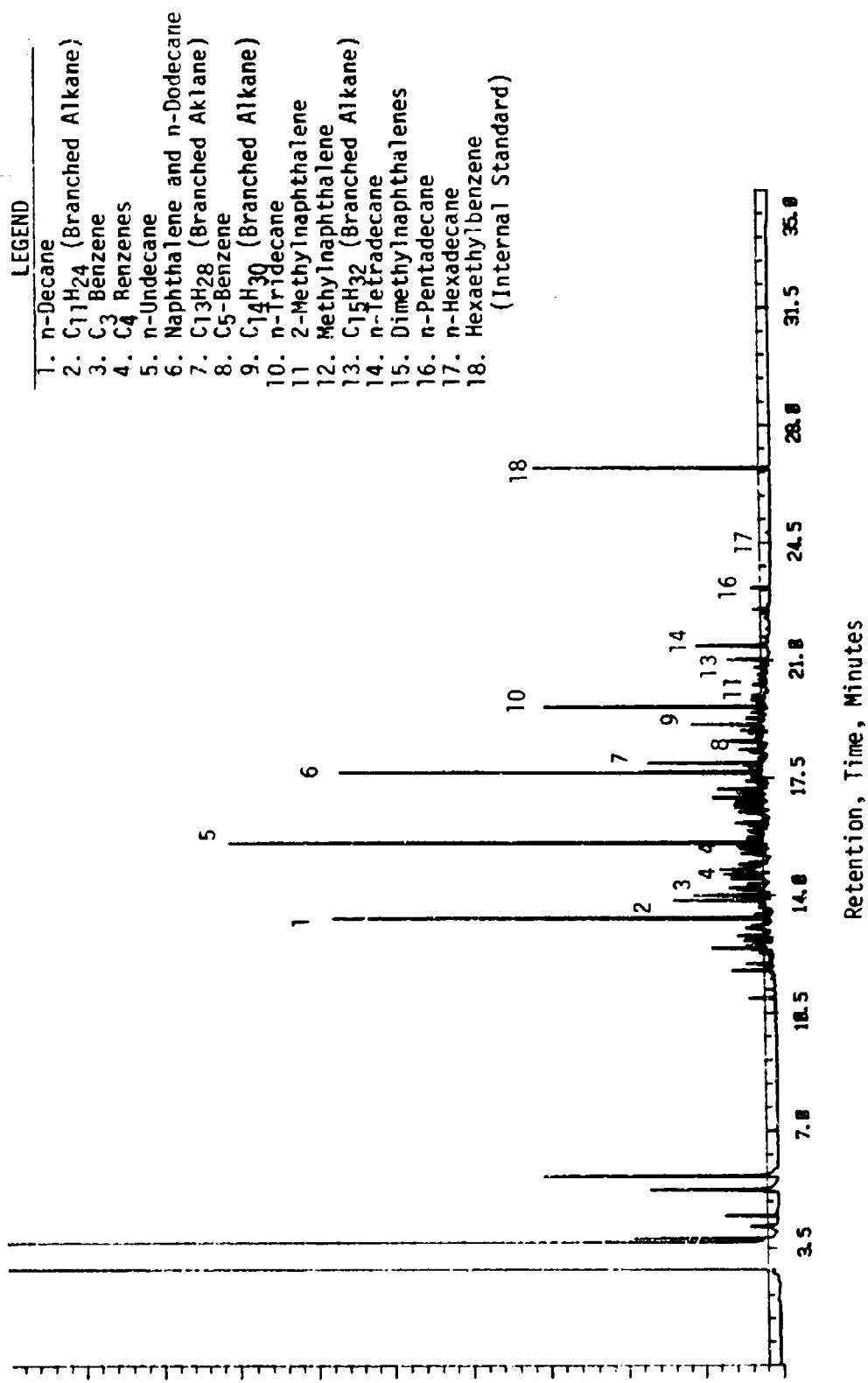


Figure 13. Chromatogram for JP-8 Shale Fuel

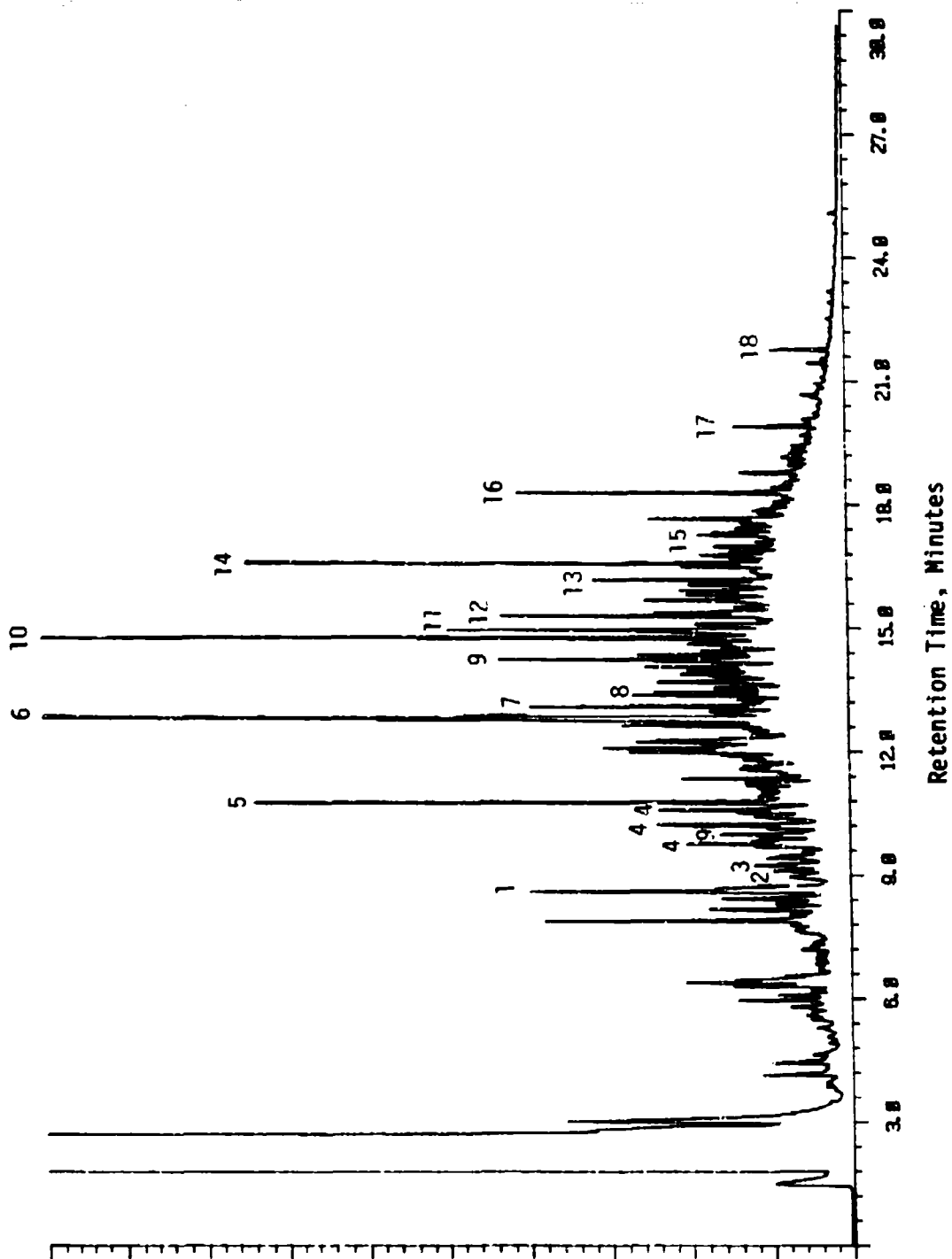


Figure 14. Chromatogram for XAD Sample of Exhaust from TF-39 Engine Operating on JP-8 Fuel at Idle (See Lengend on Figure 13)

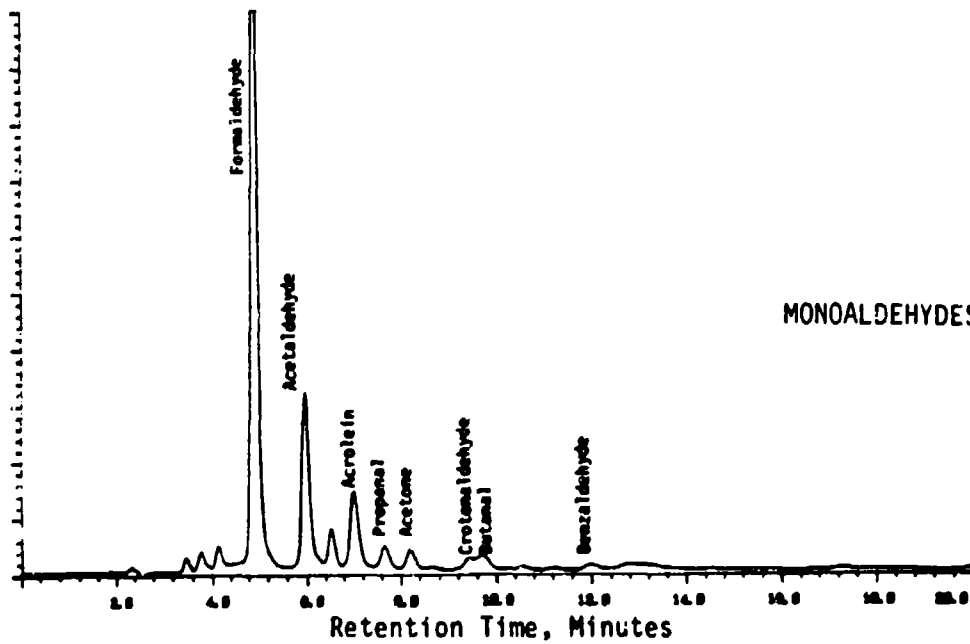
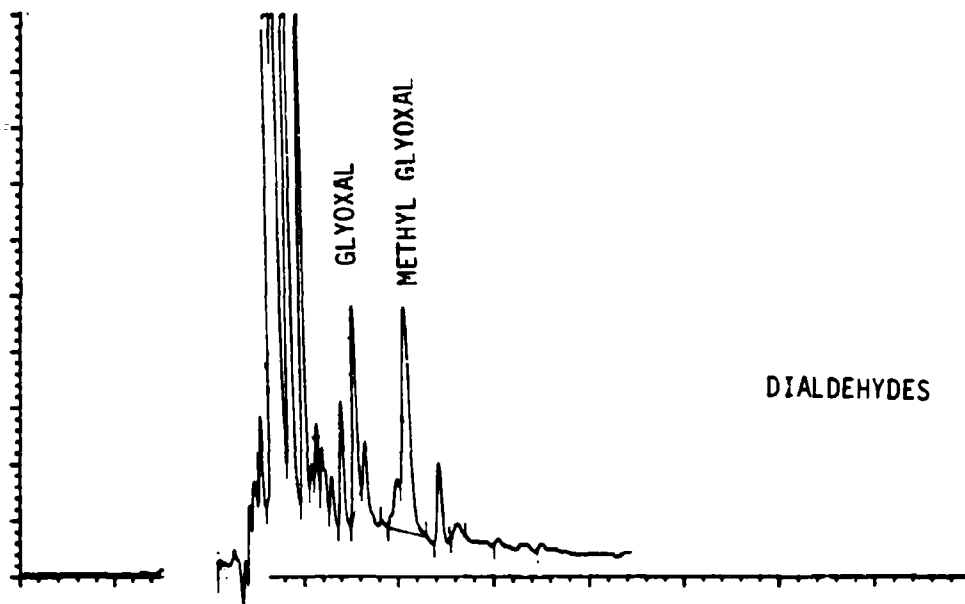


Figure 15. HPLC Chromatogram of Aldehyde Emissions from CFM-56 Engine Operating at Idle on JP-5 Fuel

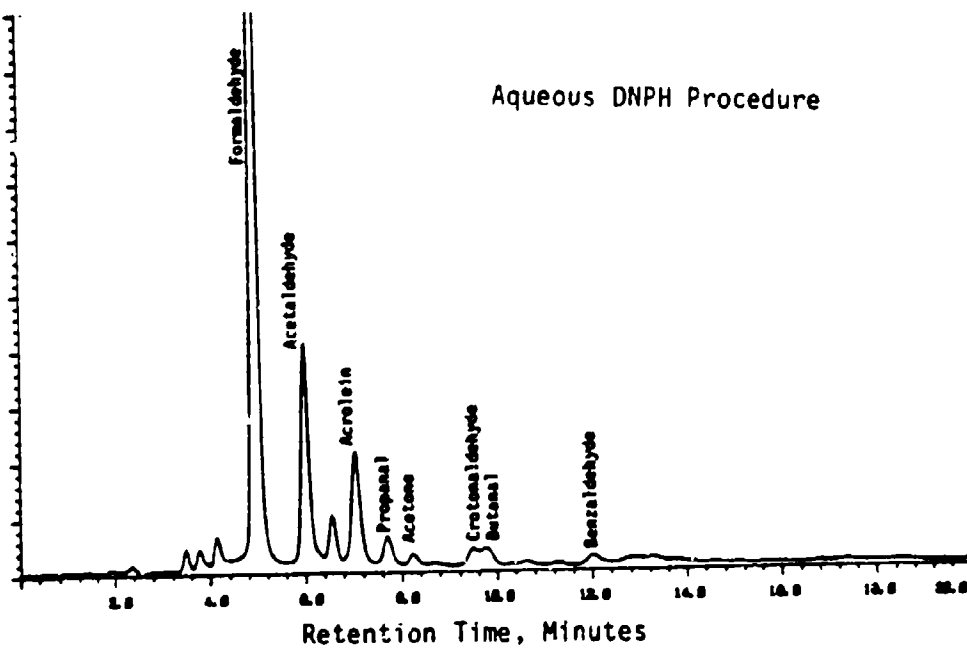
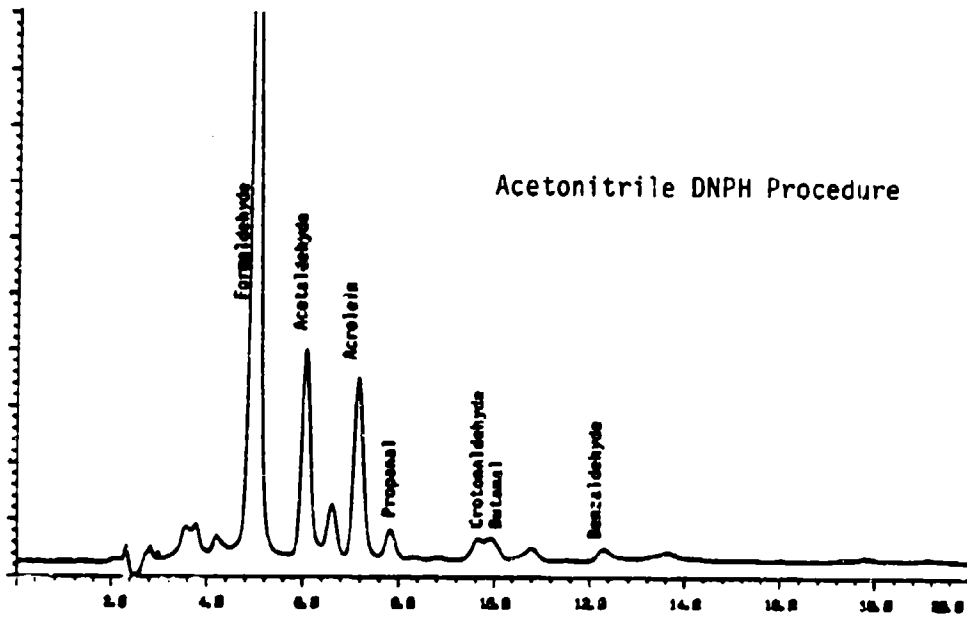


Figure 16. HPLC Chromatogram of Aldehyde Emissions from CFM-56 Engine Operating on JP-8 Shale Fuel

4. PNA Analysis

A summary of the PNA analytical data obtained for selected XAD samples is presented in Table 13. The species determined were consistent with those found earlier in the combustor rig exhaust (Reference 8). Fuel-spectrum scan GC/MS analyses of selected samples did not reveal detectable levels of any other PNA compounds.

The PNA levels found are in general agreement with those found earlier for the TF-39 combustor rig. The significance of these emission levels, compared to other mobile sources, is discussed in Section V.

B. TASK 4 PHOTOCHEMISTRY EXPERIMENTS

Experiments were conducted in the outdoor smog chambers from May through November, 1983. The experiments undertaken over this period generally fall into one of three classifications:

- Chamber characterization and validation
- TF-39 engine exhaust reactivity experiments
- CFM-56 engine exhaust reactivity experiments.

The results of these experiments are presented in this section. The results are interpreted in Section V.

1. Chamber Characterization and Validation

Before the actual engine exhaust photochemistry experiments were initiated, it was necessary to characterize certain aspects of chamber performance and verify the comparability of the two chambers. Chamber characterization and validation were undertaken between May and mid-July, 1983. The characteristics determined included leak rate, ozone decay rate, and clean-air ozone formation. Validation experiments consisted of a baseline photochemical reactivity assessment, using the reference hydrocarbon mixture, and a system demonstration employing actual engine exhaust.

a. Chamber Dilution

Chamber dilution rates were determined from the first-order decay of SF₆ and/or CO, which are essentially inert in the chamber over the time scales of these experiments. It was desirable to maintain

TABLE 13. PHA ANALYSIS DATA

	CONCENTRATION IN GIVEN SAMPLE, $\mu\text{g}/\text{m}^3$												FUEL $\mu\text{g}/\text{g}$					
	TF-39				CFR 56													
	IAO	IAO	IAO	IAO	IAO	IAO	IAO	IAO	IAO	IAO	IAO	IAO	IAO	IAO	IAO	IAO	IAO	IAO
01	09	03	012	015	010	01	016	04	015	07	013							
JP4	JP4	JP5	JP5	JP5	Blank	JP4	JP5	JP5	JP5	JP5	JP5	JP5	JP5	JP5	JP5	JP5	JP5	JP5
Idle	Idle	30% Thrust	80% Thrust	Idle	Idle	Idle	Idle	Idle	Idle	30% Thrust	80% Thrust	Idle	JP4	JP5	JP5	JP5	JP5	JP5
Naphthalene	670	470	870	26	2.1	1700	0.79	380	620	410	1.5	1.9	1040	920	2900	4600		
2-Methyl Naphthalene	290	300	680	4.8	<0.10	1960	0.06	160	330	180	<0.01	0.10	480	720	3000	2000		
1-Methyl Naphthalene	200	200	450	3.5	<0.10	1210	0.04	170	380	270	<0.01	0.03	380	600	1700	1200		
Dimethyl Naphthalene(1)	24	29	58	0.91	<0.01	Data Lost	<0.01	3.8	24	7.6	<0.01	<0.01	18	82	120	100		
"	(2)	35	40	2.5	<0.01	"	<0.01	2.1	34	14	<0.01	<0.01	18	130	190	270		
"	(3)	11	17	0.68	<0.01	"	<0.01	2.1	99	4.2	<0.01	<0.01	5.8	32	51	42		
"	(4)	5.3	7.5	0.14	<0.01	"	<0.01	1.0	3.6	1.7	<0.01	<0.01	2.3	16	9.8	9.8		
Phenanthrene	8.4	8.5	7.7	0.49	0.21	9.6	0.13	2.5	5.1	2.5	0.65	1.2	4.6	6.6	3.8	1.3		
Anthracene	1.2	1.7	0.94	0.035	0.050	1.2	0.01	0.10	0.56	0.26	0.020	0.057	0.54	1.1	0.13	0.02		
Fluoranthene	2.7	3.6	1.1	0.17	0.10	4.2	0.05	0.72	1.3	0.58	0.17	0.20	1.6	1.1	0.93	0.37		
Pyrene	3.4	5.9	1.1	0.17	0.008	4.8	0.03	0.69	1.6	1.0	0.14	0.16	2.0	1.8	0.88	0.31		
Benzo(a)Anthracene	0.38	0.42	0.006	0.074	0.10	0.10	<0.01	0.25	0.10	0.098	0.10	0.055	0.16	0.20	1.3	0.15		
Chrysene	0.33	0.42	0.019	0.043	0.010	0.010	0.01	0.039	0.10	0.043	<0.01	<0.010	0.17	0.43	<0.10	<0.10		
Benzo(e)Pyrene	0.37	0.38	0.056	0.20	0.11	0.11	<0.010	0.35	0.11	0.15	0.17	0.090	2.19	0.43	0.29	0.42		
Benzo(a)Pyrene	0.20	0.25	0.042	0.12	0.066	0.065	0.020	0.23	0.058	0.088	0.069	0.043	0.11	0.25	<0.10	<0.10		
Perylene	0.03	<0.010	<0.010	<0.010	<0.010	<0.010	<0.010	<0.010	<0.010	<0.010	<0.010	<0.010	<0.010	<0.10	<0.10	<0.10		
Coronene	0.008	0.018	<0.010	<0.010	<0.010	<0.010	<0.010	<0.005	<0.010	<0.010	<0.010	<0.010	<0.010	<0.10	<0.10	<0.10		

^a C₇-Naphthalenes calculated at four species groups. See text.

the total dilution from sampling and leakage during an experiment at no more than 40 percent of the chamber contents. Thus the allowable hourly dilution rate would be 0.10 hr^{-1} for a 5-hour experiment, 0.07 hr^{-1} for a 7-hour run, and 0.05 hr^{-1} for a run lasting 10 hours. Since nearly all of the engine exhaust experiments reached maximum O_3 levels in 4-7 hours, a dilution rate of 0.07 hr^{-1} was the goal. The sampling requirements for the monitoring instruments contributed 0.021 hr^{-1} to the total dilution rate, so that leakage had to be held to 0.05 hr^{-1} or less. The chamber leak rate depends on windspeed and wind gustiness, and on the diurnal temperature variation. Winds "pump" the chamber walls, causing greater air leakage. Increasing ambient temperature during the day results in strong increases in chamber temperature, due to the "green house effect." Increasing chamber temperature causes expansion of the chamber air, with little leakage. However, as the temperature decreases later in the day, the chamber volume contracts and there is a tendency to draw ambient air into the chamber, thus increasing the leakage.

Chamber dilution rates were measured several times before beginning each of the major series of engine exhaust experiments. The results of these dilution rate characterization studies are shown in Table 14. The rates in the May-July period were low. Dilution on September 20 and 21 was considerably higher, no doubt due to the occurrence of strong gusty winds on these days. The results prior to the TF-39 experiments show that the chambers were well within the hourly dilution rate criterion of 0.07 hr^{-1} . The dilution rates were somewhat higher before the CFM-56 experiments, at least in part because of the windy conditions experienced on the days of dilution rate measurement. Actual dilution rates were measured during each engine exhaust experiment, and these data will be discussed during the interpretation of the exhaust experiments.

b. Ozone Decay Rate

One means of characterizing the condition of a photochemical reaction chamber is to determine the rate of ozone decay in clean air in the dark. Ozone loss is primarily by reaction with the

TABLE 14. CHAMBER DILUTION RATES DURING CHARACTERIZATION EXPERIMENTS (in hr⁻¹)

Date	Chamber A	Chamber B
Before TF-39 Experiments		
5-17-83	0.057	0.068
6-9-83	0.021	0.029
7-13-83	0.026	0.032
7-18-83	0.048	0.049
Before CFM-56 Experiments		
9-20-83	0.090	0.083
9-21-83	0.109	0.097

chamber walls. A low and stable loss rate usually indicates a well-conditioned chamber. A high or increasing rate suggests some problems with increasing activity of the chamber surfaces.

The ozone decay rate is determined from the total first order O₃ decay in the dark of low (<1 ppm) O₃ concentrations, less the measured dilution rate. Ozone decay rates were measured shortly after the chambers were assembled and just before each major engine test sequence. The results are given in Table 15. Both chambers behave similarly, increasing confidence in their comparability. The ozone decay rate was highest shortly after the chambers were assembled, before the surfaces had been conditioned. Between May 4 and July 13, the chambers were conditioned overnight with several ppm O₃, and several conditioning runs, including propylene/butane/NO_x and engine exhaust irradiations were completed. The tabulated data show that the O₃ decay rate was low and stable once the chambers were conditioned, and that the rate was nearly identical for the two chambers. For comparison, the O₃ decay rate in our 17.3 m³ Teflon[®]-lined indoor chamber is typically 0.036 hr⁻¹ and the decay rate in the 5.8 m³ Teflon[®]-coated SAPRC chamber is 0.029 hr⁻¹ (Reference 10). Decay rates measured in much larger outdoor Teflon[®] chambers of 45 to 60 m³ volume ranged from 0.0029 to 0.016 hr⁻¹ (Reference 11). After conditioning, the O₃ decay rates in the outdoor chambers used for this study were lower than the rates in either of the cited indoor chambers, and higher than the rates in the much larger outdoor chambers, as expected based on the difference in surface-to-volume ratio. The O₃ decay rate data suggest that the condition of the chamber walls was satisfactory for these experiments.

c. Clean Air Ozone Formation

One means of ascertaining the cleanliness of the smog chambers and clean air supply is irradiation of clean air while monitoring O₃ formation. Two clean air irradiations were carried out before the start of the TF-39 experiments, but after conditioning and baseline reactivity experiments with the reference hydrocarbon/NO_x/CO mixture. The ozone formation rate in these experiments corresponded to 0.008 to 0.013 ppm hr⁻¹ for both chambers. In comparison with the peak

TABLE 15. OZONE DECAY RATE IN OUTDOOR
SMOG CHAMBERS (CORRECTED FOR DILUTION)

Date	hr^{-1}		Comment
	Chamber A	Chamber B	
May 4, 1983	0.080	0.080	Prior to conditioning
July 13, 1983	0.018	0.018	After conditioning/ before TF-39
September 20, 1983	0.021	0.022	Before CFM-56

O₃ concentrations observed during the actual engine exhaust irradiations (frequently 0.6-0.8 ppm), the rate of O₃ formation in the clean chamber is small.

Experiments performed before the start of the CFM-56 series and in the middle of that series showed even lower rates of O₃ formation from clean air irradiations. Experiments conducted on September 22 and October 18, 1983 showed afternoon O₃ formation rates in the range 0.001 to 0.006 ppm hr⁻¹. These also are quite low compared to O₃ production in the actual chamber experiments.

It should be noted that one should not expect an additive effect on O₃ concentration when exhaust is added to the chamber, because the chemistry is greatly perturbed. Thus, it is not recommended to subtract the O₃ production in clean air from the O₃ produced in the exhaust runs to obtain "exhaust-contributed O₃."

d. Actinometry

Ultraviolet light is the driving force behind the photochemical reactions, and was therefore monitored during the chamber irradiations. UV intensity was monitored by an Eppley UV radiometer which was factory-calibrated just prior to this study. The radiometer is sensitive over the wavelength range of 290-385 nm. It was mounted on the roof of the mobile laboratory 3 meters above ground and 6 meters from the centerline between the two chambers. The instrument was mounted on a white surface.

The most useful UV intensity parameter for chamber irradiations of organic/NO_x mixtures is the photolysis rate of NO₂, designated as k₁. To relate the output of the radiometer to k₁, the method of Wu and Niki (Reference 12) was employed for NO₂ photolysis while UV intensity was monitored with the radiometer. For each actinometry experiment, approximately 300 ppb NO₂ was injected and rapidly mixed in one of the chambers. The O₃, NO and NO₂ concentrations were monitored and k₁ calculated from

$$k_1 = \frac{27.5 [O_3][NO]}{[NO_2]} + (0.068)[O_3] \quad (1)$$

Radiometer response was recorded in $\text{mcal cm}^{-2} \text{ min}^{-1}$. The k_1 values were determined 3-10 minutes after injecting NO_2 . Actinometry experiments were conducted between July and November. Measurements were made at various times during the day to derive the relationship between k_1 and UV intensity, as measured by the radiometer.

The radiometer and/or data system produced a positive signal corresponding to $14.7 \frac{\text{m cal}}{\text{cm}^2 \text{ min}}$ in the absence of UV radiation. All data shown in the following figures have been corrected for this offset, but the offset has not been subtracted from the plotted chamber data included in Appendix A.

For the actinometry experiments, the radiometer output has been corrected for the positive offset and then converted from $\text{mcal cm}^{-2} \text{ min}^{-1}$ to mw cm^{-2} . A plot of UV intensity as measured by the radiometer versus NO_2 photolysis rate, k_1 , is shown in Figure 17. A linear relationship is observed, with a slope of $0.12 \text{ min}^{-1}/\text{mw-cm}^{-2}$. Taking into account this slope, the appropriate conversion factor and the radiometer offset, k_1 can be calculated from the radiometer data using Equation (2),

$$k_1 = (0.12)(0.06974)(\text{Radiometer Output} - 14.7) \quad (2)$$

where k_1 is in min^{-1} ,

Radiometer Output is in $\text{mcal cm}^{-2} \text{ min}^{-1}$

and 0.06974 is the conversion factor.

Jackson et al. (Reference 13) reported that the relationship between k_1 and radiometer measurements is linear, while Zafonte et al. (Reference 14) and Harvey et al. (Reference 15) have observed a curvilinear relationship. Saeger (Reference 16) found poor correlation between radiometric UV measurements and measured k_1 values. More recently, Bahe and Schurath (Reference 17) reported a linear relationship between k_1 and global radiation. They suggested that the lack of curvature resulted from the fact that data from all seasons and various meteorological conditions were used. The data reported in Figure 17 were obtained between July and October, under mostly clear sky conditions. A simple linear relationship appears to fit the data

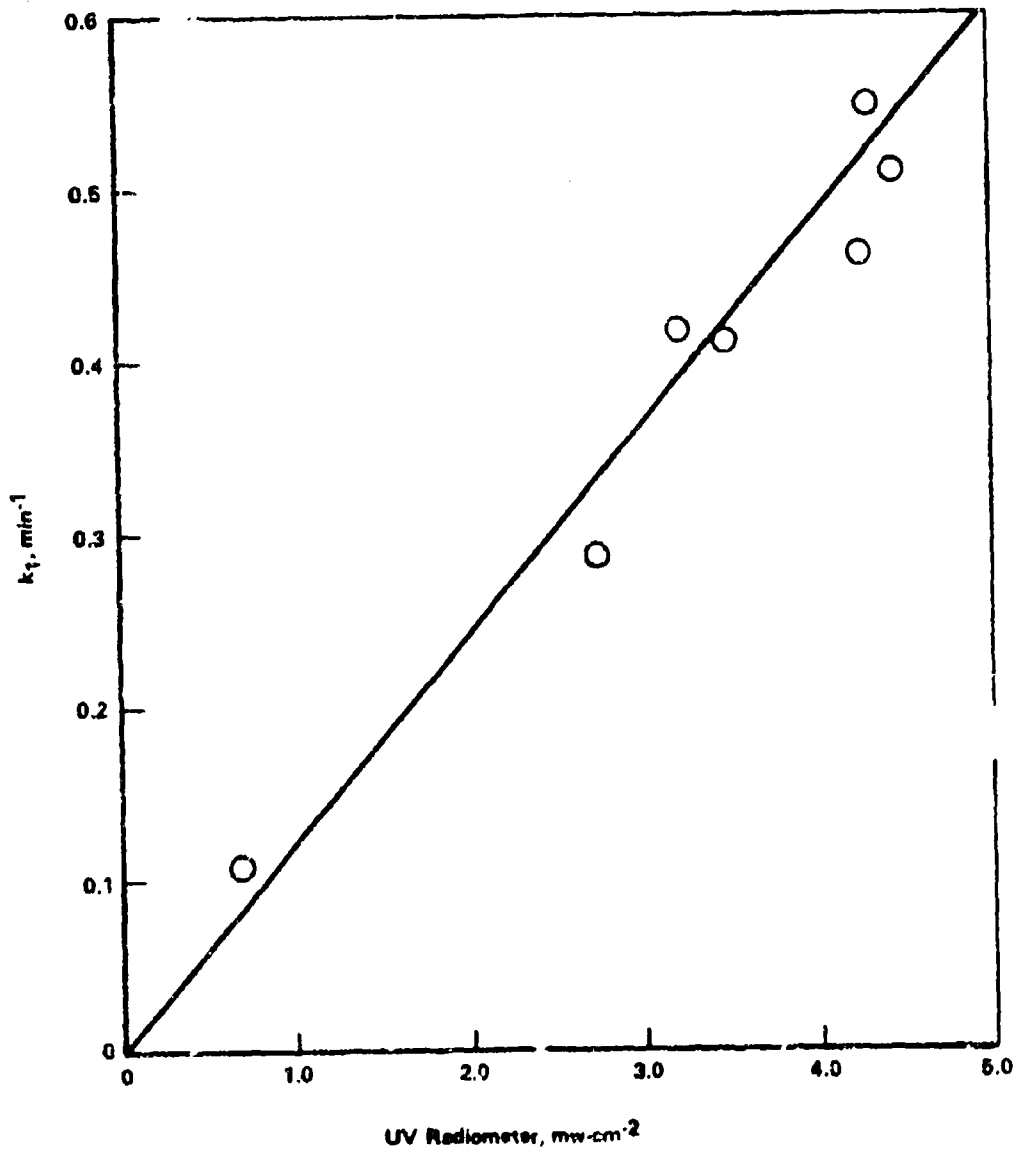


Figure 17. Plot of K_1 Measurements vs UV Radiometer Signal

quite well. A comparison of these results with the data of Zafonte et al. (Reference 14) is found in Figure 18. The agreement between the two data sets is reasonably good, although our data do not show the curvature appearing in the data collected in California.

e. Baseline Reactivity Experiment

Baseline reactivity experiments were run in both chambers to condition the chamber surfaces to smog constituents and to demonstrate the comparability of the two chambers. Several conditioning experiments were run in May and June. The reference hydrocarbon mixture, which consists of 25 percent propylene and 75 percent butane, served as the organic reagent for these experiments. The nominal concentrations employed in the conditioning experiments were:

Organic	10 ppmC
NO	0.18 ppm
NO ₂	0.37 ppm
CO	15 ppm

These nominal concentrations are based on the combustor rig experiments conducted in Task 2. The formal baseline reactivity experiment was run on June 9, 1983 under very clear, sunny, calm conditions. The SF₆-measured dilution rates were 0.021 and 0.029 hr⁻¹ for chambers A and B, respectively. The same nominal concentrations were employed as for the conditioning experiment, with the exception that all the NO_x was injected as NO in order to lower the rate of the reaction.

Plots of the light intensity and temperature during the baseline reactivity experiment are included in Figure 19. Figure 20 shows the chemistry results from the two chambers. The SF₆ data are not plotted in order to keep the figures clear, but the dilution rates were noted earlier. The CO concentration in chamber A was lower than desired, but this has little effect on the photochemical reaction. The decay of NO and production of NO₂ and O₃ were very similar in both chambers. In terms of overall performance, the two chambers are essentially identical within the experimental uncertainty with which the reagents can be injected and the products measured.

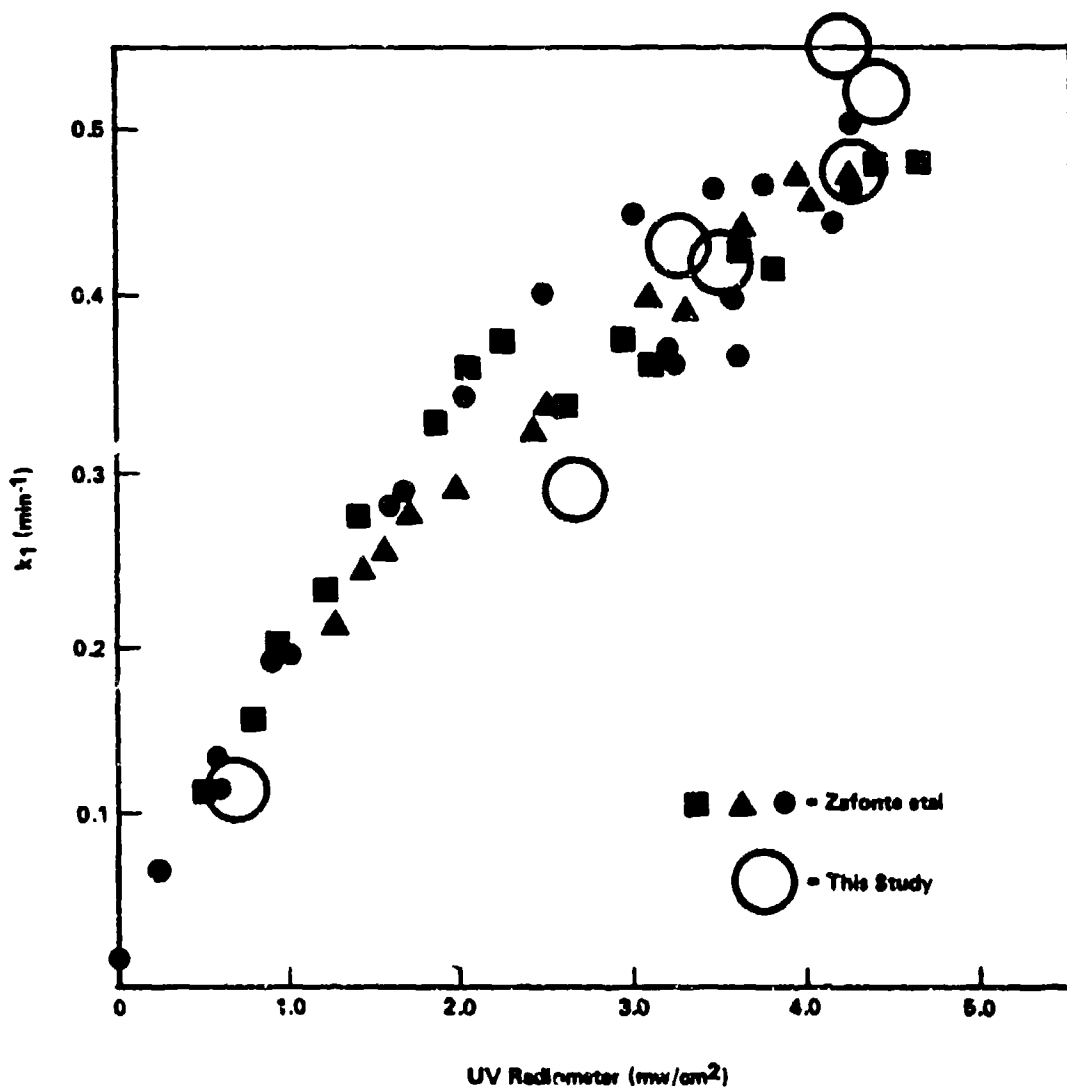


Figure 18. Comparison of Actionmetry Results from This Study With Data of Zafonte et al. (Reference 14).

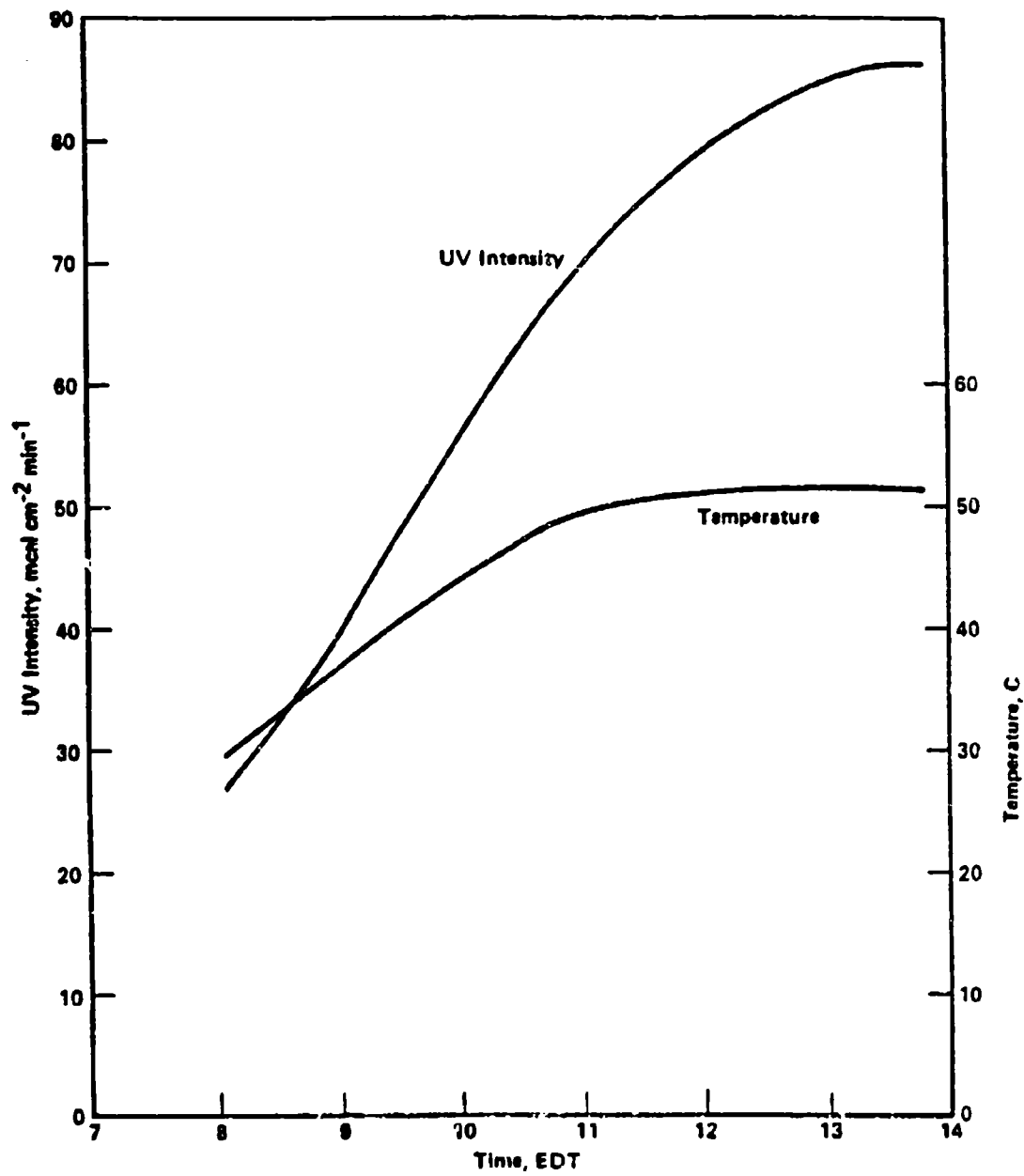


Figure 19. Temperature and UV Intensity for Chamber Experiment on June 9, 1983

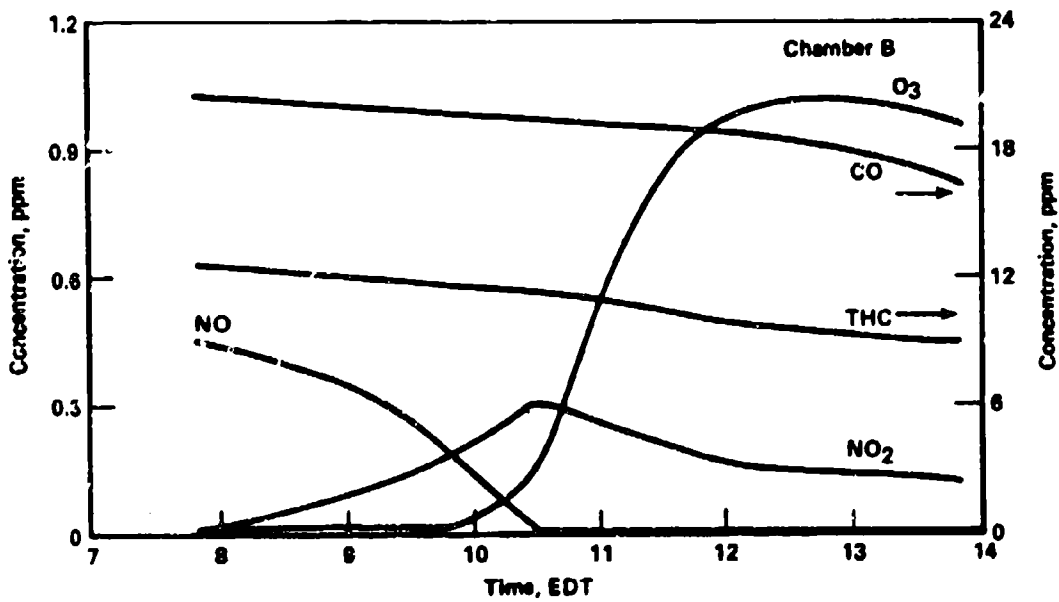
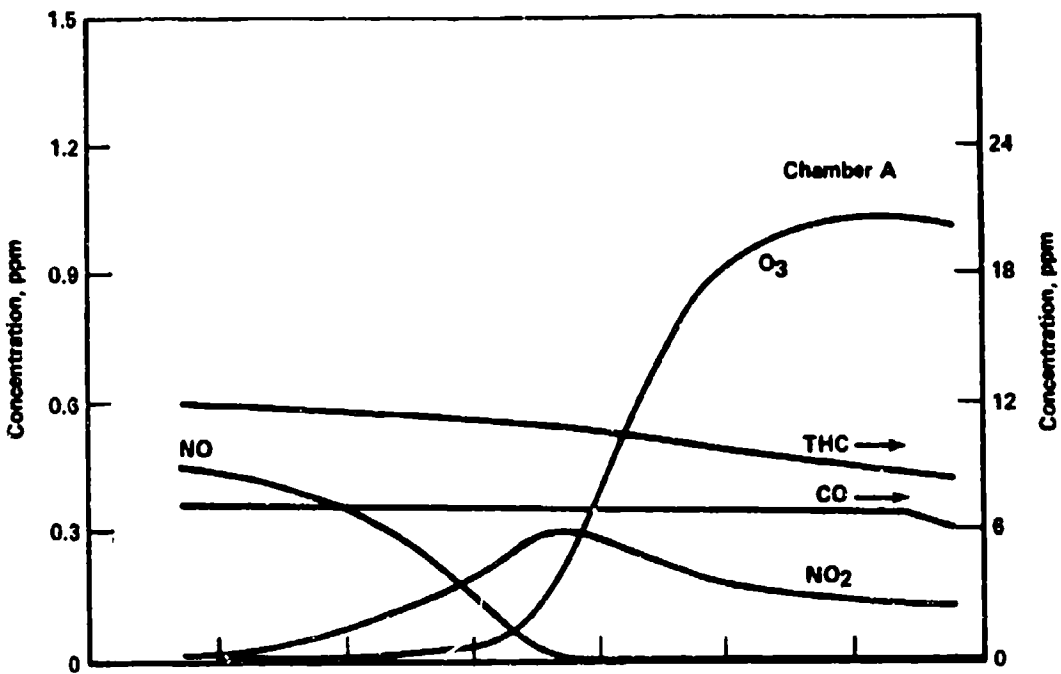


Figure 20. Dual Chamber Experiment, Butane/Propene Hydrocarbon Mix, June 9, 1983

f. System Demonstration Experiment

The objective of the system demonstration experiment was twofold: (1) to demonstrate the equivalence of the two chambers for actual engine exhaust, and (2) to demonstrate the satisfactory operation of the exhaust sampling and chamber monitoring facilities.

The system demonstration experiment was conducted on July 18, 1983. Both chambers were loaded with JP-5 exhaust from the TF-39 engine to slightly over 20 ppmC total hydrocarbon, and the reaction was followed for more than 8 hours of irradiation. A plot of the temperature, relative humidity, and UV intensity during this experiment is shown in Figure 21. Profiles of O_3 , NO_x , NO_2 , NO , total hydrocarbon (THC), and CO for both chambers are shown in Figure 22. The THC profile is delayed until 1000 EOT because the monitoring instrument was offscale. The data from the two chambers show very similar behavior for the species of interest. Of particular note is the similarity in the time and concentration of the O_3 maximum, as well as the formation of a secondary O_3 peak in both chambers. The results of aldehyde measurements in the chambers is shown in Figures 23 and 24. The initial concentrations and general behavior of the four aldehydes measures were similar, except for a somewhat higher CH_2O peak in Chamber B.

The most sensitive indicator of the comparability of the two chambers should be the secondary photoproduct, O_3 . Overlapping plots of the O_3 concentration in each chamber are provided in Figure 25. The ozone concentrations and production rates are nearly identical in the two chambers. These results confirm the comparability of the two chambers suggested by the baseline reactivity experiment, and demonstrate the operation of exhaust-handling facilities.

2. TF-39 Engine Exhaust Reactivity Experiments

The photochemical reactivity experiments employing exhausts from the TF-39 engine were conducted between July 19 and July 22, 1983. The experiments were run at Site III-C at the Peebles Test Facility.

The photochemistry experiments were conducted using the two outdoor smog chambers and support laboratory shown earlier in Figure 7. The chamber facility was located at the top of a hill above Site III-C.

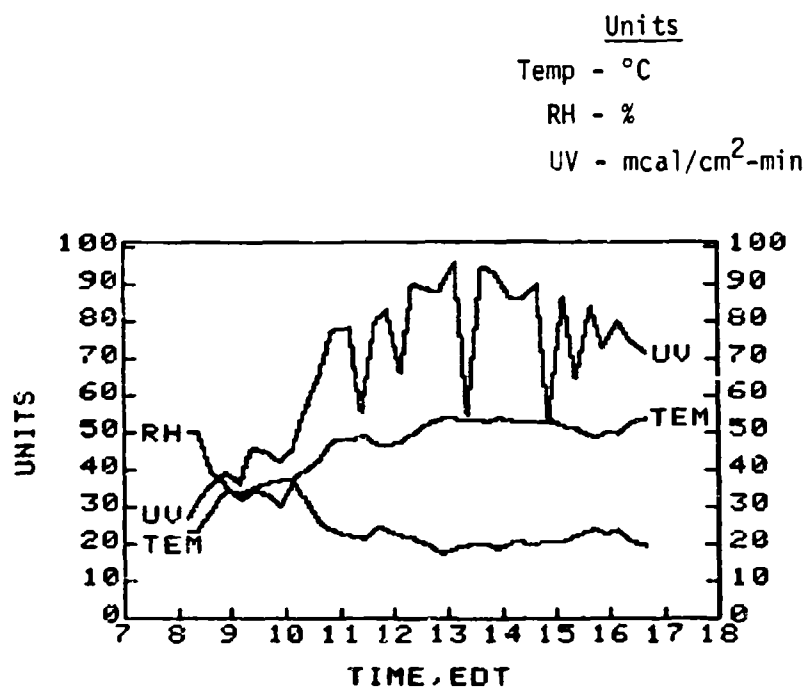
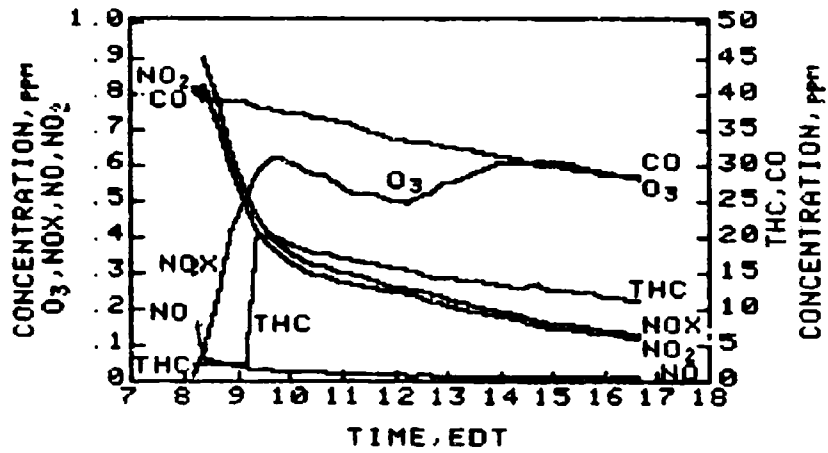
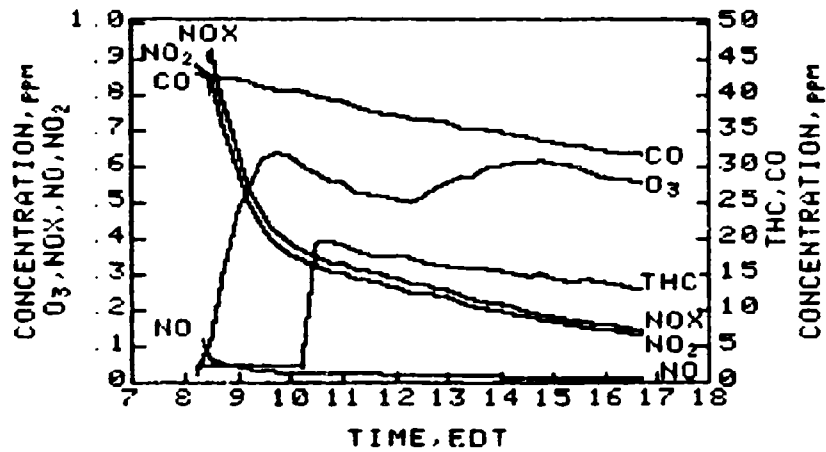


Figure 21. Profiles from AF-1 Chamber A, July 18, 1983



PROFILES FROM AF-1 CHAMBER A JULY 18 1983



PROFILES FROM AF-1 CHAMBER B JULY 18 1983

Figure 22. Profiles from AF-1 Chambers A and B July 18, 1983

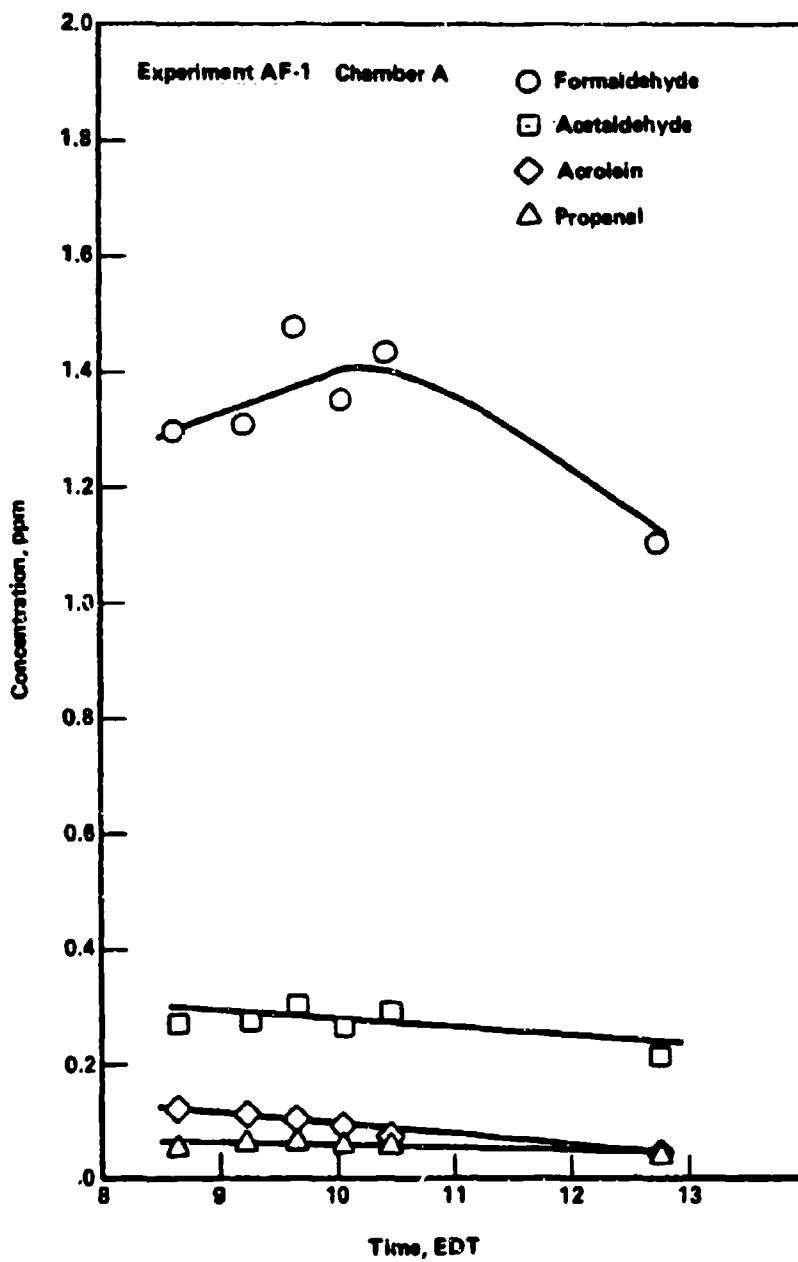


Figure 23. Aldehyde Formation in Chamber A During System Demonstration Experiment (AF-1)

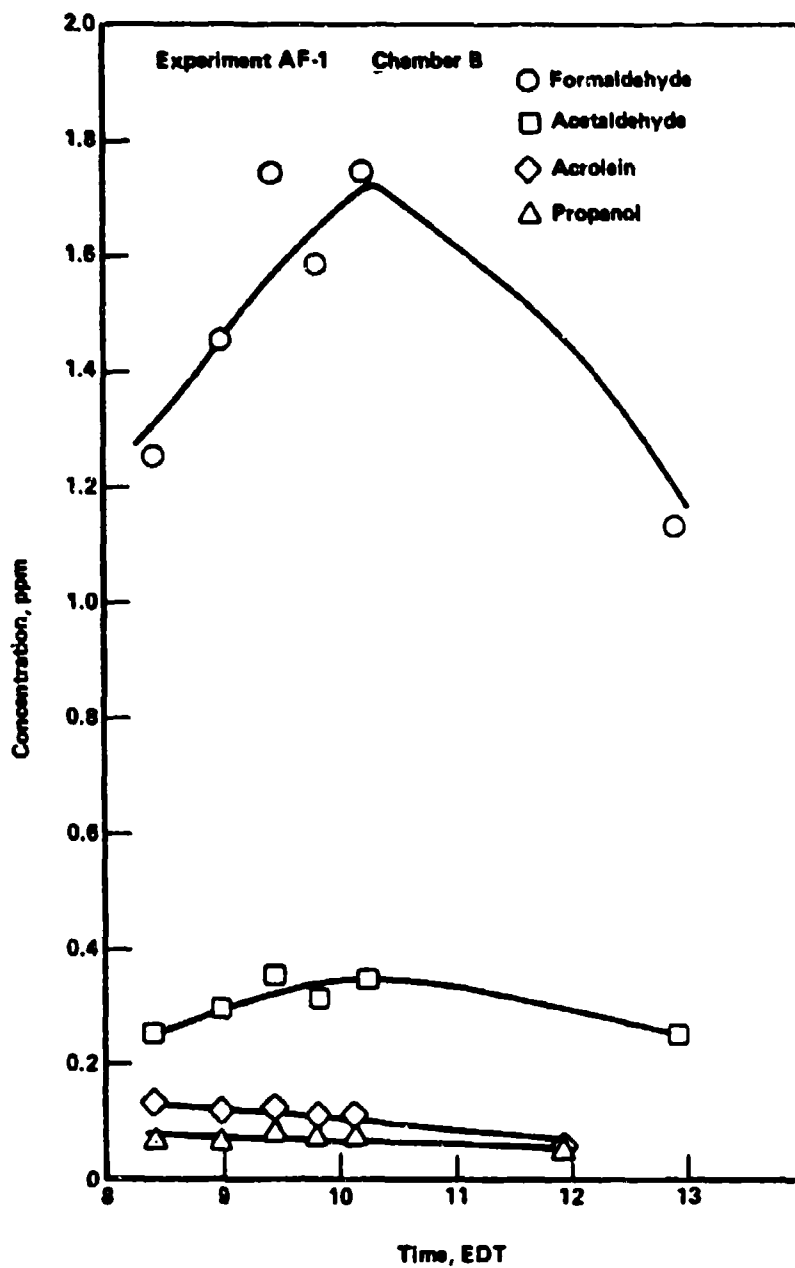


Figure 24. Aldehyde Formation in Chamber B During System Demonstration Experiment (AF-1)

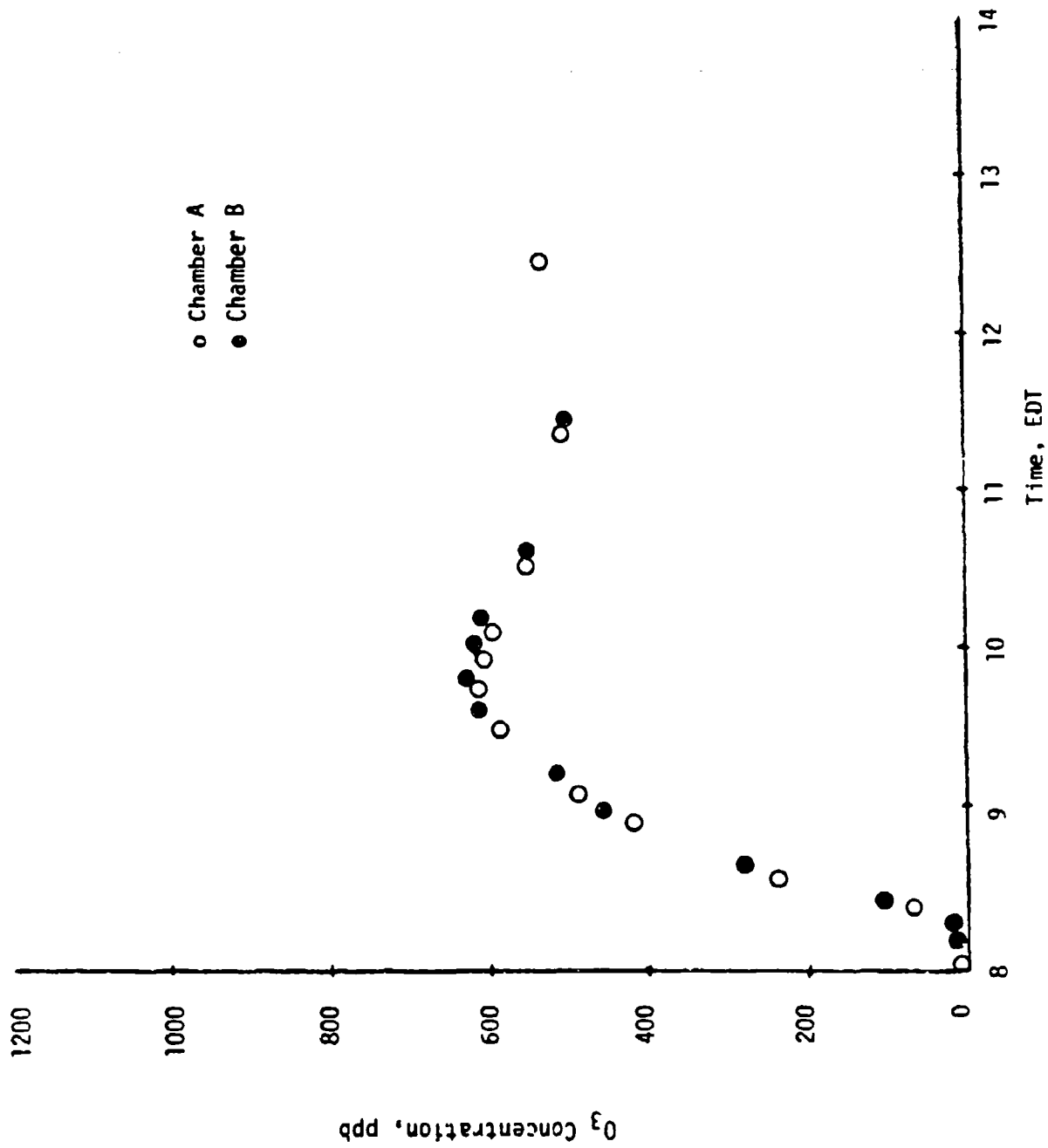


Figure 25. Plots of O₃ Concentration from Chamber A and Chamber B During System Demonstration Experiment, July 18, 1983

The chambers were transported down to the engine before dawn each day for exhaust transfer. After loading the exhaust chamber, it was moved back into position and the reference chamber was loaded with the reference mixture. The composition of the reference mixture was based on the exhaust composition observed during the System Demonstration experiment. Selection of the reference mixture composition was discussed earlier. After loading, SF₆ was added to both chambers as an inert tracer to track dilution rate.

Table 16 gives the test schedule for the TF-39 exhaust photochemistry experiments. The chambers were switched for each experiment to minimize the effect of contamination from low-volatility exhaust constituents.

The results of the TF-39 engine exhaust photochemistry experiments are included as time profiles in Appendix A. The plots are keyed to the experimental conditions shown in Table 16 by experiment number. A summary of the ozone and light-scattering aerosol results from the TF-39 runs is provided in Table 17. Detailed analysis of the experimental results is included in Section V.

3. CFM-56 Engine Exhaust Reactivity Experiments

The photochemical reactivity experiments employing exhaust from the CFM-56 engine were conducted between October 18 and November 7, 1983. These experiments were planned for earlier in the summer, but engine-scheduling difficulties required that the tests be run in October and early November. The experiments were run at Site IV A at the Peebles Test Facility. Weather during the period was less than ideal, with considerable cloudiness and frequent heavy rain, as two major storms traversed the upper midwest. Four photochemistry experiments were carried out in the outdoor chambers in October. Of these, only two had sufficient solar intensity to develop typical photochemical smog pollutant profiles. However, the other two low-intensity experiments showed evidence of considerable chemical reaction and may prove to be useful for data interpretation and modeling purposes. Two additional photochemistry experiments were conducted on November 3 and November 7, 1983. These experiments completed the matrix of emissions and photochemistry tests scheduled for the CFM-56

TABLE 16. SCHEDULE OF TF-39 ENGINE PHOTOCHEMISTRY EXPERIMENTS

Experiment	Date	Engine	Power	Fuel	Photochemistry	Weather
AF-1	July 18	TF-39	Idle	JP-5	System Demonstration	Sunny, humid
AF-2	July 19	TF-39	Idle	JP-5	Chamber A - Reference Hydrocarbon Mix Chamber B - Exhaust	Sunny, humid
AF-3	July 20	TF-39	Idle	JP-4	Chamber A - Exhaust Chamber B - Reference	Sunny, humid
AF-4	July 21	TF-39	Idle	JP-4	Chamber A - Reference Chamber B - Exhaust	Sunny, humid
AF-5	July 22	TF-39	Idle	Shale (JP-8)	Chamber A - Exhaust Chamber B - Reference	Sunny, humid; overcast after 1300 EDT

TABLE 17. OZONE AND b_{scat} RESULTS FOR TF-39 ENGINE EXHAUST PHOTOCHEMISTRY EXPERIMENTS

Experiment	Date	Fuel	Exhaust Chamber			Reference Chamber		
			Max. O ₃ (ppb)	Time of Max. (EDT)	$\frac{b_{\text{scat}}}{(10^{-4} \text{ m}^{-1})}$	Max. O ₃ (ppb)	Time of Max. (EDT)	$\frac{b_{\text{scat}}}{(10^{-4} \text{ m}^{-1})}$
AF-2	July 19	JP-5	0.574	1345	16.9	0.863	1327	0.4
AF-3	July 20	JP-4	0.603	1402	2.2	0.721	1336	0.5
AF-4	July 21	JP-4	0.612	1325	2.1	0.720	1250	0.5
AF-5	July 22	Shale	0.665	1135	14.0	0.836	1140	0.3

engine. A descriptive listing of the CFM-56 engine exhaust photochemistry experiments is provided in Table 18.

The results of the CFM-56 engine exhaust photochemistry experiments are included as time profiles in Appendix A. The plots are keyed by experiment number to the listing in Table 18. A summary of the ozone and light-scattering aerosol results from the CFM-56 runs is provided in Table 19. Detailed analysis of the results is included in Section V.

TABLE 18. SCHEDULE OF CFM-56 ENGINE EXHAUST PHOTOCHEMISTRY EXPERIMENTS

Experiment	Date	Engine	Power	Fuel	Photochemistry Experiment	Weather
AF-6	October 19	CFM-56	Idle	JP-5	Chamber A - Reference Chamber B - Exhaust	Hazy sun
AF-7	October 24	CFM-56	Idle	JP-8	Chamber A - Exhaust Chamber B - Reference	Overcast, rain
AF-8	October 25	CFM-56	Idle	JP-4	Chamber A - Exhaust Chamber B - Reference	Overcast, drizzle
AF-9	October 26	CFM-56	Idle	JP-4	Chamber A - Reference Chamber B - Exhaust	Partly sunny
AF-10	November 3	CFM-56	Idle	JP-5	Chamber A - Exhaust Chamber B - Reference	Mostly cloudy
AF-11	November 7	CFM-56	Idle	JP-8	Chamber A - Reference Chamber B - Exhaust	Partly sunny

TABLE 19. OZONE AND b_{scat} RESULTS FOR CFM-56 ENGINE EXHAUST PHOTOCHEMISTRY EXPERIMENTS

Experiment	Date	Fuel	Exhaust Chamber			Reference Chamber		
			Max. O ₃ (ppb)	Time of Max. (EDT)	b_{scat} (10^{-4} m^{-1})	Max. O ₃ (ppb)	Time of Max. (EDT)	b_{scat} (10^{-4} m^{-1})
AF-6	October 19	JP-5	0.646	1433	ND ^a	0.419	1543	ND
AF-8	October 25	JP-4	0.037	1617	ND	0.279	1422	ND
AF-9	October 25	JP-4	0.665	1514	8.2	0.468	1231	0.4
AF-10	November 3	JP-5	0.085	1250	12.5	0.368	1250	0.3
AF-11	November 7	JP-8	0.639	1614	33.0	0.708	1154	0.4

^aND = No data due to equipment malfunction.

SECTION V
DISCUSSION

A. TASK 3 ENGINE EXHAUST MEASUREMENTS

1. Carbon Balance

A major objective of this study was to improve upon the agreement between the sum of individual hydrocarbon species and the total hydrocarbon level indicated on the FID detector. A previous study (Reference 6) had achieved a carbon balance of about 35 percent at the idle (10 percent) power setting. A summary of the carbon balances achieved at the various test conditions in the current study is given in Table 20. These data have been corrected for oxygenated compound response on the FID as described in a previous report (Reference 8). The data in Table 20 demonstrate a major improvement over earlier studies in accounting for organic carbon compounds. An average carbon balance of 98 ± 10 percent was attained. The most consistent carbon balance, 97 ± 4 , was achieved under idle conditions, while a balance of 100 ± 16 was achieved for the higher (30 and 80 percent) thrust settings. The greater variability at the higher thrusts is caused by inaccuracies resulting from the much lower total hydrocarbon content of the exhaust at these thrusts.

Although the hydrocarbon emissions from the CFM-56 were two or three times lower than those from the TF-39, no difference was observed in the carbon balances for the two engines. No consistent pattern in terms of total hydrocarbon emissions or carbon balance could be found between the various fuels, although JP-4 appeared to yield a slightly better carbon balance for both engines.

The achievement of a better carbon balance in this study, compared to previous studies, is believed to be due to the higher accuracy and more complete compound coverage of the analytical techniques employed. The on-line cryogenic GC/FID system has been demonstrated to achieve greater than 90 percent recovery for a wide range of C₂ to C₁₀ organic compounds. Likewise, the XAD adsorptive trapping approach has good efficiency for compounds in the C₉-C₂₀ volatility range.

TABLE 20. COMPARISON OF TOTAL ORGANICS BY CONTINUOUS FID
VERSUS SPECIATION METHODS (ppmC)

Engine	Condition/Fuel	Total Organics By Continuous FID		Total Organics by Species Summation ^a	Carbon Balance, % ^b	
		FID-1	FID-2			
TF-3S	Idle/JP-4	401	412	407	428	105
	Idle/JP-4	375	394	385	386	100
	Idle/JP-5	336	350	343	325	95
	30%/JP-5	12.9	14.7	13.8	13.1	95
	80%/JP-5	4.83	4.35	4.59	5.20	113
	Idle/JP-8	355	367	361	359	99
	Idle/JP-4	132	119	126	127	101
	Idle/JP-5	184	174	179	178	99
CFM-56	Idle/JP-5	116	105	111	100	90
	30%/JP-5	1.53	3.10	2.31	2.58	112
	80%/JP-5	4.22	5.20	4.71	3.68	78
	Idle/JP-8	209	199	204	189	93
	AVERAGE					98 + 9.5

^aCorrected for oxygenated carbon response.

^b(Species Summation/Cont. FID Average) x 100.

2. Individual Hydrocarbon Species

The individual hydrocarbon species quantified in the emissions have been presented in Tables 6-8 (Section IV). At idle, the predominant species are ethylene, propylene, acetylene, 1-butene, methane, and formaldehyde. Generally these six materials accounted for 30-40 percent of the total hydrocarbon emissions. These species, in addition to several other olefins and carbonyl compounds found in the exhaust, are cracking or partial oxidation products not found in the fuel. The distribution of these compounds and their level, relative to the total emissions, do not appear to be greatly affected by fuel type.

The other major component of the emissions is unburned fuel. This component consists predominantly of normal paraffins (C₉ to C₁₇ for JP-8 and JP-5 fuel and C₄-C₁₆ for JP-4 fuel) with smaller amounts of alkyl substituted aromatics, cycloparaffins, and branched alkanes. The distribution of these species in the exhaust is greatly affected by fuel type, as shown by comparing the data in Tables 6-8. The similarity of the emission profile to the fuel sample itself is demonstrated in Figure 9, for JP-5 fuel.

Inspection of the data in Table 7 reveals that the total hydrocarbon emissions are greatly reduced at both the 30 and 80 percent thrust conditions. The unburned fuel component, represented by C₁₀-C₁₆ paraffins, is virtually eliminated at both of these thrust settings. For the TF-39 engine at 30 percent thrust setting, the predominant species emitted are methane, ethylene, propylene, acetylene, benzene, formaldehyde, and acetaldehyde. However, for the CFM-56, the major organic species emitted at 30 percent thrust is methane, with all other materials being much lower in concentration.

At the 80 percent thrust setting, all of the individual hydrocarbons, with the exception of methane, are very low. However, as shown in Table 7, at this thrust setting, two siloxanes become the predominant nonmethane hydrocarbon species. The identities of these two materials have been determined by GC/MS to be 1,1,3,3,5,5-hexamethyl-2,4,6-trioxo-1,3,5-trisilacyclohexane and the octamethyl, tetrasiloxane-homologue. It is unclear whether these compounds are derived from engine operation,

or whether they are artifacts of the sampling system; however, they were not present at the idle thrust setting.

3. Distribution of Emissions By Compound Class

In order to more easily interpret the detailed hydrocarbon emission data, the exhaust organic distribution according to important classes of compounds is presented in Tables 21-23 for the three fuel types. The most abundant compound class, in each case, is olefins.

Comparison of the TF-39 and CFM-56 emissions by compound class reveals that most of the compound classes are two to three times lower for the CFM-56. An important exception is aldehydes, which are similar for the two engines when JP-5 or JP-8 is used and only a factor of two lower when JP-4 is used. These data are graphically illustrated in Figure 26, wherein the levels of the various compound classes for the TF-39 combustor rig, TF-39 engine, and CFM-56 engine using JP-5 fuel are plotted. While most compound classes are lower by a factor of two for the CFM-56 engine, compared to the TF-39 engine, aldehyde and ketone levels are virtually identical.

The finding of a higher relative abundance of aldehydes in the CFM-56 exhaust is very significant since this class represents perhaps the most important emission from both toxicological and photochemical viewpoints. This aspect of the data is discussed more fully in a later portion of the report.

4. Distribution of Emissions By Carbon Number

The distribution of emissions by volatility is of some importance since these data most clearly distinguish the cracking and partial oxidation products from the unburned fuel component. The carbon number distributions for selected exhaust samples and the three fuels are presented in Tables 24 and 25, respectively.

As shown in Table 24, a primary maximum distribution for the exhaust hydrocarbons is found in the C₂ to C₃ region, represented predominantly by ethylene. At idle a secondary maximum, corresponding to unburned fuel, is found in the C₁₁-C₁₂ region for JP-8, C₆-C₇ region for JP-4, and C₁₂-C₁₃ region for JP-5. At higher thrust settings, the

TABLE 21. MAJOR ORGANIC SPECIES SUMMARIZED BY COMPOUND CLASS,
IN EXHAUST OF JET ENGINES OPERATING WITH JP-4 FUEL^a

Compound	TF-39 Engine				CFM-56 Engine	
	Idle (1st run)		Idle (2nd day)		Idle	
	7/19/83		7/20/83		(10/20/83)	
	x	S.D.	x	S.D.	x	S.D.
Paraffins	89.66	3.76	84.50	9.84	17.46	1.24
Acetylene	18.32	0.23	16.71	2.29	4.29	0.73
Olefins	128.97	3.89	129.28	17.71	39.95	2.04
Aromatics	33.87	2.15	34.72	2.81	8.96	0.77
Aldehydes	39.40	6.81	39.17	3.17	19.57	1.43
Ketones	1.40	0.45	1.08	0.17	0.65	0.11
Alcohols	0.60	0.11	0.68	0.06	0.25	0.01
TOTAL	312.20	17.40	306.14	36.05	91.13	6.33

^a \bar{x} = Average concentration for three replicate
determinations, ppmC.
S.D. = Standard deviation.

TABLE 22. MAJOR ORGANIC SPECIES SUMMARIZED BY COMPOUND CLASS IN EXHAUST OF JET ENGINES OPERATING WITH JP-5 FUEL^a

Compound	TF-39 Engine						CFM-56 Engine								
	Idle			80%			Idle (10/19/83)			30%			80%		
	\bar{x}	S.D.	\bar{x}	S.D.	\bar{x}	S.D.	\bar{x}	S.D.	\bar{x}	S.D.	\bar{x}	S.D.	\bar{x}	S.D.	
Paraffins	31.74	1.33	1.94	0.19	1.35	0.39	16.25	1.74	8.37	0.42	0.79	0.06	0.56	0.07	
Acetylene	16.85	0.65	1.23	0.26	N.D.	N.D.	9.67	0.83	5.75	0.58	N.D.	N.D.	N.D.	N.D.	
Olefins	117.18	6.52	4.34	1.31	0.09	0.05	61.97	2.79	41.51	1.43	0.04	0.02	0.12	0.03	
Aromatics	20.08	1.10	0.80	0.04	0.18	0.005	11.44	0.97	6.53	0.33	0.04	0.02	0.03	0.005	
Aldehydes	36.29	6.18	2.39	0.51	0.50	0.19	31.71	0.68	16.33	2.01	0.20	0.04	0.29	0.02	
Ketones	0.78	0.30	0.20	0.14	0.17	0.10	0.61	0.18	0.52	0.09	0.16	0.06	0.07	0.007	
Alcohols (Phenol)	0.64	0.03	N.D.	N.D.	N.D.	N.D.	0.40	0.04	0.35	0.00	N.D.	N.D.	N.D.	N.D.	
TOTAL	223.56	16.11	10.90	2.45	2.29	0.74	132.05	7.23	79.36	4.90	1.23	0.20	1.07	0.13	

^a \bar{x} = Average concentration for three replicate determinations, ppmf.
S.D. = Standard deviation.

TABLE 23. MAJOR ORGANIC SPECIES SUMMARIZED BY COMPOUND CLASS IN EXHAUST OF JET ENGINES OPERATING WITH JP-8 FUEL^a

Compound	TF-39 Engine		CFM-56 Engine	
	Idle		Idle	
	\bar{x}	S.D.	\bar{x}	S.D.
Paraffins	43.35	3.61	20.10	1.58
Acetylene	15.20	0.69	9.99	1.30
Olefins	116.35	5.85	65.72	4.41
Aromatics	29.68	3.32	15.81	1.22
Aldehydes	33.53	2.05	30.67	1.78
Ketones	0.79	0.06	0.56	0.13
Alcohols	1.49	0.17	0.69	0.14
TOTAL	240.39	15.75	143.54	10.56

^a \bar{x} = Average concentration for three replicate determinations, ppmC.
S.D. = Standard deviation.

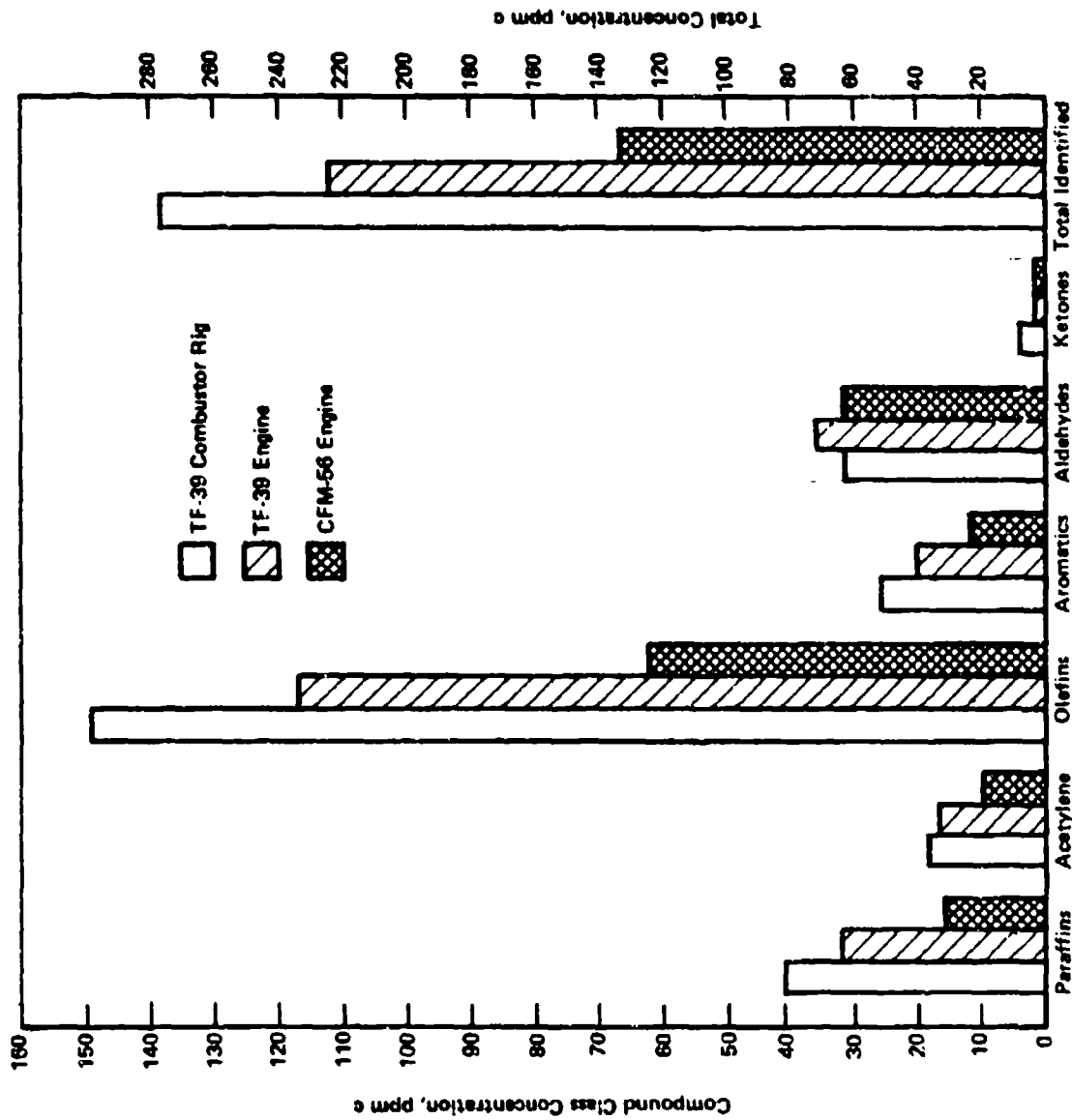


Figure 26. Compound Class Distributions for Emissions Using JP-5 Fuel and Ground Idle Test Point

TABLE 24. TOTAL ORGANIC SPECIES IN EXHAUST OF SELECTED TEST RUNS, DISTRIBUTION BY CARBON NUMBER (ppmC)

Compound	TF-39 Engine					CFM-56 Engine	
	JP-4 Fuel		JP-5 Fuel			JP-8 Fuel	JP-5 Fuel
	Idle	Idle	Idle	30%	80%	Idle	Idle
C ₁ to C ₂	28.8	24.2	21.0	2.70	1.58	24.2	19.2
C ₂ to C ₃	102.6	85.8	82.2	3.44	0.37	83.2	50.2
C ₃ to C ₄	42.4	34.0	28.3	1.21	0.17	29.8	15.8
C ₄ to C ₅	43.3	38.1	35.7	1.20	0.11	36.4	18.8
C ₅ to C ₆	34.3	30.2	17.1	0.50	0.08	17.7	8.4
C ₆ to C ₇	50.6	43.6	18.0	0.80	0.05	17.9	8.6
C ₇ to C ₈	36.8	30.2	10.8	0.20	0.18	10.8	5.0
C ₈ to C ₉	26.9	24.1	11.8	0.30	0.13	10.9	4.5
C ₉ to C ₁₀	22.2	17.7	13.9	0.50	0.08	28.0	4.5
C ₁₀ to C ₁₁	17.5	17.8	12.0	0.10	0.18	34.7	5.6
C ₁₁ to C ₁₂	13.4	12.3	19.2	0.44	0.33	35.0	8.1
C ₁₂ to C ₁₃	10.8	13.3	20.7	0.10	0.05	25.1	10.4
C ₁₃ to C ₁₄	9.7	10.4	19.5	0.17	0.17	17.1	8.7
C ₁₄ to C ₁₅	5.8	6.5	13.6	0.01	0.02	8.3	5.7
C ₁₅ to C ₁₆	2.9	3.4	7.0	0.02	0.01	3.7	2.6
C ₁₆ and above	1.9	3.3	5.6	0.09	0.02	3.1	1.8
Total organics	450	395	336	11.8	3.53	386	178

TABLE 25. HYDROCARBON DISTRIBUTION BY CARBON NUMBER IN VARIOUS FUELS

Range	% (Carbon Basis)		
	JP-4	JP-5	JP-8 (Shale)
C ₄ -C ₅	0.95	-	-
C ₅ -C ₆	6.0	-	-
C ₆ -C ₇	18.9	-	-
C ₇ -C ₈	20.5	-	-
C ₈ -C ₉	13.0	0.9	1.4
C ₉ -C ₁₀	9.6	7.9	10.0
C ₁₀ -C ₁₁	8.0	21.7	27.8
C ₁₁ -C ₁₂	9.9	23.4	26.1
C ₁₂ -C ₁₃	8.0	22.4	24.2
C ₁₃ -C ₁₄	3.5	13.3	6.9
C ₁₄ -C ₁₅	1.2	6.0	2.8
C ₁₅ -C ₁₆	0.32	1.9	1.0
C ₁₆ and Above	-	0.9	0.4

secondary maximum is not observed. At 80 percent thrust the C₁-C₂ region (methane and formaldehyde) accounts for 50 percent of the total emissions.

5. Ratio of Selected Aromatic and Aliphatic Compound Pairs

In the earlier portion of this study (Reference 8), a relatively higher ratio of aromatic compounds to aliphatic compounds was found for the exhaust compared to the fuel. This phenomenon is believed to be due to less efficient combustion of the aromatic compounds in the fuel. Table 26 demonstrates this effect for the TF-39 and CFM-56 engines operating on JP-5 fuel. As shown in Table 26, the naphthalene/n-C₁₂ ratio is increased 20-90 fold for the exhaust compared to the fuel. Significant enhancement of alkylbenzenes, methylnaphthalenes, and phenanthrene are also observed.

This finding is significant since the unburned fuel component of the exhaust is more highly aromatic than the fuel itself. Therefore, this factor must be taken into account when evaluating the environmental impact of the emissions.

6. Comparison of TF-39 Combustor Rig and Full-Scale Engine

An interesting aspect of this study is the availability of detailed emission data from both a TF-39 combustor rig and full scale engine. The use of a combustor rig for studying emissions composition is highly advantageous because of the much lower costs associated with its operation. However, such an approach can be used only if the combustor rig accurately simulates the engine in terms of emissions.

Data for the TF-39 combustor rig and engine have been compared from several aspects in this study. Figure 27 shows the emission distribution by carbon number for the combustor rig and engine. The relative amounts generally agree within 1-2 percent, although the combustor rig has proportionally higher emissions in the unburned fuel region (C₁₀-C₁₆).

A comparison of levels of specific compounds from the two systems is shown in Table 27. The total hydrocarbon level for the combustor rig is a factor of 1.4 times greater than the engine, as expected, due to the inclusion of bypass air in the engine exhaust

TABLE 26. SELECTED AROMATIC/ALIPHATIC RATIOS
FOR EMISSIONS USING JP5 FUEL

Compound Pair	Ratio of Aromatic/Aliphatic Concentrations			
	TF-39 Combustor Rig	TF-39 Engine	CFM-56 Engine	JP-5 Fuel
C ₄ -Benzene/n-C ₁₁	0.44	0.31	0.67	0.049
Naphthalene/n-C ₁₂	0.38	0.70	1.3	0.016
1-Methyl Naphthalene/n-C ₁₃	0.15	0.31	0.42	0.032
Dimethyl Naphthalenes/n-C ₁₄	0.33	0.20	0.45	0.011
Phenanthrene/n-C ₁₆	0.17	0.055	0.055	0.0008

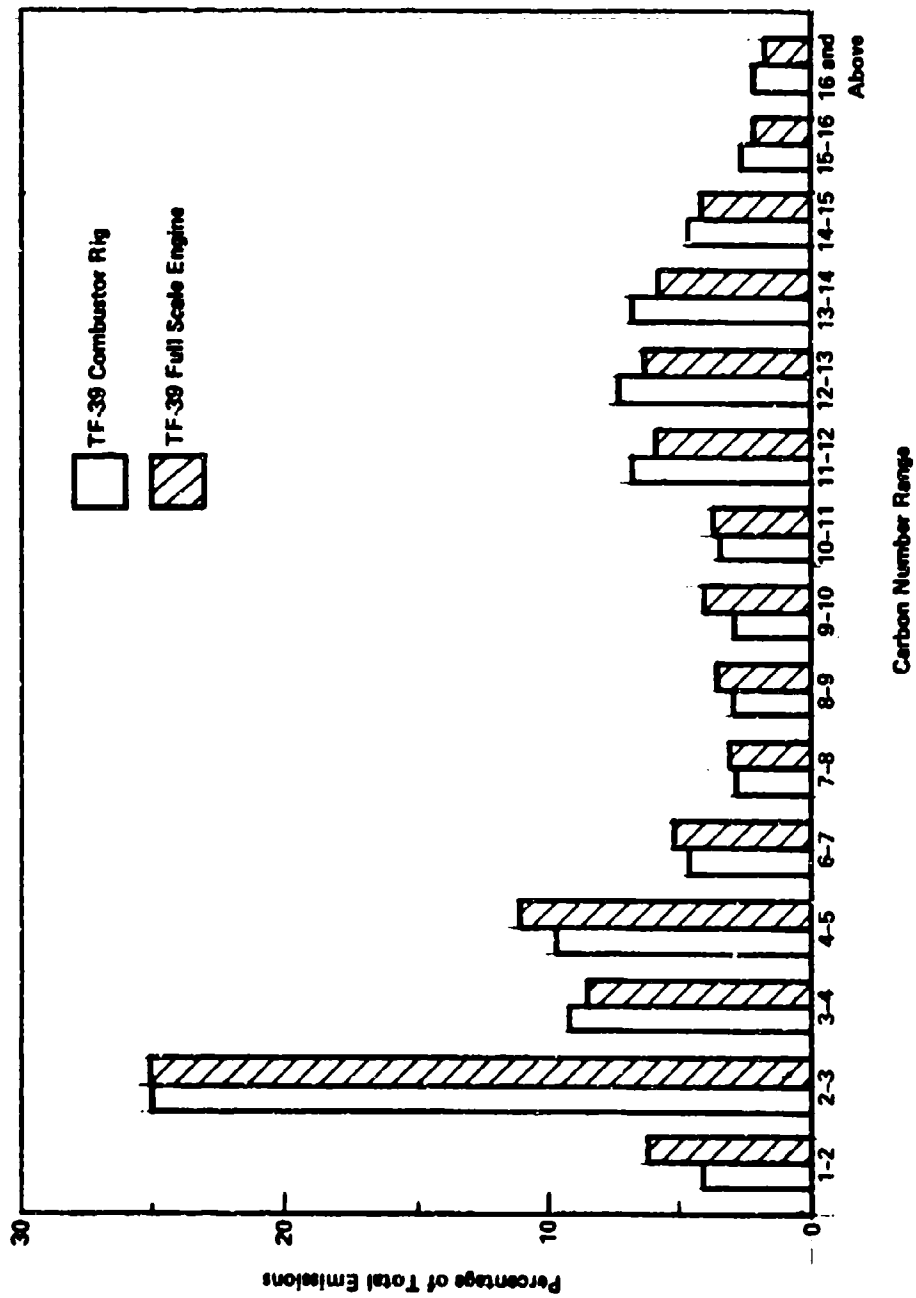


Figure 27. Comparison of Distributions of Organic Emissions from TF-39 Combustor Rig and Full-Scale Engine

TABLE 27. COMPARISON OF EMISSION LEVELS OF SELECTED COMPOUNDS FROM TF-39 COMBUSTOR RIG AND FULL-SCALE ENGINE OPERATING ON JP-5 FUEL AT GROUND IDLE

Compound	Concentration, ppmC		Ratio ^a
	Combustor Rig	Full Scale Engine	
Methane	10.4 ± 1.1	9.4 ± 0.09	1.10
Ethane	2.9 ± 1.6	2.0 ± 0.13	1.45
Ethylene	81.6 ± 4.9	62 ± 3.2	1.32
Acetylene	21.0 ± 1.7	17 ± 0.65	1.23
Benzene	9.3 ± 0.94	7.5 ± 0.25	1.24
n-Octane	0.53 ± 0.15	0.34 ± 0.05	1.55
n-Decane	2.0 ± 0.24	1.6 ± 0.05	1.25
n-Dodecane	6.6 ± 0.76	2.8 ± 0.09	2.35
n-Hexadecane	0.60 ± 0.09	0.27 ± 0.008	2.22
Naphthalene	2.3 ± 0.31	1.99 ± 0.23	1.15
Phenanthrene	26 ± 2	7.7	3.4
Formaldehyde	14 ± 6.3	14.6 ± 3.0	0.97
Acetaldehyde	6.3 ± 1.2	7.5 ± 0.83	0.84
Acrolein	6.2 ± 1.4	6.2 ± 1.1	1.0
Total Hydrocarbons	502 ± 47	346 ± 33.9	1.45

^aRatio = Combustor Rig/Engine.

sample. The ratios for specific compounds are generally between 1.0 and 1.5, in good agreement with the total hydrocarbon ratio. However, the higher boiling paraffins (e.g. n-dodecane and n-hexadecane) are significantly higher for the combustor rig.

Interestingly naphthalene, which has a volatility similar to to n-dodecane, had a lower ratio, 1.15, in general agreement with the total hydrocarbon ratio. Phenanthrene, as well as higher molecular weight PNAs, was significantly lower for the engine than for the combustor rig.

Compound class distributions for the TF-39 engine and combustor rig are shown in Figure 26. Very good agreement was observed (i.e., each class yields an emission ratio similar to the total hydrocarbon emission ratio) for the two combustion systems.

Based on these data, the combustor rig appears to be an adequate surrogate for the full-scale engine. It should be emphasized that the combustion rig employed for these comparisons is a full-scale 1/6th sector of an actual TF-39 engine. The PNA levels are not expected to agree well because of the complex factors leading to their formation and the low levels present. Higher boiling hydrocarbons in the unburned fuel region for JP-5 appear to yield poorer agreement than do the cracking and partial oxidation products (i.e., olefins and aldehydes).

7. Carbonyl Compounds--Method Performance

The levels of aldehydes and ketones in the exhaust have been presented in Tables 6-8. As discussed earlier in Section III, two alternative DNPH methods were employed. The latter method, employing acetonitrile as a solvent, was used primarily for the CFM-56 engine with only minimal data being gathered by this technique during the TF-39 experiments. The primary advantage of the latter technique is the capability to form DNPH derivatives with dicarbonyl compounds such as glyoxal and methyl glyoxal.

As shown in Tables 6-8, significant levels of these two dicarbonyl compounds were detected. Methyl glyoxal is significant since it is highly reactive, photochemically. Apparently, the presence of these materials in combustion exhaust has not been reported previously.

Since both DNPH procedures can detect monocarbonyl compounds, a comparison of the results obtained by the two methods was made. These

data are presented in Table 28. Representative chromatograms for the two techniques from the same test (TF-39 using JP-8 shale fuel) are shown in Figure 16. A typical chromatogram for the dicarbonyl determinations is shown in Figure 15.

The data in Table 28 demonstrate agreement within \pm 10-20 percent between the two DNPH procedures. Slightly higher average values for formaldehyde, acrolein, and propanal were obtained using the acetonitrile-based procedure, whereas slightly lower average values were achieved for acetaldehyde. Benzaldehyde levels agreed extremely well for the two techniques. Based on these data, the acetonitrile DNPH method appears to be the method of choice since a wider range of compounds can be determined.

8. Comparison of Jet Turbine Engine Emission Rates to Other Mobile Sources

Previous efforts to establish the relative importance of aircraft engine emissions on ambient air quality have been hampered by the lack of a satisfactory data base concerning the composition of the exhaust stream. Consequently, a primary objective of this study was to establish such a data base. The excellent carbon balances achieved (Table 20) and extensive compositional data (Tables 6-8) demonstrate that the results of this study can serve as a reliable data base for environmental input assessments.

However, knowledge of the detailed composition of an emission source is not sufficient to make such assessments. Additional information required includes: (1) emission inventories for all significant sources with the geographical region of interest, (2) mathematical models which accurately describe the dispersion of aircraft emission in the atmosphere, and (3) detailed knowledge of the meteorological conditions within the geographical region of interest.

Since these pieces of information will be specific for a given geographical location, a generalized statement of the relative importance of aircraft emissions would not be meaningful. To give the reader some perspective on the significance of the compositional data provided in this report, two approaches have been used. First, the photochemical

TABLE 28. COMPARISON OF AQUEOUS AND ACETONITRILE (ACCN) DNPH PROCEDURES FOR ALDEHYDES

Test Conditions	Concentration of Aldehyde Using Given Method, ppm														
	Formaldehyde			Acetaldehyde			Acrolein			Propenal			Benzaldehyde		
	Average	ACCN	% Deviation	Average	ACCN	% Deviation	Average	ACCN	% Deviation	Average	ACCN	% Deviation	Average	ACCN	% Deviation
CFMS6/JPS/101e	13.4	16.2	2.5	6.0	4.7	12	4.2	5.0	6.7	1.1	0.90	10	0.96	0.93	1.6
CFMS6/JPS/101e	7.3	8.6	0.6	2.5	3.6	10	0.90	2.3	64	0.57	1.7	47	0.42	0.40	6.7
CFMS6/JPS/101e	8.1	8.4	1.0	3.2	3.5	4.5	2.1	2.3	4.5	1.2	2.1	27	0.40	0.54	5.9
CFMS6/JPS/101e	7.1	8.0	10	2.7	3.9	18	0.90	2.4	43	0.66	2.3	55	0.36	0.54	20
CFMS6/JPA/101e	8.5	8.5	0	1.9	3.2	25	2.3	2.8	9.8	1.0	1.4	17	0.53	0.40	5.0
CFMS6/JPS(Shale)/101e	13.0	12.5	2.0	5.4	4.2	13	3.7	4.6	11	1.4	1.1	12	1.1	1.2	4.3
CFMS6/JPS(Shale)/101e	13.6	13.6	0	5.8	4.3	15	4.0	4.6	7.0	1.3	1.0	13	1.0	1.4	
CFMS6/JPS/305 Throat	0.079	0.11	17	0.020	0.021	14	<0.01	<0.01	--	<0.01	<0.01	--	<0.01	<0.01	--
CFMS6/JPS/305 Throat	0.081	0.11	15	0.030	0.012	150*	<0.01	<0.01	--	<0.01	<0.01	--	<0.01	<0.01	--
CFMS6/JPS/605 Throat	0.16	0.24	20	0.044	0.042	27	<0.01	<0.01	--	<0.01	<0.01	--	<0.01	<0.01	--
FF39/JPA/101e	13.3	17.9	15	7.1	7.0	0.7	5.3	5.8	4.5	2.4	1.6	20	1.5	1.4	2.4
FF39/JPA/101e	12.2	10.9	21	7.2	6.4	5.9	5.8	6.9	8.7	2.5	1.8	17	2.6	1.3	30
FF39/JPA/101e	16.7	10.3	4.5	7.4	6.9	3.5	5.6	6.9	10	2.5	1.8	16	1.0	1.4	17
FF39/JPS(Shale)/101e	14.9	10.4	10	5.6	4.8	7.7	5.3	7.2	13	2.3	1.4	24	1.2	1.4	7.7
FF39/JPS(Shale)/101e	14.8	18.4	12	6.2	4.8	13	5.8	7.4	12	2.4	1.5	23	1.8	1.6	5.9
FF39/JPS(Shale)/101e	12.9	16.7	12	6.6	5.2	12	5.9	6.7	6.2	2.3	1.4	24	1.6	1.5	3.5
FF39/JPS/605 Throat	0.48	0.20	60	0.17	0.082	38	0.016	0.7	6.5	0.024	0.010	14	<0.01	<0.01	--
Average Deviation			12			12			14			22			9.8

Linear Regression Data (x = Acetonitrile, y = aqueous)		
Slope	0.84	1.13
Y-Intercept	-0.10	-0.36
Correlation Coefficient	0.960	0.951

* Not included in calculating average deviation.

reactivity of the exhaust sample has been compared to other exhaust streams using a reactivity scheme. These comparisons are provided in Section V.B. Secondly, the aircraft emission levels for a few selected organic compounds, deemed to be of toxicological significance, have been compared to the levels found from other sources. These comparisons are presented below.

We anticipate that the data contained in this report will be used to make similar comparison for other compounds, as well as for assessing effects on ambient air quality within specific geographical regions. Consequently, no attempt has been made to conduct detailed comparisons, beyond those described above, in the current study. Two recent review articles provide useful insight into methods for making such comparisons (Reference 18,19).

a. Benzene

Benzene is an environmentally significant compound because it is known to cause leukemia in workers exposed to relatively high levels. Recently the workplace standard for this compound has been set at 1 ppm (6 ppmC). Emission levels of benzene in this study were in the range of 1-7 ppmC (i.e., at or below the workplace standard).

A comparison of benzene emissions from automobiles operating on the 1975 Federal Test Procedure, with and without catalytic converters (Reference 20) and jet engines is presented in Table 29. As shown by these data, the CFM-56 emissions are in the same range as for the automobiles equipped with catalytic converters, whereas the TF-39 emissions are significantly higher, approaching the emission level for automobiles not equipped with catalytic converters.

b. PNA Emissions

PNA levels in gasoline and diesel engine emissions have been controversial, because of the difficulty in obtaining accurate data. Consequently, a detailed comparison of jet engine emissions of PNAs to other mobile sources is difficult. Table 30 presents a comparison of benzo(a)pyrene emission levels from various mobile sources (Reference 21). These data indicate that BAP emissions from jet engines

TABLE 29. COMPARISON OF BENZENE EMISSIONS
FROM VARIOUS MOBILE SOURCES

Source	Benzene Emissions, mg/g of Fuel
Automobile, Catalytic	0.13
Automobile, Noncatalytic	0.75
CFM-56, JP-5 Fuel	0.10
TF-39, JP-5 Fuel	0.42
CFM-56, JP-4 Fuel	0.094
CFM-56, JP-8 Fuel	0.20

TABLE 30. COMPARISON OF BENZO(a)PYRENE
EMISSIONS FROM VARIOUS SOURCES

Source	BAP, $\mu\text{g/g}$ of Fuel
Automobile, Diesel	0.16
Automobile, Diesel	0.030
Automobile, Unleaded Gasoline	0.014
Automobile, Leaded Gasoline	0.097
Truck, Diesel	0.0038
Truck, Gasoline	0.065
CFM-56, JP-5	0.0053
TF-39, JP-5	0.0051
CFM-56, JP-4	0.024
CFM-56, JP-8	0.012

are generally lower than from internal combustion engines. In this case the CFM-56 emission levels were slightly higher than for the TF-39. However, the observed difference between the two engines is not significant, given the variability in the determination.

Considerable caution must be exercised in interpreting these data, primarily because a representative proportion of the particle-bound PNA fraction was not necessarily collected. In the Task 2 effort (Reference 8) an analysis of the particle sample revealed that less than 2 percent of the total PNAs was bound to the particles, the vast majority being in the vapor phase. In addition, no nitro-substituted PNAs (a significant compound class from a biological viewpoint) were found. Nonetheless, the primary emphasis of this work has been the gas-phase hydrocarbon composition and more detailed particle characterization studies (Reference 7) should be consulted when making PNA comparisons to other emission sources.

c. Carbonyl Emissions

Aldehydes and ketones represent perhaps the most significant component class of jet aircraft emissions, from a health standpoint. This compound class is also photochemically very significant. Formaldehyde has been shown to cause nasal tumors and several aldehydes are severe eye irritants.

Table 31 lists formaldehyde emission levels for a variety of mobile sources (Reference 22). As shown by these data, the jet aircraft aldehyde emission levels are generally higher than the diesel or catalyst-equipped automobile, and approach the level for the non-catalyst-equipped automobile. A comparison of individual aldehyde distributions for various mobile sources is shown in Figure 28. In general the emission profiles are similar, benzaldehyde composition being the only exception.

As noted earlier, glyoxal and methyl glyoxal emissions were found to be significant components of the jet engine exhaust. However, emission data for these compounds from other sources are not available. Hence the relative contribution of jet engines can not be determined for these compounds.

TABLE 31. FORMALDEHYDE EMISSIONS FROM A VARIETY OF MOBILE SOURCES

Source	Formaldehyde Level, ppm
Automobile, Noncatalytic	24
Automobile, Catalytic	3.6
Light-Duty Diesel (1978)	5.7
Light-Duty Diesel (1980)	7.0
TF-39 Engine, JP-4	14.6
CFM-56 Engine, JP-4	9.3
CFM-56 Engine, JP-5	10.3
CFM-56 Engine, JP-8 (Shale)	13.3

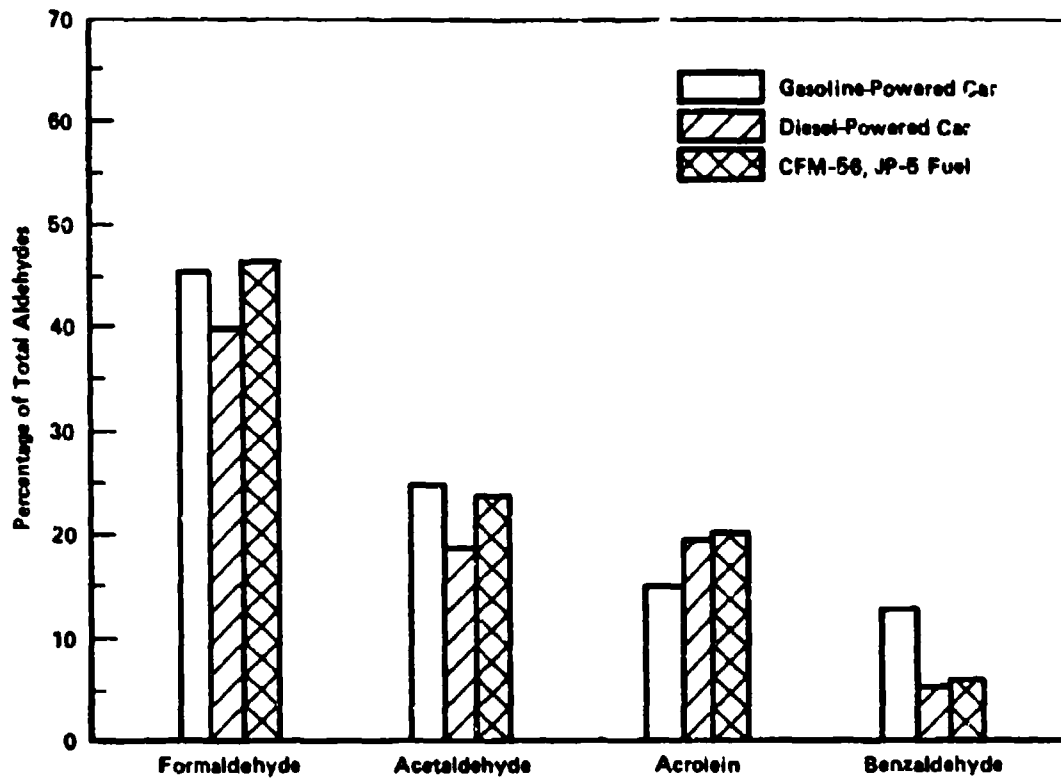


Figure 28. Percentage of Aldehydes in Exhaust from Three Combustion Sources

B. TASK 4 PHOTOCHEMISTRY EXPERIMENTS

1. Introduction

One of the major objectives of this study is to investigate the photochemical reactivity of gas turbine engine exhaust. In this context, photochemical reactivity is defined as the potential of organic species or organic mixtures to react in ambient air to produce ozone. The two principal environmental issues relating to organic emissions from turbine engines are toxicity (discussed earlier) and photochemical reactivity. In 1973, the U.S. Environmental Protection Agency promulgated emission regulations for certain categories of aircraft engines, and proposed revisions and additional regulations in 1978 (Reference 23). Approximately 98 percent of the organic emissions from commercial turbine engine aircraft in the vicinity of airports occur during engine idle and taxiing operations (Reference 24). In the 1978 regulations proposal, EPA stated, "... emissions from major air terminals dominated by commercial traffic continue to appear sufficient in magnitude to justify Federal standards applicable to commercial aircraft. At major terminals, the annual emissions due to aircraft alone are of the order of thousands of tons per year for each gaseous pollutant, while in comparison, a stationary source is defined as major under new section 302 (j) of the Clean Air Act if it emits 100 tons per year or more of any pollutant." Gas turbine aircraft engines emit significant quantities of organic compounds in the vicinity of airports. If these emissions are photochemically reactive, they may, under some conditions, contribute to the formation of photochemical smog in the vicinity of airports and possibly downwind of airports. It therefore is important to assess the reactivity of jet engine exhaust.

There are no direct measurements of the photochemical reactivity of jet engine exhaust, such as exist for automobile and diesel engine exhaust. Basic kinetic data and individual compound reactivity information derived from laboratory smog chambers have been used, together with very limited turbine engine organic composition data, to estimate the contribution of turbine engine emissions to photochemical air pollution (References 24 and 25). However, such estimates suffer from the paucity of comprehensive exhaust composition data, and the need to assume that a

linear summation of individual compound reactivities adequately represents the reactivity of a complex mixture. This assumption is invalid for many compositions due to synergistic, as well as inhibitory, effects which occur in mixtures. Because of these shortcomings in the estimation of reactivity from existing data, direct measurements of exhaust reactivity were undertaken in this study.

Many factors affect the production of ozone and other smog manifestations by a complex mixture such as jet engine exhaust. Important variables include organic composition, reactivity of organic constituents, ratio of organics to NO_x , ultraviolet light intensity, and temperature. In this study, reactivity is being assessed through the use of outdoor smog chambers, to assure that the experiments are performed under realistic environmental conditions and because well-controlled indoor smog chambers are not amenable to field installation next to a jet engine. The reactivity of exhaust from two different engines operating on three different fuels has been assessed in this study. Each experiment was conducted on a different day. Environmental conditions vary from day to day, so a reference chamber employing a constant composition of smog precursors was operated alongside the exhaust chamber to provide a means of accounting for day-to-day variations in environmental conditions. Numerous experiments were undertaken to characterize the two chambers and to demonstrate the comparability of the chambers with regard to ozone formation. These experiments were discussed in Section IV.

For purposes of this study, the primary variable defining reactivity is maximum ozone concentration. Other variables have been used to represent reactivity, including the rate of NO oxidation, the rate of hydrocarbon consumption, degree of eye irritation, and production of secondary aerosol. However, the driving force behind this study is ozone formation, since air quality standards for O_3 are on record.

The experimental aspects of the photochemical reactivity measurements are provided in Section III. Results of the photochemistry experiments are given in Section IV. The remainder of this Section is devoted to an analysis of the photochemistry experimental results.

2. TF-39 Photochemistry Experiments

The results of the TF-39 engine exhaust photochemistry experiments are shown in graphical form in Appendix A. A representative set of profiles from experiment AF-3 is shown in Figures 29-31. The exhaust and reference chambers are identified in Table 16. The experiment was initiated shortly after 0600 EDT. UV intensity (uncorrected, see Section IV) increased from $23 \text{ mcal-cm}^{-2} \text{ min}^{-1}$ to $80\text{-}90 \text{ mcal-cm}^{-2} \text{ min}^{-1}$, and remained at that level from 1200 to 1500 EDT. Temperature in the chambers peaked at 50°C . The temperature in the chambers is always elevated above ambient due to the "greenhouse" effect. The relative humidity in the exhaust chamber exceeded that in the reference chamber due to the moisture introduced with the exhaust. The relative humidity in both chambers decreased as the temperature climbed.

Concentration profiles of exhaust reactants and products are shown in Figure 30. The profiles demonstrate the classic characteristics of photochemical smog formation. Total hydrocarbons decrease as NO is converted to NO_2 . After most of the NO has been converted to NO_2 , the ozone concentration rises rapidly. A double peak was observed in the exhaust chamber, with the maximum O_3 concentration of 0.603 ppm occurring at 1402 EDT. The four measured aldehydes were present in the exhaust and therefore are present initially in the exhaust chamber. Formaldehyde is by far the dominant aldehyde. Three of the four aldehydes increase with irradiation until approximately 1000 EDT. Thereafter, the rate of consumption exceeds the rate of production. The concentration of acrolein remains relatively constant until 1100 EDT and decreases thereafter. The profiles from the reference chamber are shown in Figure 31. The behavior of the species in the reference chamber is very similar to that observed in the exhaust chamber. The concentration of O_3 peaked at 1336 EDT at a value of 0.721 ppm. Neither formaldehyde nor acetaldehyde were present initially in the reference mixture, but after 4 hours of irradiation, 294 ppb of formaldehyde and 216 ppb of acetaldehyde had formed.

A summary of the composition of the exhaust used in the TF-39 photochemistry experiments is included in Table 32. Experiments AF-3

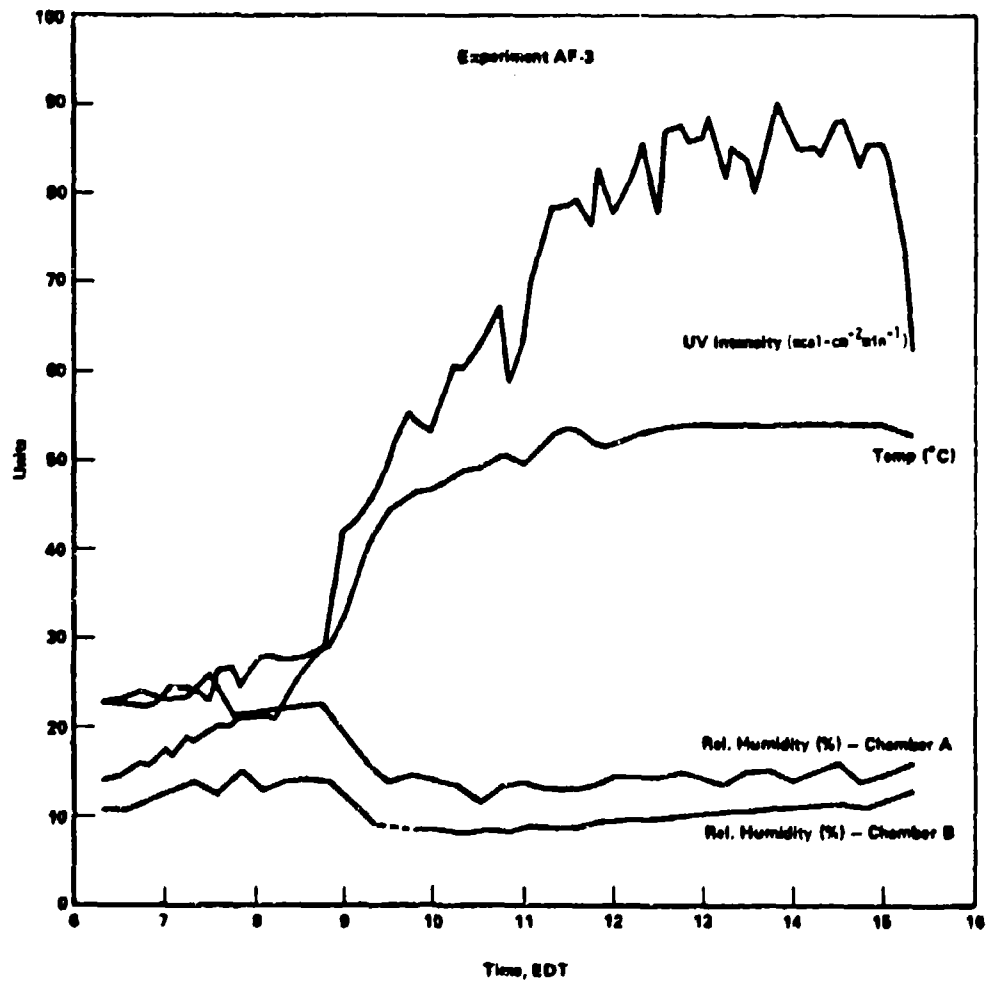


Figure 29. Smog Chamber Profiles from AF-3
Using TF-39 Engine and JP-4 Fuel

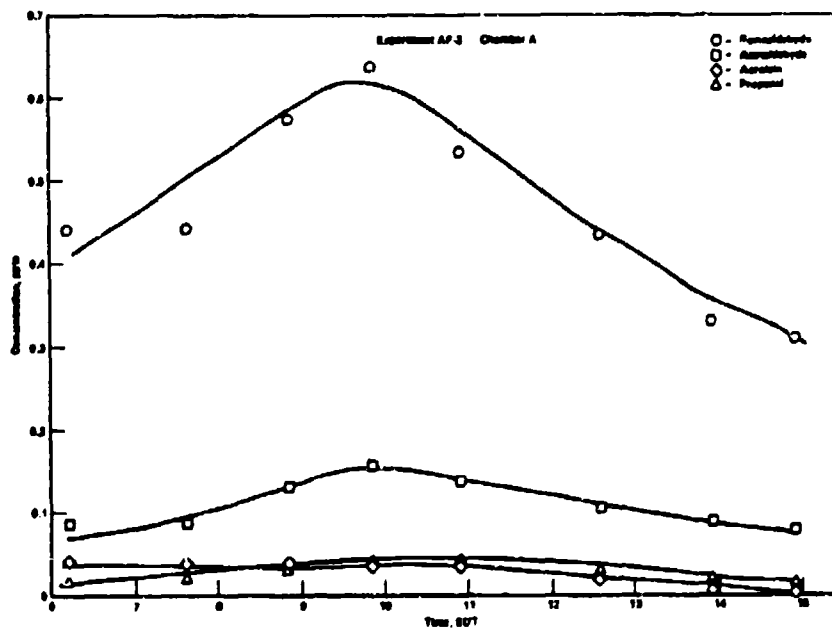
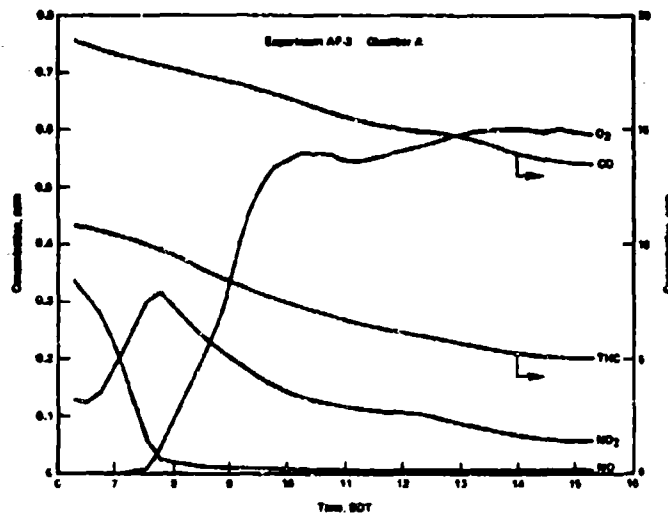


Figure 30. Smog Chamber Profiles from AF-3 Using TF-39 Engine and JP-4 Fuel (Exhaust Chamber)

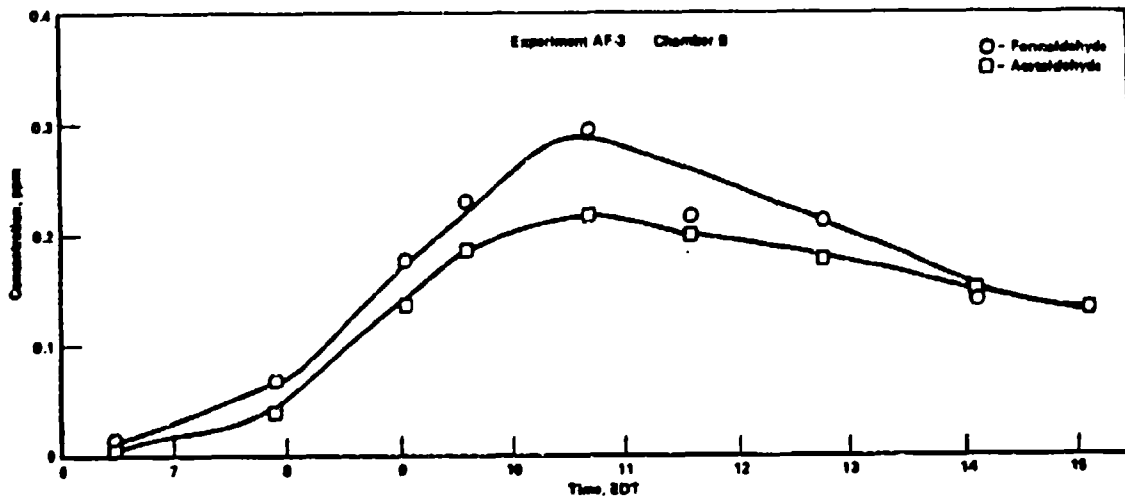
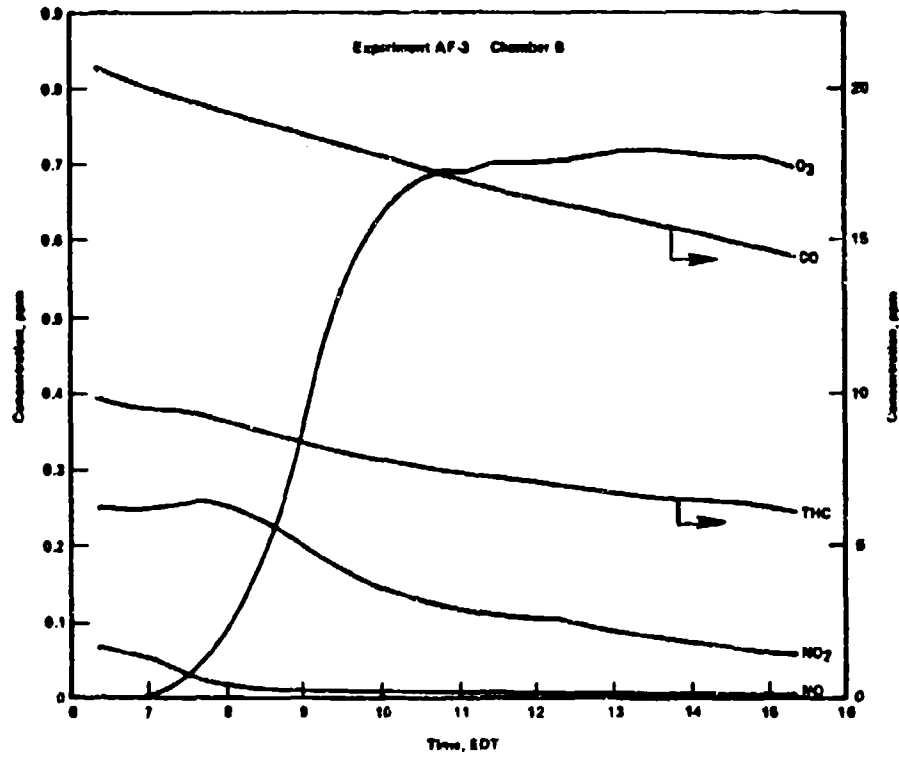


Figure 31. Smog Chamber Profiles from AF-3 Using TF-39 Engine and JP-4 Fuel (Reference Chamber)

TABLE 32. COMPOSITION OF TF-39 EXHAUST USED IN
PHOTOCHEMISTRY EXPERIMENTS

Experiment	Date	Fuel	Exhaust Composition				
			THC, ppmC	NO _x , ppm	CO, ppm	THC/NO _x	NO/NO _x
AF-2	July 19	JP-5	350	19.9	542	17.6	0.61
AF-3	July 20	JP-4	412	17.0	552	24.2	0.66
AF-4	July 21	JP-4	394	17.1	543	23.0	0.55
AF-5	July 22	Shale (JP-8)	367	18.9	544	19.4	0.58

and AF-4 are duplicate runs which can be employed to estimate reproducibility. Some daily variations in emissions are expected because the emissions are somewhat dependent on ambient temperature and humidity. Nevertheless, comparison of the AF-3 and AF-4 compositions in Table 32 indicates very good repeatability. The THC, NO_x and CO concentrations are all within ± 3 percent of the mean of the two runs. As a consequence, the THC/ NO_x ratios are quite similar. This is important because photochemical ozone production is highly dependent on the initial THC/ NO_x ratio. The greatest difference between the two experiments is found in the NO/ NO_x ratio. The higher NO/ NO_x ratio observed for AF-3 suggests that O_3 production in that run may have a longer induction period as NO is oxidized to NO_2 . Perhaps the more surprising feature of these exhaust ratios is the significant amount of NO_2 initially present in the exhaust. The NO_2 contribution to total NO_x ranges from 34 to 45 percent, which is substantially higher than 10-15 percent generally suggested for most combustion sources. The relatively high levels of NO_2 present initially will contribute to the photochemical reactivity of the exhaust by speeding the onset of O_3 formation.

Overall, the exhaust composition data in Table 32 show relatively high THC/ NO_x ratios, and the presence of substantial levels of NO_2 in the exhaust. Both of these factors will tend to promote the rate of O_3 generation under photochemically active conditions, and will enhance the maximum O_3 concentration ultimately achieved, if all other factors are equal. The ratios THC/ NO_x and NO/ NO_x are sufficiently similar for the four experiments that only minor variations in the photochemical reactivity are anticipated due to these factors. Consequently, the major factors influencing the reactivity of these four experiments are expected to be exhaust organic composition and variations in meteorological conditions.

The maximum pollutant concentrations observed for the four photochemistry experiments with TF-39 exhaust are listed in Table 33. The repeatability of the chamber experiments can be judged from a comparison of AF-3 and AF-4. JP-4 exhaust was employed for both runs. The maximum O_3 concentrations from the exhaust chamber were within ± 1 percent of the mean, demonstrating excellent reproducibility, especially when one considers that meteorological variations can influence the O_3 maxima.

TABLE 33. MAXIMUM REACTION PRODUCT CONCENTRAIONS OBSERVED
IN TF-39 SMOG CHAMBER EXPERIMENTS

Experiment	Date	Fuel	Maximum Exhaust Chamber Concentrations, ppb			Maximum Reference Chamber Concentrations, ppb				
			Formaldehyde	Acetaldehyde	Acrolein	Propanal	O ₃	Formaldehyde	Acetaldehyde	
AF-2	July 19	JP-5	574	802	142	48	30	863	237	227
AF-3	July 20	JP-4	603	637	156	41	41	721	294	216
AF-4	July 21	JP-4	612	548	115	36	27	720	304	194
AF-5	July 22	Shale	665	650	120	35	24	826	265	222

On these two days, the meteorological conditions which influence O₃ formation must have been very similar, because the concentrations of O₃ produced in the reference chamber are nearly identical. The levels of aldehydes generated by the reference mixture also are quite similar for these two experiments, providing further confirmation of the repeatability of the experiments. The maximum aldehyde levels observed in the exhaust chamber vary considerably from AF-3 to AF-4. This observation is partially explained by differences in the exhaust aldehyde levels initially injected into the chamber. These data were presented earlier in Table 6.

The photochemical reactivity of these four experiments is best ascertained by comparing the O₃ results plotted in Figure 32. As already noted, the maximum O₃ concentrations produced by the exhaust and reference mixtures in the duplicate JP-4 experiments, AF-3 and AF-4, are nearly identical. On the other 2 days (experiments AF-2 and AF-5), the reference mixture produced higher O₃ concentrations, suggesting that the meteorological conditions were more conducive to O₃ formation on those days. The dilute exhaust also generated a higher O₃ maximum during the shale-derived JP-8 fuel experiment (AF-5), indicating that the relative reactivity of the JP-4 and shale-derived JP-8 fuel exhausts are similar. However, the maximum O₃ concentration in the JP-5 exhaust run (AF-2) is lower than the other experiments, despite the fact that the reference mixture yielded the highest concentration of all four runs. This observation suggests that the relative reactivity of JP-5 exhaust may be lower than JP-4 and shale fuel exhaust. This lower reactivity may be related to the organic composition of the exhaust, the lower initial THC/NO_x (Table 32) or some combination of the two. The influence of the organic composition of the exhaust on reactivity is discussed shortly.

One means of describing the relative reactivity of the exhaust makes use of the O₃ maximum in the reference chamber to normalize the experiments with respect to meteorological conditions. Due to induction times which may delay the onset of O₃ formation and likely nonlinearities in the chemical systems, this approach is most appropriate when the reactivities of the exhaust and reference mixtures are similar and variations in meteorological conditions are not dramatic. These conditions are met quite well by the

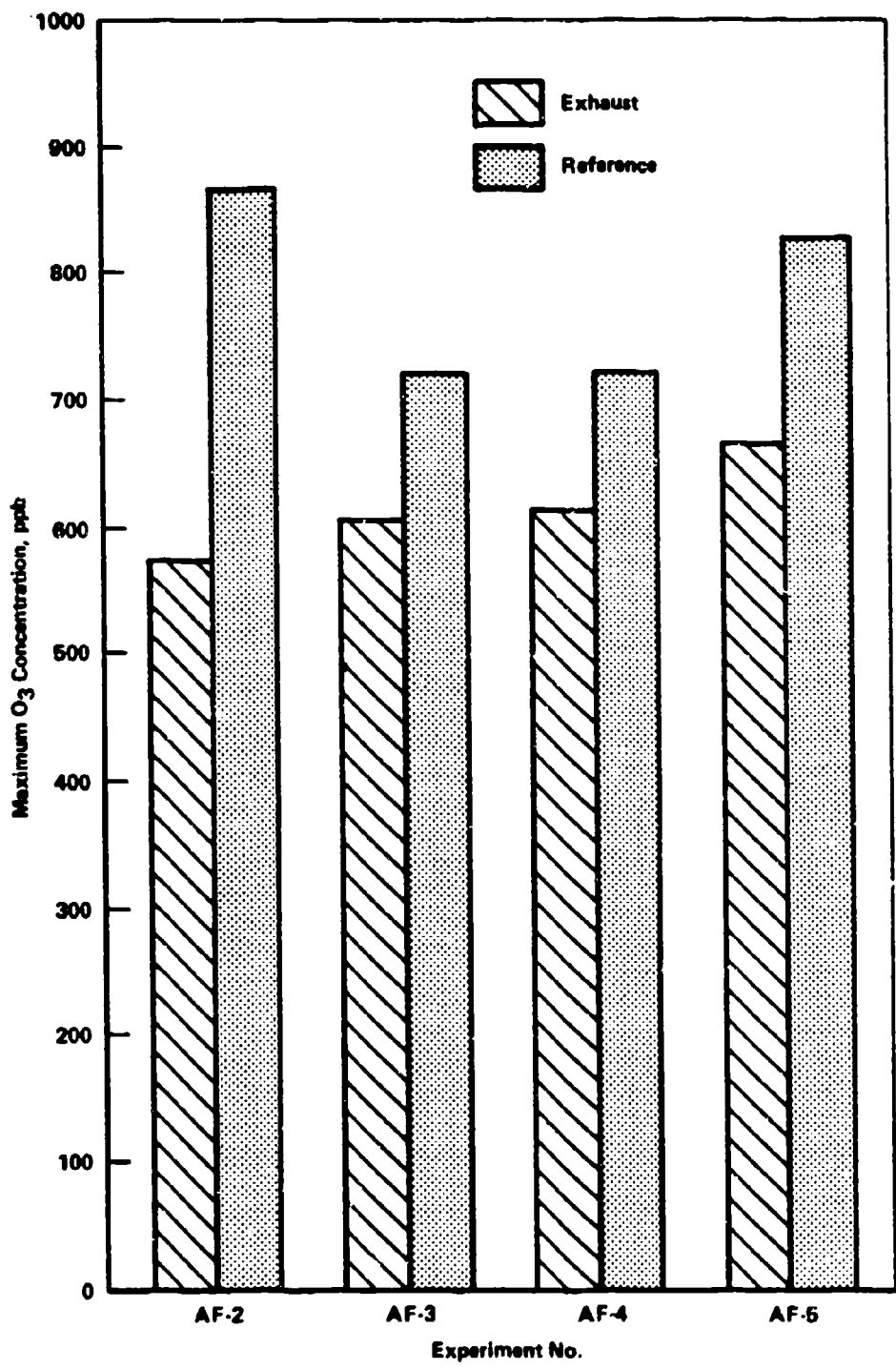


Figure 32. Maximum O₃ from TF-39 Experiments

TF-39 experiments. The ratio of maximum O_3 in the exhaust chamber to maximum O_3 in the reference chamber is listed in Table 34. This table illustrates the lower relative reactivity of JP-5 exhaust generated by the TF-39 engine. Based on the normalized reactivity, the JP-5 exhaust from the TF-39 engine is approximately 20 percent less reactive than either the JP-4 or shale-derived JP-8 fuel exhausts for conditions of strong photochemical activity.

The reference chamber results can only be used to normalize the exhaust reactivity if the two chambers behave comparably and if the reference chamber loadings are similar from experiment to experiment. The comparability of the chambers is excellent, judging from the baseline reactivity experiment and the system demonstration experiment discussed in Section IV. The repeatability of the initial reference chamber concentrations can be addressed by comparing the initial THC levels and THC/NO_x ratios. The initial THC concentrations in the reference chamber were very similar, ranging from 10.2 to 10.4 ppmC, and the important THC/NO_x ratio varied by less than ± 4 percent from the mean of 29.5 at the start of the four experiments. The comparability of the two chambers and the excellent reproducibility in the reference chamber loadings indicate that differences in reference chamber O_3 concentration are due to meteorological variations, rather than chamber or loadings factors, and that the reference chamber data can be used to normalize the exhaust chamber results with respect to meteorological variations.

It is useful to determine how differences in initial exhaust concentrations might effect the ultimate reactivity of an experiment. This can be accomplished by comparing the results from the system demonstration experiment (AF-1, Figure 22) with AF-2 (Appendix A). Both experiments made use of JP-5 exhaust from the TF-39 engine, but the chamber loadings for the system demonstration experiment were twice the AF-2 loadings. The THC/NO_x ratios were similar for both experiments. The difference in maximum ozone concentration between AF-1 and AF-2 was only 10 percent, despite the factor of two difference in initial exhaust loading. The conclusion to be drawn from this observation is that minor variations in initial exhaust loading should have little effect on the ultimate ozone concentration produced by the exhaust.

TABLE 34. TF-39 EXHAUST REACTIVITY RELATIVE
TO REFERENCE MIXTURE

Fuel	Normalized Reactivity
JP-4	0.8
JP-5	0.7
JP-8 (shale)	0.8

One other feature of the TF-39 engine exhaust photochemistry experiments which warrants discussion is the production of light-scattering aerosol. The results of integrating nephelometer measurements of the light-scattering coefficient (b_{scat}) made at the end of each experiment are shown in Table 17. These data represent secondary, or photochemically produced, aerosol since all primary particulate matter (i.e. smoke) was filtered out of the exhaust by a high-efficiency quartz fiber filter during the chamber-loading process (see Section III). As noted in Table 17, the reference mixture produced consistently low levels of light-scattering aerosol. This is consistent with the very volatile, low molecular weight, and nonaromatic nature of the reference organic mixture. The duplicate JP-4 exhaust experiments generated nearly equal concentrations of light-scattering aerosol, with b_{scat} values of 2.1 and $2.2 \times 10^{-4} \text{ m}^{-1}$. The light-scattering coefficients from the JP-5 and JP-8 (shale-derived) exhausts were substantially higher. This is in keeping with the lower volatility of the exhaust compounds produced by these two fuels. In general, low volatility and/or aromatic hydrocarbons react in photochemical systems to produce condensable species which end up in the aerosol phase. Compared to the JP-4 exhaust, the JP-5 and JP-8 (shale) exhausts reacted to produce substantially greater amounts of secondary light-scattering aerosol. From these limited results it is difficult to assess the environmental consequences of this observation, other than to note that the exhausts from these two fuels will react in the atmosphere under photochemically active conditions to produce visibility-degrading particulate matter to a much greater extent than the JP-4 exhaust.

3. CFM-56 Photochemistry Experiments

The results of the CFM-56 engine exhaust photochemistry experiments are shown in graphical form in Appendix A. Summaries of the experimental conditions and results were presented in Tables 18 and 19. The general features of these profiles are very similar to those obtained from the TF-39 engine exhaust. The main differences in the two sets of engine experiments are the lower UV intensities and lower chamber temperatures of the CFM-56 experiments. The reduced temperatures and light intensities result from the fact that the CFM-56 experiments were conducted in October

and November. The engine was unavailable for experiments earlier in the year. One of the experiments, AF-7, was conducted under very overcast, occasionally rainy conditions, and has not been reported. It was subsequently repeated under more favorable conditions. Two other experiments, AF-8 and AF-10, were carried out under overcast or mostly cloudy skies. These two runs are included because they exhibited some degree of reactivity and might be useful in future kinetic modeling applications.

A summary of the composition of the exhaust used in the CFM-56 experiments is provided in Table 35. Compared to the TF-39 emissions noted in Table 32, the CFM-56 engine emitted much less THC and slightly more NO_x and CO. As a consequence, the THC/ NO_x ratio is substantially lower than in the TF-39 exhaust. The NO/ NO_x ratios are generally higher. Both of these factors are expected to increase the induction time of the photochemistry experiments, relative to the TF-39 exhaust runs. The longer induction time before the appearance of O_3 is a result of the longer time required to oxidize NO to NO_2 under the CFM-56 exhaust conditions.

The summary data in Table 18 show that two experiments were carried out in an attempt to evaluate the repeatability of chamber experiments with CFM-56 exhaust. Unfortunately, due to poor weather, one of the runs in each of the attempted duplicate pairs (AF-8/AF-9 and AF-6/AF-10) had insufficient sunlight intensity to overcome the induction time, thus precluding an evaluation of reproducibility. Because the baseline reactivity, system demonstration, and TF-39 experiments demonstrated excellent repeatability, and, lacking any data to the contrary, we assume in the following discussion that the performance of the two chambers is comparable and that the chamber experiments are reproducible.

The maximum pollutant concentrations observed in the five photochemistry experiments with CFM-56 engine exhaust are listed in Table 36. There is considerable scatter in the aldehyde data, with two formaldehyde values from AF-10 considered suspect due to unusual features in the chromatogram. We attribute the remainder of the scatter to real differences in exhaust composition and daily variations in the photochemical conditions leading to aldehyde production. The tabulated O_3 maxima are plotted in bar-graph format in Figure 33. As mentioned earlier, the meteorological

TABLE 35. COMPOSITION OF CFM-56 EXHAUST USED IN
PHOTOCHEMISTRY EXPERIMENTS

Experiment	Date	Fuel	Exhaust Composition				
			THC ppmC	NO _x ppm	CO ppm	THC/NO _x	NO/NO _x
AF-6	October 19	JP-5	174	19.2	770	9.1	0.91
AF-8	October 25	JP-4	99	20.3	611	4.9	0.66
AF-9	October 26	JP-4	126	20.7	679	6.1	0.63
AF-10	November 3	JP-5	105	21.4	617	4.9	0.70
AF-11	November 7	Shale (JP-8)	148	22.1	695	6.7	0.72

TABLE 36. MAXIMUM REACTION PRODUCT CONCENTRATIONS OBSERVED
IN THE CFM-56 SMOG CHAMBER EXPERIMENTS

Experiment	Date	Fuel	Maximum Exhaust Chamber Concentrations, ppb			Maximum Reference Chamber Concentrations, ppb			
			Formaldehyde	Acetaldehyde	Acrolein	Propanal	O ₃	Formaldehyde	Acetaldehyde
AF-6	October 19	JP-5	646	138	75	34	419	414	211
AF-8	October 25	JP-4	037	--	--	--	279	--	--
AF-9	October 26	JP-4	665	188	23	112	468	273	194
AF-10	November 3	JP-5	085	170	87	<25	368	1,300 ^a	200
AF-11	November 7	Shale	639	186	27	95	708	383	279

^aThis value is suspect because of the unusual shape of the chromatographic peak.

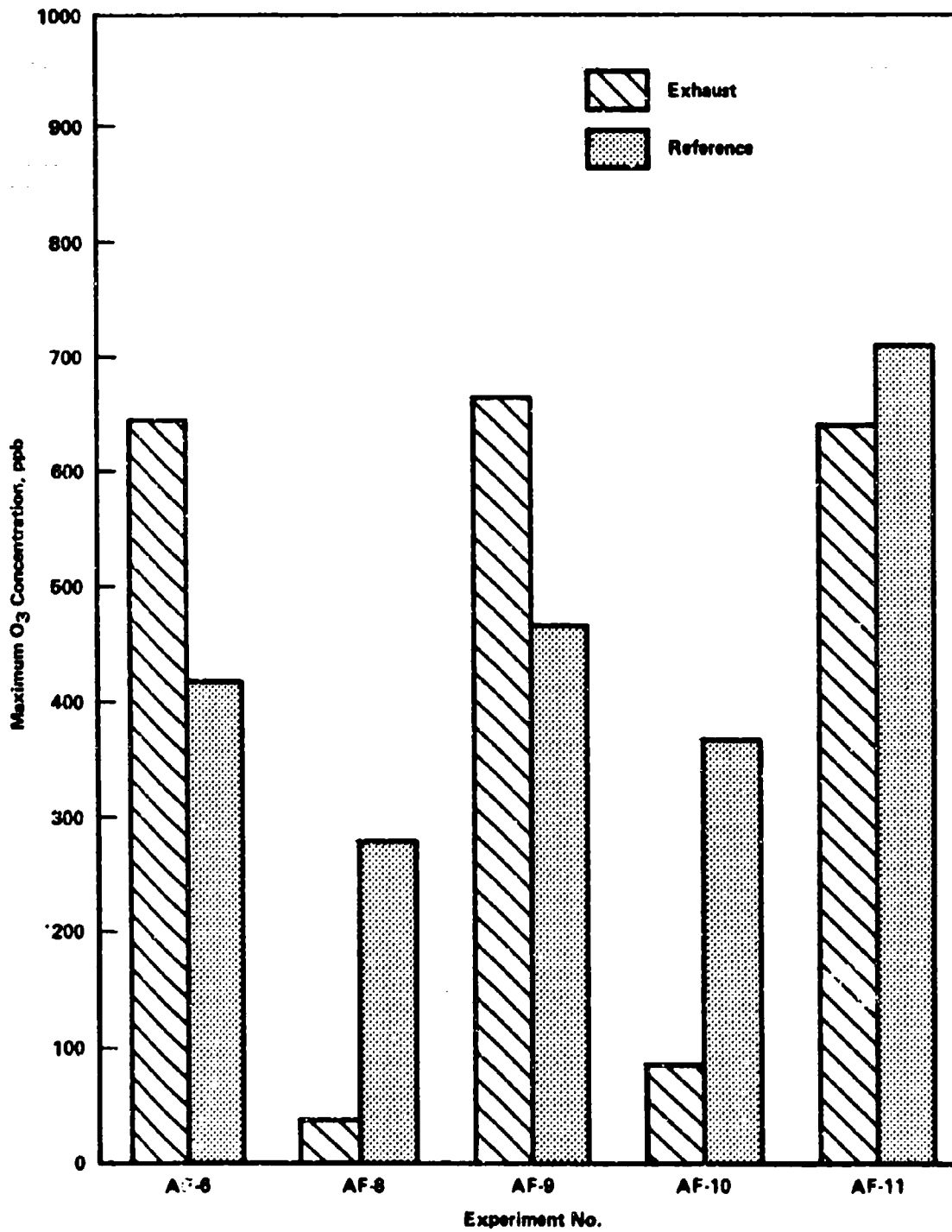


Figure 33. Maximum O₃ from CFM-56 Experiments

conditions for photochemical reaction were unfavorable for experiments AF-8 and AF-10. The reference mixture generated significant levels of O_3 on both days, although the exhaust reactions produced very little O_3 due to the long induction times at low light intensities mentioned previously. The integrated UV intensities from all nine exhaust photochemistry experiments are listed in Table 37. The data show that experiments AF-8 and AF-10 experienced the lowest UV intensities, and, as a consequence, the maximum O_3 concentrations were much lower than in the other experiments. Because these two experiments were conducted under atypical conditions relative to the other runs, they are not discussed further in this report. However, the results may be useful in future modeling studies, where a range of meteorological conditions would extend the modeling data base.

The exhaust and reference chamber O_3 data from the CFM-56 experiments are plotted in Figure 33. The three most useful runs for our purposes are AF-6, AF-9, and AF-11. As noted in Table 36, AF-6 made use of JP-5 exhaust, AF-9 used JP-4 and AF-11 employed exhaust from the shale-derived JP-8 fuel. The reference mixture produced differing maximum O_3 levels for these three runs, due to differences in meteorological conditions and, in the case of AF-6, to a problem with chamber loading. The reference chamber was overloaded by 0.1 ppm NO at the start of AF-6. While this only represents an 18 percent difference in the THC/NO_x, the effect on O_3 formation is large because NO inhibits O_3 production and prolongs the induction period. The data in Table 19 show that the O_3 maximum in the reference chamber precedes that in the exhaust chamber for all experiments except AF-6. Unquestionably, the excess NO in AF-6 has delayed the onset of O_3 formation and possibly affected the maximum O_3 concentration achieved in the experiment. Under the circumstances, it is prudent to consider the reference chamber O_3 maximum from AF-6 as a lower limit, and exercise caution in normalizing the exhaust results for this experiment. If it is assumed that the maximum O_3 which would have been produced in AF-6 with the correct NO loading would have been similar to the maximum concentration observed in the other CFM-56 experiments (i.e. 0.708 ppm in AF-11), then upper and lower limits for reference chamber O_3 can be assigned, and the normalized JP-5 exhaust reactivity can be estimated to lie between the corresponding upper and lower limits. The normalized reactivities

TABLE 37. INTEGRATED UV INTENSITIES^a (cal-cm⁻²)

Experiment	At Time Of Exhaust Chamber O ₃ Maximum	At Time Of Reference Chamber O ₃ Maximum	At End Of Experiment
AF-2	17.03	15.62	22.20
AF-3	18.12	16.35	23.59
AF-4	16.26	13.76	24.56
AF-5	8.67	8.87	13.21
AF-6	11.10	13.84	15.06
AF-8	3.15	2.48	3.75
AF-9	11.36	5.24	12.33
AF-10	3.13	3.13	7.11
AF-11	10.04	5.36	10.17

^aCorrected for offset noted in Section III.

estimated from the CFM-56 experiments are listed in Table 38. The reactivity range for JP-5 exhaust is based on the limits noted above. These results indicate that the exhaust from the shale-derived JP-8 fuel is slightly less reactive than the reference mixture; the JP-4 exhaust is considerably more reactive than the reference mixture; and the JP-5 exhaust may be of similar or greater reactivity than the reference mix. The shale fuel exhaust is about 40 percent less reactive than JP-4 exhaust, while JP-5 exhaust could be slightly greater or significantly less reactive than JP-4, owing to the uncertainty in the JP-5 reactivity.

In the discussion of the TF-39 exhaust reactivity, two criteria had to be met to justify the normalization of the exhaust reactivity through use of reference mixture reactivity: (1) the behavior of the two chambers must be comparable and (2) meteorological conditions should be similar for all experiments in the set. With respect to the CFM-56 exhaust experiments, the first condition has been met, but the meteorological criterion is not so certain. For experiments AF-8 and AF-10 the meteorological conditions were so unfavorable to photochemical reaction that the exhaust chamber barely reached the onset of O₃ formation. Even for the other three CFM-56 runs, the meteorology was much more variable than for the TF-39 experiments, and the effect of this variability on reactivity is uncertain. For this reason, the reader must remember that the CFM-56 relative reactivities are considered to be less reliable than those estimated from the TF-39 runs. However, there is little doubt that the CFM-56 exhaust from the three fuels is of similar or greater reactivity compared to the reference mixture.

The light-scattering aerosol results from the CFM-56 experiments are given in Table 19. Data are missing for AF-6 and AF-8 due to an instrument malfunction. Based on the three remaining runs, the exhaust from the shale-derived JP-8 fuel yielded the highest scattering coefficient, with JP-5 exhaust second and JP-4 producing the least light scattering. The b_{scat} values in the reference chamber are low and reproducible. It is noteworthy that the JP-5 exhaust produced substantial amounts of light-scattering aerosol, even though very little O₃ was produced under prevailing meteorological conditions. As noted earlier, the relative amounts of secondary aerosol generated by the three exhausts is in keeping with the

TABLE 38. CFM-56 EXHAUST REACTIVITY RELATIVE TO REFERENCE MIXTURE

Fuel	Normalized Reactivity
JP-4	1.4
JP-5	0.9 - 1.5
JP-8 (shale)	0.9

known tendency of low-volatility or highly aromatic mixtures to generate photochemical aerosol. In this case, the composition of the three fuels would suggest this relative order of secondary aerosol formation.

4. Comparison of TF-39 and CFM-56 Exhaust Reactivities

In terms of emissions, the TF-39 is a current-generation engine and is not equipped with emission abatement features. The CFM-56, on the other hand, represents an advanced engine specifically designed for low emissions. The emissions measurements presented earlier in this report document the reduced emissions of the CFM-56 relative to the TF-39 engine. The question addressed in this section concerns the relative photochemical reactivity of emissions from the two engines.

All of the photochemical reactivity experiments conducted during this project were run with an initial hydrocarbon concentration of 10 ppmC. Because the hydrocarbon concentration in the CFM-56 exhaust was considerably lower than the TF-39, a larger volume of exhaust was injected into the chambers for the CFM-56 experiments. Comparison of exhaust reactivity between the two engines is on a mass basis, because the chambers were loaded to a fixed ppmC concentration.

The relative reactivity of exhaust from the two engines is compared for each fuel type in Table 39. The reactivity (relative to the reference mixture) of the CFM-56 exhaust is higher than that of the TF-39 exhaust in all cases. The greatest reactivity difference across engines occurs for the JP-4 exhaust, and the smallest difference was found with JP-8 exhaust. The JP-5 experiments cannot be compared quantitatively due to the uncertainty associated with the CFM-56 results. Nevertheless, it is clear that the JP-5 exhaust from the CFM-56 engine is more reactive than the TF-39, and may be substantially more reactive.

An interesting question concerns the relative reactivity of equal volumes of exhaust from the two engines. This question can only be addressed in a rather hypothetical way using the results of this study. It is possible to speculate on this issue, using the results from AF-1, the system demonstration experiment. If we had conducted experiments with equal volumes of exhaust, the organic concentration in the TF-39

TABLE 39. COMPARISON OF NORMALIZED PHOTOCHEMICAL REACTIVITIES ACROSS ENGINES AND FUELS (based on equal mass of organic emissions)

	TF-39	CFM-56
JP-4	0.8 ^a	1:4
JP-5	0.7	0.9-1.5
JP-8 (shale)	0.8	0.9

^aBased on duplicate experiments.

chamber would have been 2-4 times that in the comparable CFM-56 experiment, depending on the fuel and ambient conditions which influence emissions. Thus, if we can show the effect on maximum O₃ of increased chamber hydrocarbon loading with the TF-39 engine, then we can speculate on the reactivity differences for equal exhaust volumes. The System Demonstration Experiment (AF-1) is useful in this regard, since it was initiated with 23 ppmC hydrocarbon, or 2.3 times the normal loading. Figure 22 and Table 17 show that this experiment produced only about 6 percent more O₃ than the corresponding experiment at 10 ppmC run the next day under nearly identical meteorological conditions. This suggests that the relative reactivity of equal volumes of TF-39 and CFM-56 exhaust will differ little from the relative reactivity as determined on a mass basis. However, the effect of chamber loading on maximum O₃ could be different for the exhaust from the other fuels, due to the differences in organic composition. For this reason, speculation on volumetric reactivity comparisons may not hold for the other two fuels. If this speculation is valid for JP-5 exhaust, however, it suggests that, although the CFM-56 organic emissions are considerably lower than the TF-39, the increased reactivity of the organics in the CFM-56 exhaust cause it to be more reactive than the TF-39, in spite of the lowered emissions. At this time, this speculation is unsupported by direct experimental data, and may be unfounded. Forthcoming combustor rig experiments which will focus on photochemical reactivity should shed light on this subject. It will also be important to compare the reactivities in a consistent manner, since the concentration of organics in equal volumes of exhaust is influenced by bypass air, and the ratio of bypass flow to core flow varies between engine types.

5. Influence of Exhaust Composition on Photochemical Reactivity

It is of interest to know the relative contribution of various organic compound classes to the photochemical reactivity of turbine engine exhaust. Reactivity contributions can be estimated using a reactivity index for each compound and a linear summation procedure. The reactivity of a mixture of organic species is calculated as

$$\text{Total Reactivity} = \sum_{i=1}^{i=n} m_i r_i$$

where m equals molar concentration (ppmV) of an organic compound and r is the reactivity index for that compound. The molar concentrations for each compound were determined by dividing the species data in Tables 6-8 by the number of carbon atoms in each compound. Unresolved or unknown peaks are generally part of the unburned fuel and were assigned a carbon number representative of the particular fuel. The resulting molar distribution in the exhaust from the two engines and three fuels is shown in Table 40. The distribution is nearly independent for a given engine. There is a significant difference between engines, however, with the CFM-56 engine yielding a higher percentage of aldehydes. The photochemically reactive alkenes and aldehydes made up 74 percent of the organic emissions, on a molar average basis.

The reactivity index used for these calculations was derived by Dimitriades (Reference 26) from several published smog chamber studies. This particular index was chosen because it is based on the most comprehensive data base, it uses O_3 maximum as its reactivity criterion, and it is a five-class scheme, so it can distinguish various levels of reactivity. The classification scheme is shown in Table 41. The molar concentrations and total calculated reactivities for the engine/fuel combinations are displayed in Table 42. Where organic composition data were available from duplicate runs in Tables 6-8, the run of highest total concentration was used to calculate reactivity to improve accuracy. The data show considerable differences in both concentration and total reactivity, as expected from the results in Tables 6-8.

The reactivity data have been further subdivided to show the contribution of the various classes of organic compounds to total reactivity. These results are listed in Table 43. A number of features of the compound class reactivity results are noteworthy. The aromatic hydrocarbons contribute no more than 2 percent of the total reactivity for any fuel/engine combination. The alkanes contribute up to 12 percent, and their contribution is greatest for JP-4, which has also the highest paraffinic content in the fuel (Table 12). For all three fuels, the alkane contribution is slightly greater for the TF-39 engine. The greatest

TABLE 40. MOLAR DISTRIBUTION OF EXHAUST ORGANIC COMPOUNDS^a (mole %)

	JP-4		JP-5		JP-8	
	TF-39	CFM-56	TF-39	CFM-56	TF-39	CFM-56
Alkanes	28	26	29	21	25	21
Alkenes	49	42	45	46	50	46
Aromatics	3	2	3	2	4	3
Aldehydes	20	30	23	31	21	30

^aAssumes unknown compounds are alkanes.

TABLE 41. FIVE CLASS REACTIVITY CATEGORIZATION OF ORGANIC COMPOUNDS (Reference 26)

	Class I	Class II	Class III	Class IV	Class V
	C ₁ -C ₃ paraffins	Mono-tert-alkyl benzenes	C ₄ -paraffins	Prim- & sec-alkyl benzenes	Aliphatic olefins
	Acetylene	Cyclic ketones	Cycloparaffins	Dialkyl benzenes	o-methyl styrene
	Benzene	Tert-alkyl acetates	Alkyl acetylenes	Branched alkyl ketones	Aliphatic aldehydes
	Benzaldehyde	2-nitropropane	Styrene	Prim- & sec-alkyl alcohols	Tri- & tetra-alkyl benzenes
	Acetone		N-alkyl ketones	Cellulosolve acetate	Unsaturated ketones
	Tert-alkyl alcohols		Prim- & sec-alkyl acetates	Partially halogenated olefins	Diacetone alcohol
	Phenyl acetate		N-methyl pyrrolidone		Ethers
	Methyl benzoate		N,N-dimethyl acetamide		Cellosolves
	Ethyl amines				
	Dimethyl formamide				
	Methanol				
	Perhalogenated hydrocarbons				
	Partially halogenated paraffins				
Relative Reactivity	1.0	3.5	6.5	9.7	14.3

TABLE 42. MOLAR CONCENTRATIONS AND TOTAL REACTIVITY

	TF-39		CFM-56	
	Conc., ppmV	Reactivity	Conc., ppmV	Reactivity
JP-4	125.9	1289.0	45.0	483.5
JP-5	102.7	1084.7	64.8	706.3
JP-8	102.7	1078.8	67.6	728.2

TABLE 43. CONTRIBUTION OF COMPOUND CLASSES TO
PHOTOCHEMICAL REACTIVITY^a (percent of total)

	JP-4		JP-5		JP-8	
	TF-39	CFM-56	TF-39	CFM-56	TF-39	CFM-56
Alkanes	12	10	8	6	9	7
Alkenes	59	49	60	50	60	52
Aromatics	2	2	1	1	2	2
Aldehydes	27	39	31	42	29	39

^aUsing O_3 scale cited in Reference 26.
max.

contributor to photochemical reactivity regardless of fuel or engine, is the alkene category. This is due in large measure to the dominance of ethylene in the exhaust. On a molar basis, ethylene makes up approximately 25-30 percent of the total exhaust organics. However, other very reactive olefins are also present in abundance. The reactivity contribution of the alkenes ranges from a low of 49 percent up to 60 percent. In all cases, the contribution is significantly greater for the TF-39. The second greatest reactivity contributor in all cases is the aldehyde class, and again, there is one dominant compound in this class, namely, formaldehyde. The aldehydes, which make up 20-30 percent of the exhaust organic concentration, contribute 27-42 percent of the photochemical reactivity. As with the other compound classes, there are no significant differences among the fuels for a given engine. There is, however, a very important difference between engines. For each fuel, the aldehydes contribute substantially more to the reactivity of the CFM-56 exhaust than to the TF-39. This observation is consistent with the compositional data in Table 40.

The compound class reactivity results in Table 43 show that alkenes contribute 50-60 percent of the photochemical reactivity of the exhaust from these two engines operating at idle. Aldehydes contribute about 30 percent of the TF-39 exhaust reactivity and 40 percent of the CFM-56 reactivity. On the average, alkanes produce only 9 percent of the total reactivity, and aromatic compounds only 2 percent. There are only minor differences in reactivity from fuel to fuel for a given engine. A comparison between engines shows a much greater aldehyde contribution for the CFM-56, with corresponding lower contributions from the alkanes and alkenes.

The observations relating to aldehyde concentration are noteworthy, because of their photochemical contributions, and because certain aldehydes are known eye irritants, and formaldehyde has been shown to cause nasal tumors. Some perspective on the relative emissions of carbonyl compounds from these engines and other mobile sources was presented earlier in this report.

It is important to note that the linear summation technique used to generate the reactivity data presented here has known shortcomings,

especially in dealing with complex mixtures. As a consequence, the calculated reactivity values should be used with caution. The results are adequate for comparing relative reactivity among fuels, engines and compound classes, but the absolute values resulting from these calculations may not be significant.

6. Comparison of Observed and Calculated Photochemical Reactivities

Previous sections of this report compared measured photochemical reactivities of exhausts among fuels and between engines. The exhaust composition data also were used to compare calculated reactivities among fuels, engines and organic compound classes. It is reasonable to ask how the observed and calculated reactivities compare. To make this comparison, the experimentally determined reactivities in Table 39 and the calculated reactivities in Table 42 must be put into comparable units. The calculated reactivities must be put on a weight basis because the chamber experiments were performed in this manner. Therefore, the calculated reactivities have been divided by the exhaust concentration in ppmC to obtain reactivity per ppmC. The calculated exhaust reactivities were then normalized to the reference mixture by dividing by the calculated reference mixture reactivity. The resulting normalized reactivities are listed in Table 44. The measured and calculated reactivities listed in Table 44 have been normalized using the measured and calculated "reference mixture" reactivities, respectively. This method of treating the data will allow us to compare the measured and calculated reactivities on a similar basis.

It is clear from the data in Table 44 that both the measured and calculated reactivities for the TF-39 exhaust are relatively independent of fuel type. For each fuel, the reactivity calculated from exhaust composition is significantly higher than the measured reactivity. Putting this a different way, the reactivity predicted from exhaust composition suggests that the TF-39 exhaust is more reactive than the reference mixture, while the actual chamber data show the exhaust is less reactive than the reference mixture under these experimental conditions.

The calculated reactivities for the CFM-56 exhaust are similar for all three fuels and are higher than the calculated TF-39 reactivities.

TABLE 44. MEASURED AND CALCULATED EXHAUST REACTIVITIES
 NORMALIZED TO REFERENCE MIXTURE REACTIVITY

	TF-39		CFM-56	
	Measured	Calculated	Measured	Calculated
JP-4	0.8	1.4	1.4	1.5
JP-5	0.7	1.4	0.9 - 1.5	1.6
JP-8 (shale)	0.8	1.2	0.9	1.6

Both measured and predicted reactivities show the CFM-56 exhaust to be more reactive than the TF-39. The measured and calculated results for the CFM-56/JP-4 combination are similar. The CFM-56 results for JP-5 fuel can not be compared quantitatively because of the uncertainty in the measured value, but the measured reactivity is similar to or less than the predicted value. The measured reactivity for the CFM-56/JP-8 experiment is significantly less than the calculated reactivity. In this regard, it follows the trend observed in the TF-39 comparisons.

It is noteworthy that, in every case, the reactivity based on exhaust composition overpredicts the reactivity actually measured through smog chamber experiments. The implications of this observation will be discussed further in the next subsection.

It is clear from Table 44 that the reactivity calculations based on exhaust composition do not adequately predict the measured differences in reactivity between the two engines. The reasons for this are uncertain, although others have observed this same phenomenon (Reference 28,29). It may be that the reactivity scale use in the calculations inadequately represents the reactivity of compounds in complex mixtures. It is also possible that real exhaust compositional differences other than organic species may have affected the measured reactivity. For example, the NO_x concentration was threefold higher in the CFM-56 chamber experiment with JP-4 fuel than in the comparable TF-39 experiment. It is possible that this, or some other unknown factor which is not accounted for in the reactivity calculations, is the cause of the reactivity differences. Combustor rig exhaust photochemistry experiments, currently are in the planning stage, may shed light on this issue.

7. Comparison of Turbine Engine Exhaust Reactivity With Other Emission Sources

The exhaust reactivity results and molar concentrations listed in Table 42 can be used to calculate molar reactivities for each turbine engine/fuel combination. These results can then be compared with estimates of molar reactivities of organic emissions from other sources. Table 45 shows the molar reactivities calculated from the exhaust composition data.

TABLE 45. MOLAR REACTIVITIES CALCULATED FROM EXHAUST COMPOSITION

	TF-39 Exhaust	CFM-56 Exhaust
JP-4	10.3	10.7
JP-5	10.5	10.9
JP-8	10.5	10.8

These reactivities were derived using the five category relative reactivity scheme proposed by Dimitriadis (Reference 26) and used by Trijonis and Arledge (Reference 24). These latter authors used this scheme to estimate the molar reactivity of organics from various emission sources in the Los Angeles basin.* Spicer and Levy (Reference 27) used the same reactivity classification to estimate the reactivity of diesel and automobile organic emissions, and Levy et al. (Reference 28) used this scale to compare reactivities for auto exhaust measured in Battelle's indoor smog chamber with reactivities calculated from exhaust composition data. Table 46 lists the molar reactivities of organic emissions from a number of different sources. The report of Trijonis and Arledge (Reference 24) should be consulted for molar reactivities for a large number of other organic emission sources.

The molar reactivity of jet aircraft emissions estimated by Trijonis and Arledge (Reference 24) is only about 15 percent lower than the TF-39 estimate of this study. This is relatively good agreement considering the lack of detailed exhaust composition data available to

* A scale factor of 10.2 has been applied to the relative reactivities in Reference 24 to make them consistent with our scale.

the authors of Reference 24. The organic distribution they used to approximate jet engine emissions at idle is very different from the distribution determined in this study. The paraffinic contribution was greatly overestimated, while the levels of olefins and aldehydes were seriously underestimated. Exhaust organic reactivities for piston aircraft and gasoline-powered vehicles are somewhat lower than the jet aircraft estimates in Table 46. Diesel emissions show similar molar reactivities compared to the two turbine engines investigated in this study.

These comparisons make use of estimated reactivities generated from the measured exhaust composition. It was previously shown that the reactivities actually measured in the smog chambers did not always track the reactivities estimated from composition data. In the worst case, the measured and estimated reactivities (normalized) differ by a factor of 2. Comparisons of photochemical reactivities for diesel exhaust organics have shown measured reactivities nearly twice as high as calculated reactivities (Reference 29), and Levy et al. (Reference 28) found only weak correlation between measured and calculated reactivities. As a consequence, comparisons of the molar source reactivities in Table 46 should be tempered with knowledge of the uncertainties inherent in the estimation procedure.

A final comment is necessary to put the reactivity of turbine engine exhaust in perspective. The molar reactivity results in Table 46 show that turbine engine emissions are the most reactive of the various sources listed. However, our measurements (Table 44) indicate that they are actually substantially less reactive than the composition-based predictions suggest. To estimate the contribution to photochemical air pollution from aircraft turbine engine operations, the region of interest must be defined and relative emissions from the various sources in that region must be taken into account. The composition and reactivity data in this report can be used for this purpose by future investigators. Such comparisons have not been made in the report because no single region or set of conditions could be considered typical; each region or emissions scenario should be analyzed individually. Such an analysis has been performed for the Metropolitan Los Angeles Air Quality Control Region by

TABLE 46. MOLAR REACTIVITIES OF ORGANIC EMISSIONS
CALCULATED FROM COMPOSITION DATA

Source	Molar Reactivity	Reference
Turbine engine (TF-39) ^a	10.4	This study
Turbine engine (CFM-56) ^a	10.8	This study
Jet aircraft ^a	9.0	24
Piston aircraft	7.5	24
Automotive ^b	7.3	24
Automotive ^b	5.3 ^c	27
Automotive ^b	8.0	28
Diesel vehicle ^b	10.4	24
Diesel vehicle ^b	9.2	27

^aBased on emissions at idle.

^bBased on test cycle or in-use conditions.

^cBased on C₁-C₆ compounds only.

Trijonis and Arledge (Reference 24). These authors used the five-class reactivity scheme utilized in this study to construct a "reactive emissions inventory" for the Los Angeles area. Their data show that even though emissions from jet aircraft are among the most reactive of all the sources (Reference 24 calculations), the emission levels are such that they contribute only 0.6 percent of the total reactivity in the Los Angeles basin. This may be compared with the authors' estimated contributions for gasoline and diesel vehicles of 33.9 percent and 4.8 percent respectively. Measured reactivity results in this report suggest that the jet aircraft contributions may have been overestimated by the prediction procedure used in Reference 24 for the Los Angeles area. As a consequence, it is unlikely that the contribution to total reactivity would even be as high as 0.6 percent. Of course, the contribution may be higher in other urban areas, and it will certainly be more significant in the vicinity of major airports. Nonetheless, a value on the order of 0.5 percent, or possibly even a few percent in some locations would seem to be a prudent estimate of jet aircraft contribution to overall photochemical reactivity. Such an estimate provides some perspective on the environmental impact of jet engine emissions.

SECTION VI

CONCLUSIONS AND RECOMMENDATIONS

A. ENGINE EMISSION TESTING

Emissions from two different engines operated on three fuels at idle and one fuel (JP-5) at higher thrust settings were studied. Several important findings resulting from this task are summarized below:

- Excellent carbon balance, 98 ± 10 percent, was achieved by comparing the summation of individual hydrocarbon species to the total hydrocarbon concentration.
- At idle, five cracking products (methane, ethylene, acetylene, propylene, and 1-butene) account for 30-35 percent of the total organic emissions. Most of the remainder is unburned fuel and partial oxidation products (aldehydes, ketones, and phenols).
- The distributions of individual hydrocarbon species for the TF-39 full-scale engine and the TF-39 combustor rig compares very well, with the exception of PNAs which were three to four times lower in the engine exhaust.
- Aromatic components of all three fuels are present in a higher proportion in the exhaust than in the raw fuel, compared to paraffins of equivalent volatility.
- Although the total hydrocarbon carbon emissions are two to three times lower for the CFM-56 engine than the TF-39 engine, aldehyde emission levels are similar for the two engines.
- The dicarbonyl compounds, glyoxal and methyl glyoxal, are present at significant concentrations, 1-4 ppmC, in the exhaust samples. No data are available for these compounds from other emission sources.
- Average carbon numbers for the unburned fuel region of the emissions were 6, 11, and 12 for JP-4, JP-8 (shale derived), and JP-5 fuels, respectively.
- For the TF-39 engine at idle, compound class distributions were in the following ranges for the three fuel types: 30-90 ppmC for paraffins, 15-20 ppmC for acetylene, 110-130 ppmC for olefins, 20-30 ppmC for aromatics, and 30-40 ppmC for aldehydes and ketones. Emissions using JP-4 fuel had a significantly greater proportion of paraffins than for the other two fuels.

B. PHOTOCHEMICAL REACTIVITY

The photochemical reactivity of exhaust generated at engine idle from two different engines and three fuels was investigated using two 8.5 m³ Teflon[®] smog chambers. The conclusions drawn from the photochemistry experiments are summarized below.

- Under clear sky conditions and warm temperatures, exhaust from each fuel/engine combination was photochemically reactive. Significant levels of ozone, light-scattering aerosols, aldehydes and other photochemical smog manifestations were generated by the exhaust.
- When compared on an equal mass basis, exhaust from the CFM-56 engine is more reactive than TF-39 exhaust. However, organic concentrations in the CFM-56 exhaust are two to three times lower.
- Exhaust reactivity was nearly independent of fuel type for the TF-39 engine. For the CFM-56 engine, JP-4 exhaust was the most reactive, JP-8 (shale) was the least reactive, and JP-5 was somewhat uncertain but fell between JP-4 and JP-8.
- On a molar average basis, the photochemically reactive classes alkenes and aldehydes made up 74 percent of the organic emissions.
- The contribution to reactivity of various classes of organic compounds was estimated from the exhaust composition data and a 5-class reactivity categorization. These results are shown below.

	Percent Contribution to Photochemical Reactivity					
	TF-39 Exhaust			CFM-56 Exhaust		
	JP-4	JP-5	JP-8 (shale)	JP-4	JP-5	JP-8 (shale)
Alkanes	12	8	9	10	6	7
Alkenes	59	60	60	49	50	52
Aromatics	2	1	2	2	1	2
Aldehydes	27	31	29	39	42	39

- Exhaust reactivity estimated from the composition data and the five-class reactivity categorization, overpredicts the measured reactivity in every case, and overpredicts substantially in most cases. This suggests that previous "reactive emission inventories" which have estimated jet engine exhaust reactivity from composition data may have overestimated the jet aircraft contribution to photochemical reactivity.

C. RECOMMENDATIONS FOR FUTURE RESEARCH

Several areas of uncertainty have been identified in the present study. In some cases the uncertainties stem from incomplete information, and in other cases they represent new questions which have arisen as a result of the data obtained in this project. Recommendations to investigate these areas of uncertainty are listed below.

- The source of the siloxanes observed at high-thrust conditions is uncertain. It seems likely that these compounds are an artifact of the sampling system, but further work will be necessary to document the source of these materials.
- A direct comparison of the photochemical reactivity of turbine engine emissions with combustor rig emissions has not been made. Additional combustor rig experiments are recommended to complete this comparison.
- Further information on dialdehyde emissions would be useful. Measurements of dialdehyde emissions from a combustor rig would permit turbine engine/combustor rig comparisons.
- The photochemical reactivity of exhaust from the TF-39 and CFM-56 engines has been compared on a mass basis. The relative reactivity of equal volumes of exhaust from these engines has not been ascertained. Limited combustor rig experiments could be used to address this question.
- Further research is recommended to identify bioactive species in the exhaust.
- The present studies should be extended to determine emission rates of potentially toxic and bioactive species from other engine/fuel combinations. This will provide a data base for risk assessment.
- Studies to investigate the atmospheric lifetime and chemical fate of toxic or bioactive emissions are warranted. Either outdoor or indoor environmental chambers can be used to carry out such studies.

- By making certain assumptions, the data obtained in this study can be used to estimate indirectly the contribution of aircraft emissions to the concentration of organic compounds around and downwind of airports. The information contained in this report on individual organic species and species ratios also could be used, in conjunction with selected measurements upwind and downwind of an airport, for site-specific source attribution of organic compounds. An assessment of the applicability and utility of source reconciliation techniques using these data is recommended.

REFERENCES

1. Brooks, J. J., West, D. S., Strobel, J. E., and Stamper, L., Jet Engine Exhaust Analysis by Subtractive Chromatography, Final Report, SAM-TR-78-37, Brooks AFB, TX, December 1978.
2. Chase, J. O. and Hurn, R. W., "Measuring Gaseous Emissions from an Aircraft Turbine Engine," Proceedings of Society of Automotive Engineers Meeting, 839-845, April, 1970, .
3. Lazanc, E. R., Melvin, W. W., and Hochheiser, S., "Air Pollution Emissions from Jet Engines," J. Air Pollution Control Assn., 18 (6), 392-394, (1968).
4. Groth, R. H. and Robertson, D. J., "Reactive and Nonreactive Hydrocarbons Emissions from Gas Turbine Engines," presented at the 67th Annual Meeting of the Air Pollution Control Association, Denver, June 9-13, 1974.
5. Stumpf, S. A. and Blazowski, W. S., "Detailed Investigations of Organic Emissions from Gas Turbine Engines," Paper No. 27-1, International Conference on the Sensing of Environmental Pollutants, Las Vegas, Nevada, September 15-19, 1975.
6. Moses, C. A. and Stavinoka, L. L., "Gas Chromatographic Analysis of Exhaust Hydrocarbons from a Gas Turbine Combustor," presented at Western States Section/The Combustion Institute, Stanford Research Institute, October 20-21, 1975.
7. Robertson, D. J., Elwood, J. H., and Groth, R. H., Chemical Composition of Exhaust Particles from Gas Turbine Engines, Final Report EPA 600/2-79-041, Research Triangle Park, NC, February, 1979.
8. Berry, D. A., Holdren, M. W., Lyon, T. F., Riggin, R. M., and Spicer, C. W., Turbine Engine Exhaust Hydrocarbon Analysis, Tasks 1 and 2, Interim Report No. ESL 82-43, Tyndall AFB, FL, June, 1983.
9. Kuntz, R., Lonneman, W., Namie, G., and Hull, L. A., "Rapid Determination of Aldehydes in Air Samples," Anal. Lett., 13, 1409-1415 (1980).
10. Winer, A. M., Atkinson, R., Carter, W.P.L., Long, W. D., Aschmann, S. M. and Pitts, J. N., Jr., High Altitude Jet Fuel Photochemistry, Statewide Air Pollution Research Center report to Air Force Engineering and Services Lab., ESL-TR-82-38, Tyndall AFB, FL, October, 1982.
11. Carter, W.P.L., Ripley, P. S., Smith, C. G. and Pitts, J. N., Jr., Atmospheric Chemistry of Hydrocarbon Fuels, Statewide Air Pollution Research Center report to Air Force Engineering and Services Lab., ESL-TF-81-53, Tyndall AFB, FL, November, 1981.

12. Wu, C. H. and Niki, H., "Methods for Measuring NO₂ Photodissociation Rate. Application to Smog Chamber Studies," Environ. Sci. Tech., 9, 46 (1975).
13. Jackson, J. O., Stedman, D. H., Smith, R. G., Hecker, L. H., and Warner, P. O., "Direct NO₂ Photolysis Rate Monitor," Rev. Sci. Instrum., 46, 376 (1973).
14. Zafonte, L., Rieger, P. L., and Holmes, J. R., "Nitrogen Dioxide Photolysis in the Los Angeles Atmosphere," Environ. Sci. Tech., 11, 483-487 (1977).
15. Harvey, R. B., Stedman, D. H., and Chameides, W., "Determination of the Absolute Rate of Solar Photolysis of NO₂," J. Air Poll. Control Assoc., 27, 663-666 (1977).
16. Saeger, M., "An Experimental Determination of the Specific Photolysis Rate of Nitrogen Dioxide," MS Thesis, U. North Carolina, Chapel Hill, NC (1977).
17. Bahe, F. C., Schurath, U., and Becker, K. H., "The Frequency of NO₂ Photolysis at Ground Level, as Recorded by a Continuous Actinometer," Atm. Environ., 14, 711-718 (1980).
18. Naugle, D. F. and Fox, D. L., "Aircraft and Air Pollution," Env. Sci. Tech., 15, 391-395 (1981).
19. Naugle, D. F., "Aviation and Ambient Air Quality: A Comprehensive Literature Survey," Paper No. 80-3.3; Air Pollution Control Association Annual Meeting, June 22-27, 1980.
20. Nebel, G. J., "Benzene in Auto Exhaust," J. Air Poll. Cont. Assoc., 29, 391-392 (1979).
21. Zweidinger, R. B., "Emission Factors from Diesel and Gasoline Powered Vehicles: Correlation with the Ames Test," in Toxicological Effects of Emissions from Diesel Engines, J. Lewtas, ed., Elsevier Biomedical, pp. 83-96. (1982).
22. Lipari, F. and Swarin, S. J., "Determination of Formaldehyde and Other Aldehydes in Automobile Exhaust with an Improved 2,4-Dinitrophenylhydrazine Method," J. Chrom., 247, 297-306 (1982).
23. U.S. Environmental Protection Agency, "Control of Air Pollution from Aircraft and Aircraft Engines," Fed. Register, 43 (58), March 24, 1978.
24. Trijonis, J. C., and Arledge, K. W., Utility of Reactivity Criteria in Organic Emission Control Strategies, Application to the Los Angeles Atmosphere, EPA-600/3-76-091, Research Triangle Park, NC, August, 1976.

25. Whitten, G. Z. and Hogo, H., Introductory Study of the Chemical Behavior of Jet Emissions in Photochemical Smog, SAI final report to NASA and FAA, Contract No. NAS2-8821, May, 1976.
26. Dimitriadis, B., "The Concept of Reactivity and Its Possible Applications in Control," Proceedings of the Solvent Reactivity Conference, EPA-650/3-74-010, Research Triangle Park, NC, November, 1974.
27. Spicer, C. W. and Levy, A., The Photochemical Smog Reactivity of Diesel Exhaust Organics, Battelle-Columbus Lab. final report to Coordinating Research Council, Project CAPA-10-71, Atlanta, GA, May, 1975.
28. Levy, A., Miller, D. F., Hopper, D. R., Spicer, C. W., Trayser, D. A., and Cote, R. W., Motor Fuel Composition and Photochemical, Battelle-Columbus Lab. final report to American Petroleum Institute, Project EF-8, Washington, D.C., October, 1974.
29. Dimitriadis, B. and Carroll, H. B., Photochemical Reactivity of Diesel Exhaust--Some Preliminary Tests, Bureau of Mines Report of Investigation 7514, Washington, D.C., April, 1971.

APPENDIX A
SMOG CHAMBER PROFILES

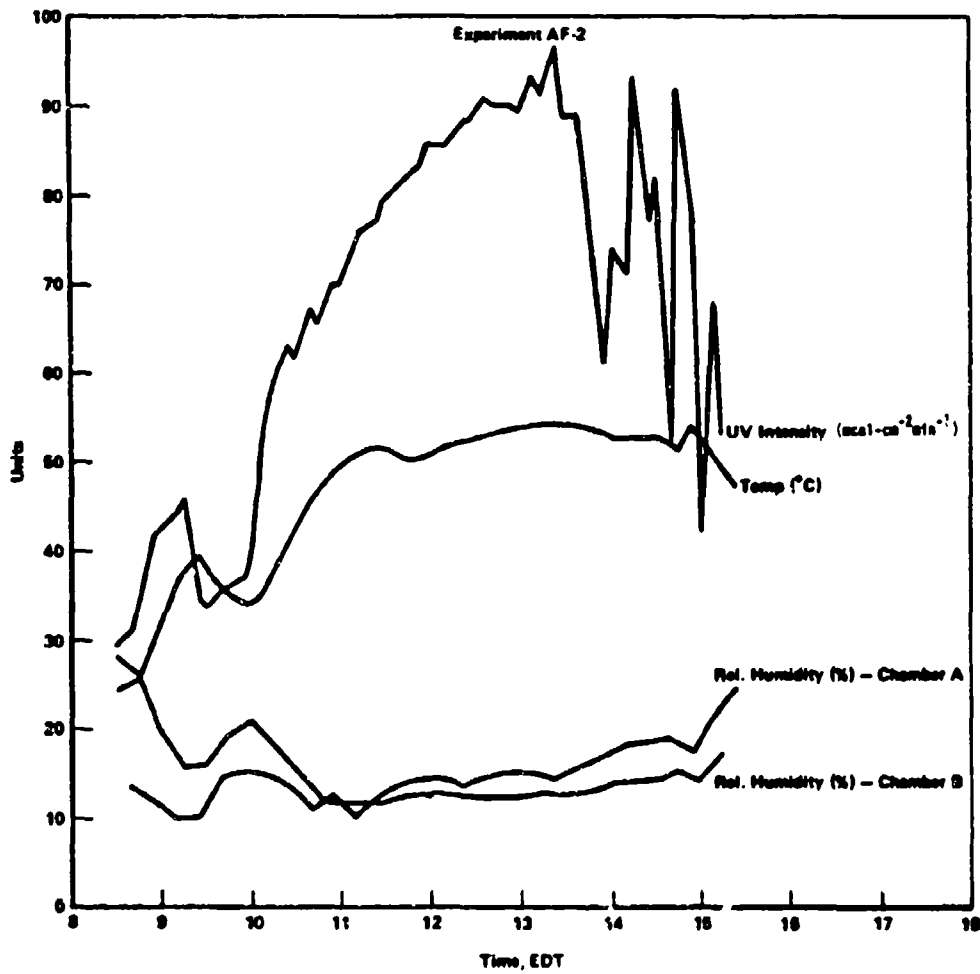


Figure A-1. Smog Chamber Profiles from AF-2
Using TF-39 Engine and JP-5 Fuel

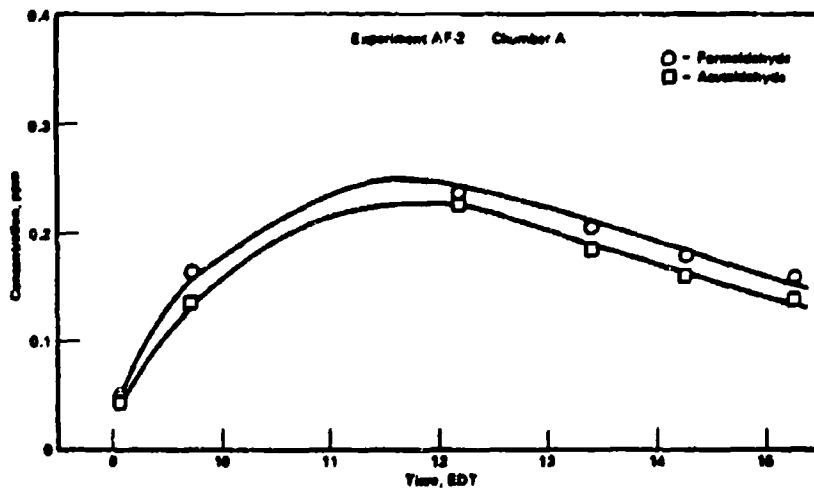
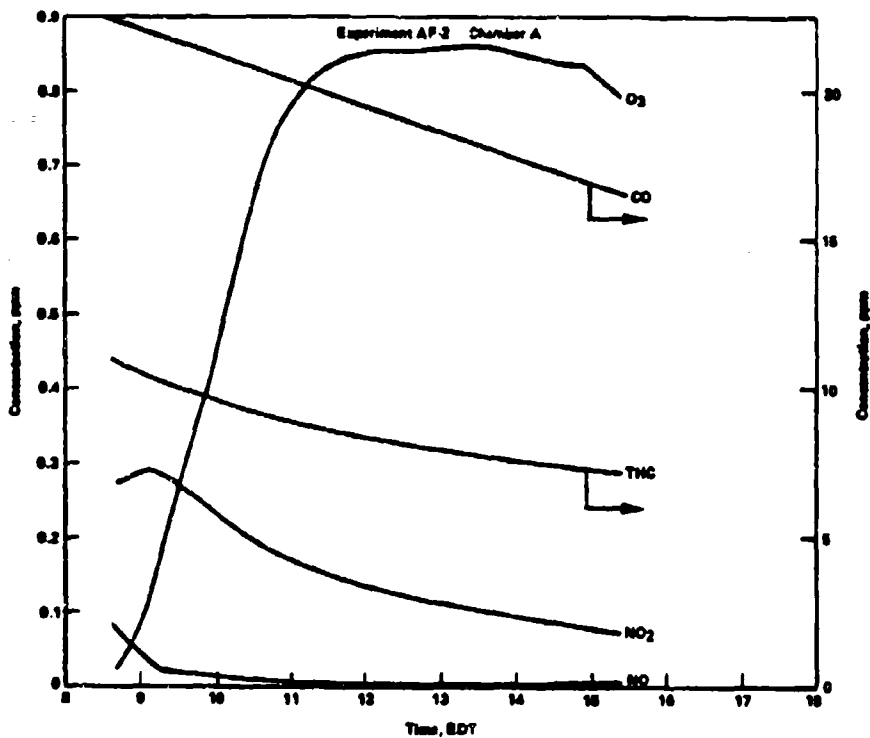


Figure A-2. Smog Chamber Profiles from AF-2 Using TF-39 Engine and JP-5 Fuel (Reference Chamber)

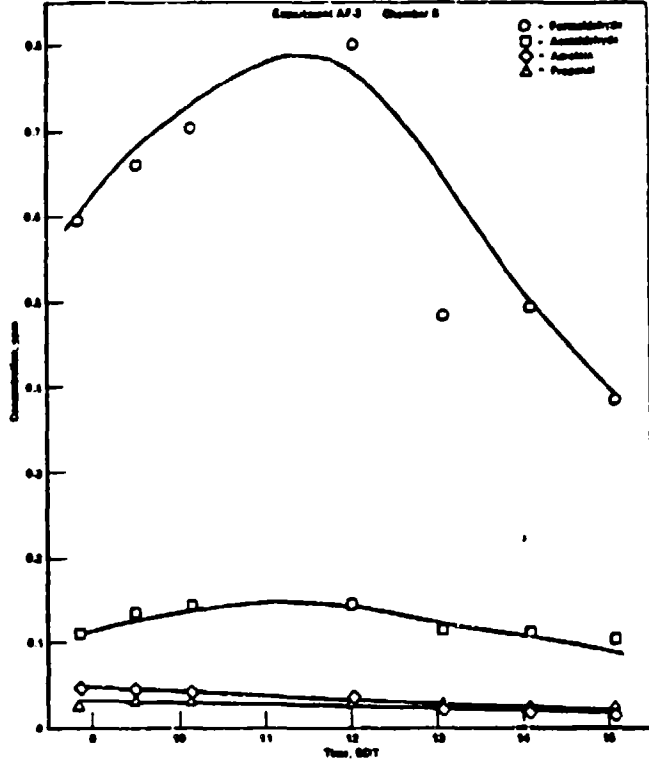
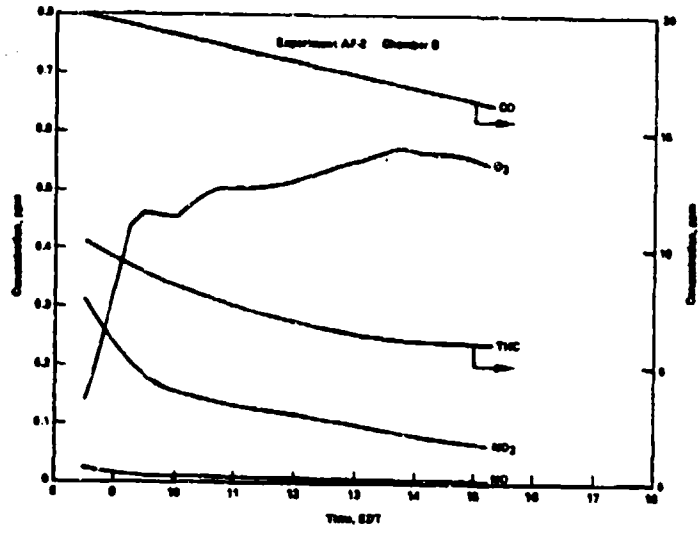


Figure A-3. Smog Chamber Profiles from AF-2 Using TF-39 Engine and JP-5 Fuel (Exhaust Chamber)

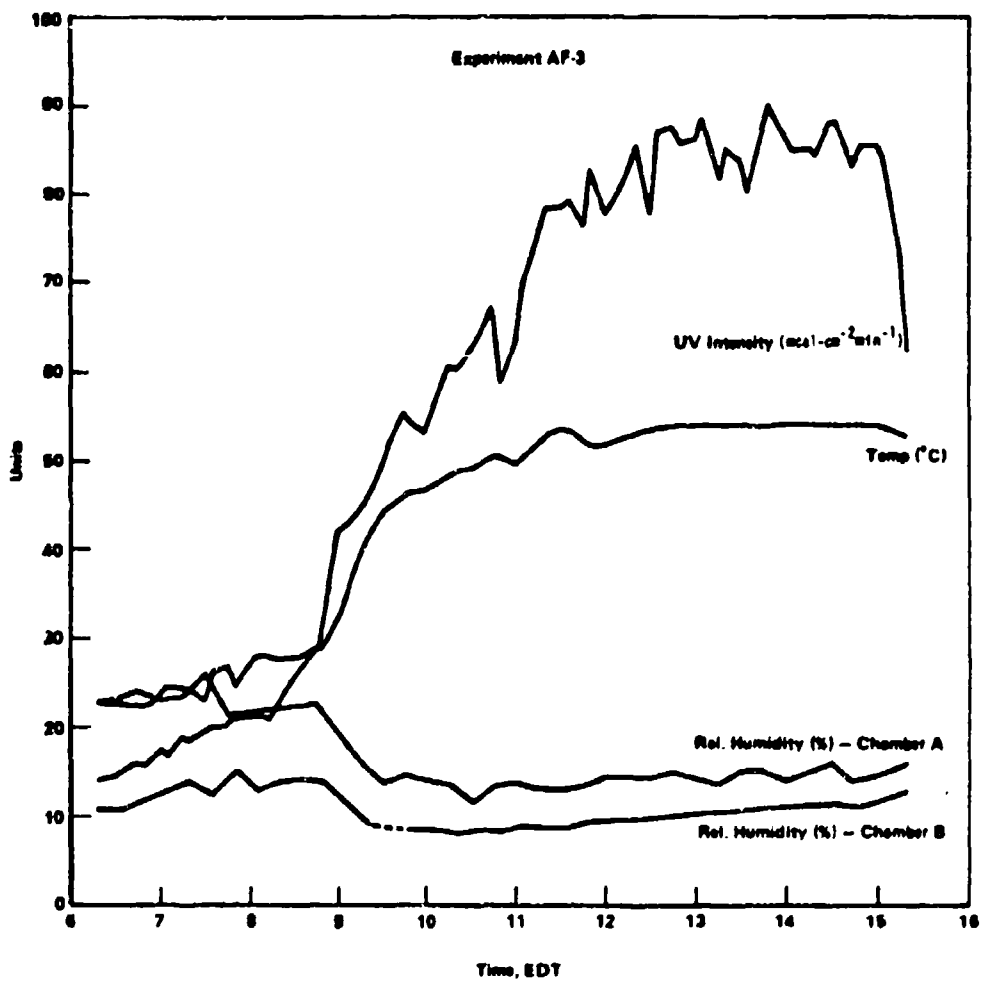


Figure A-4. Smog Chamber Profiles from AF-3
Using TF-39 Engine and JP-4 Fuel

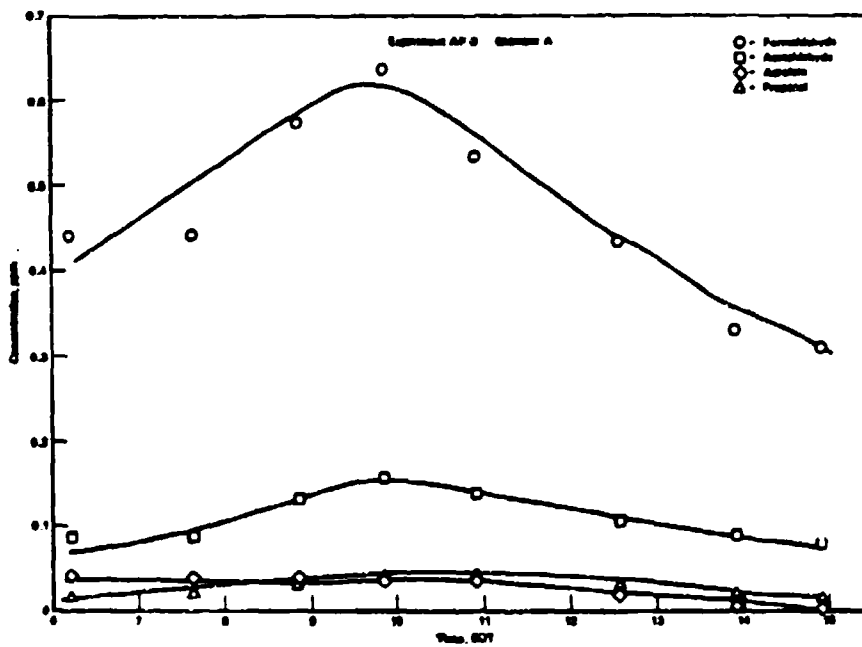
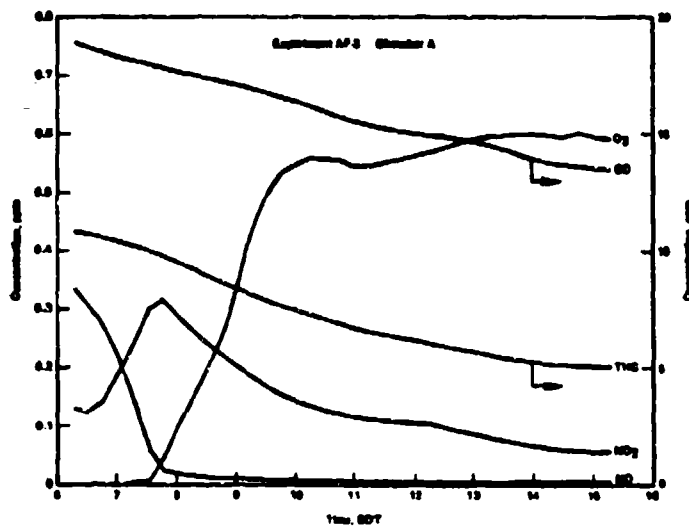


Figure A-5. Smog Chamber Profiles from AF-3 Using TF-39 Engine and JP-4 Fuel (Exhaust Chamber)

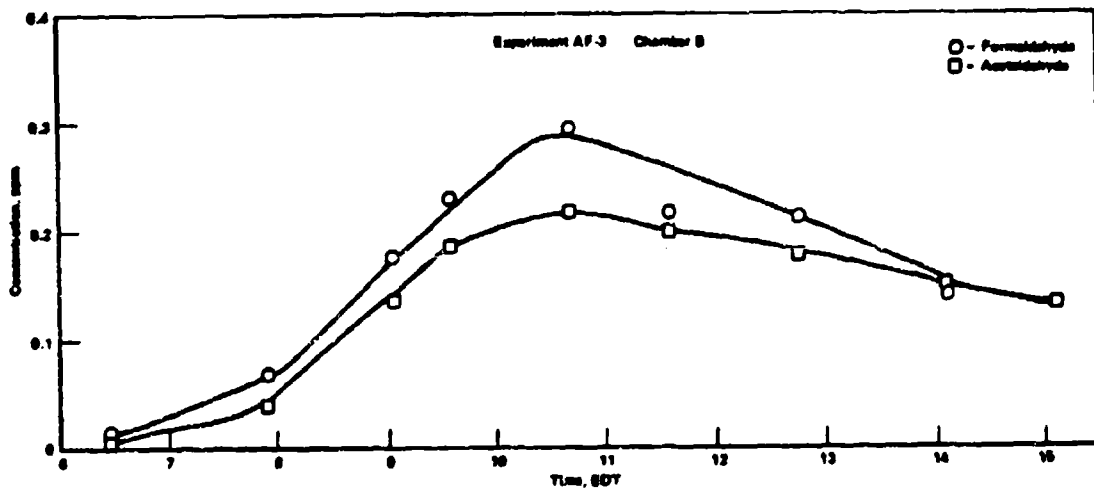
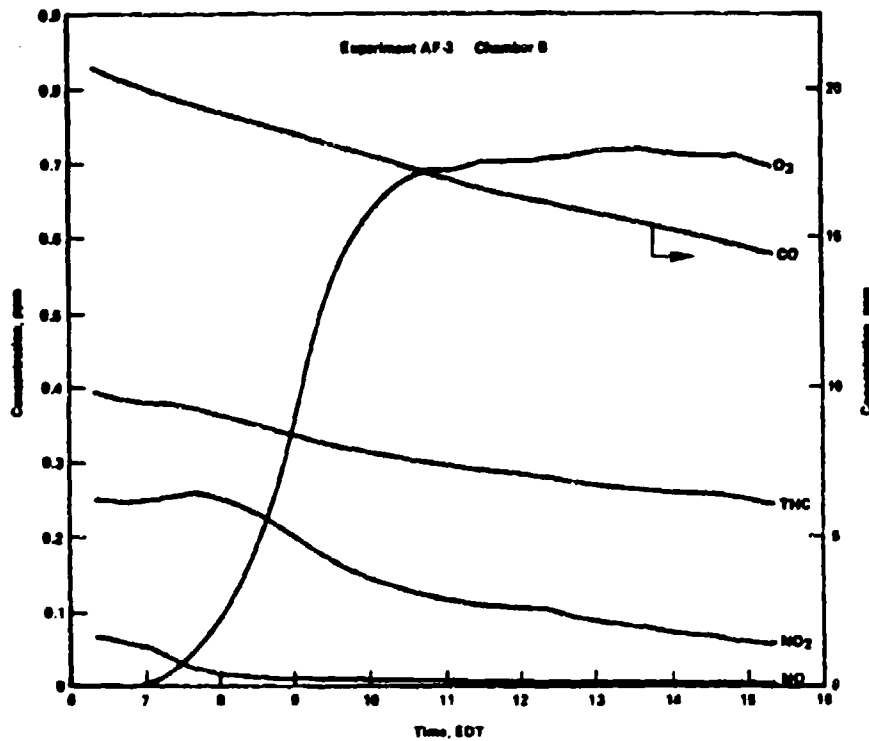


Figure A-6. Smog Chamber Profiles from AF-3 Using TF-39 Engine and JP-4 Fuel (Reference Chamber)

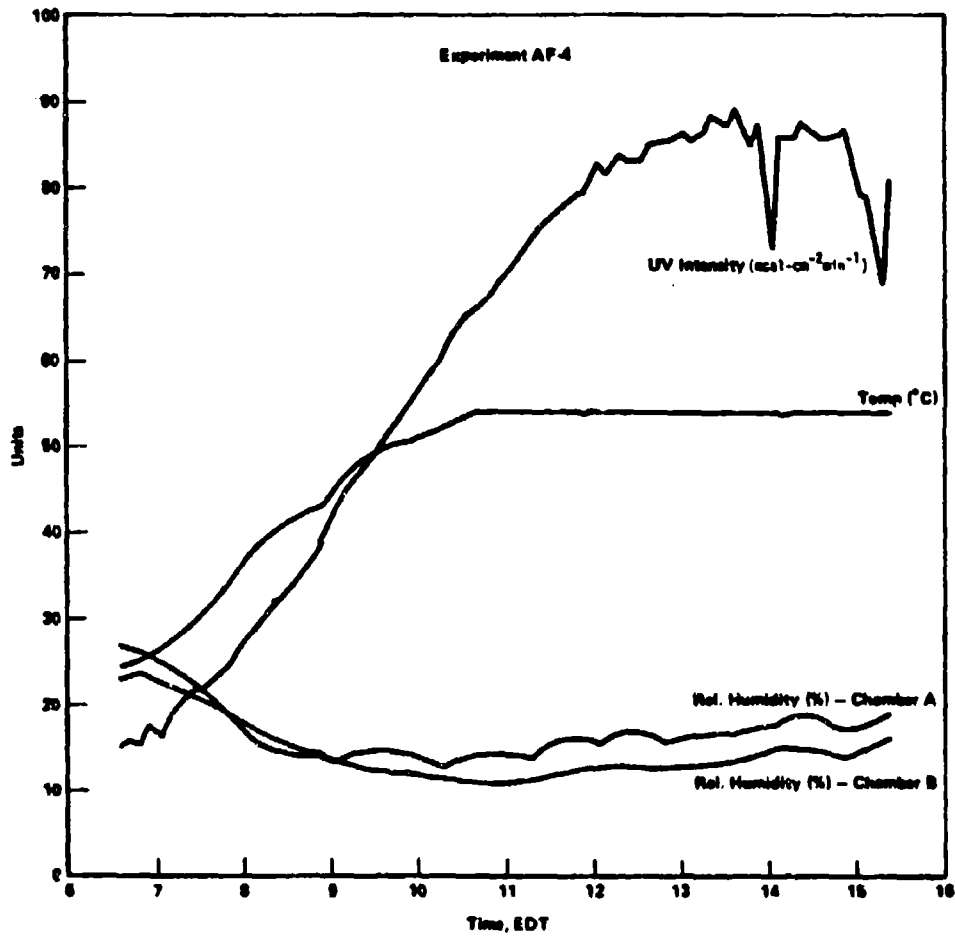


Figure A-7. Smog Chamber Profiles from AF-4
Using TF-39 Engine and JP-4 Fuel

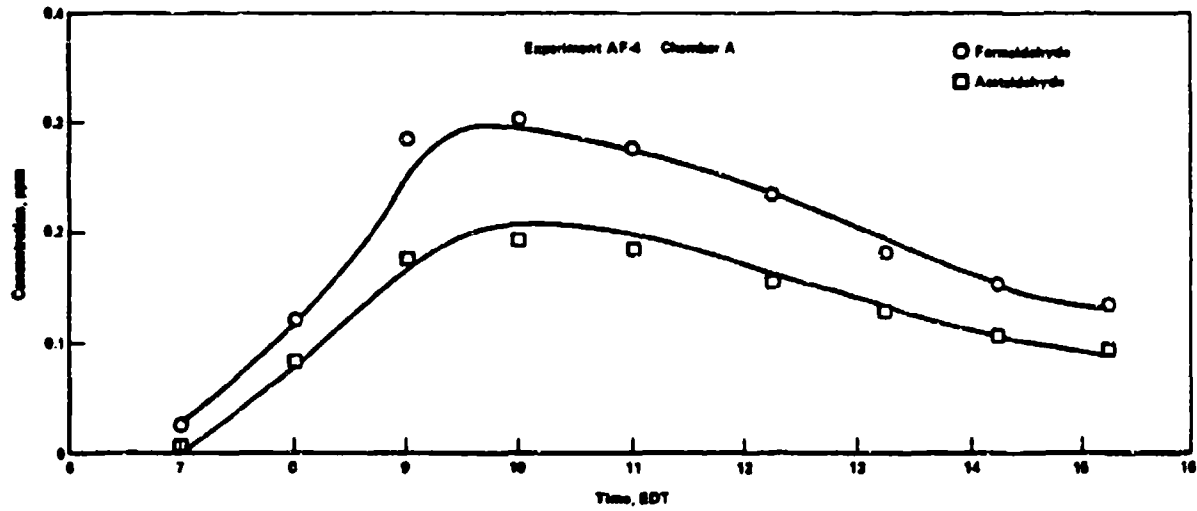
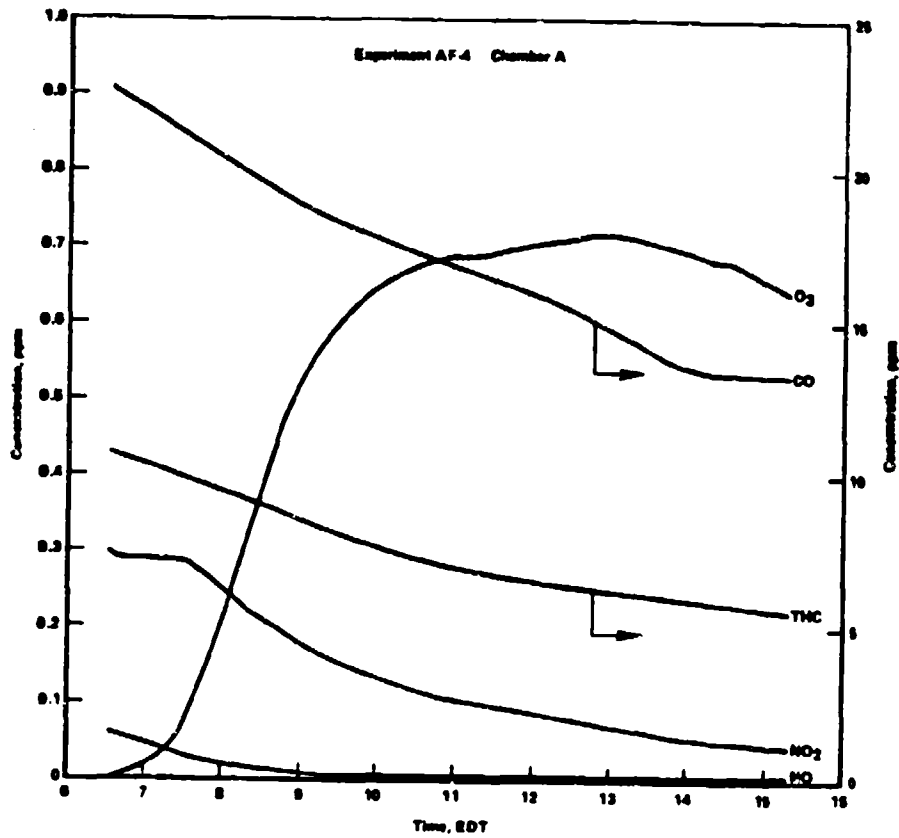


Figure A-8. Smog Chamber Profiles from AF-4 Using TF-39 Engine and JP-4 Fuel (Reference Chamber)

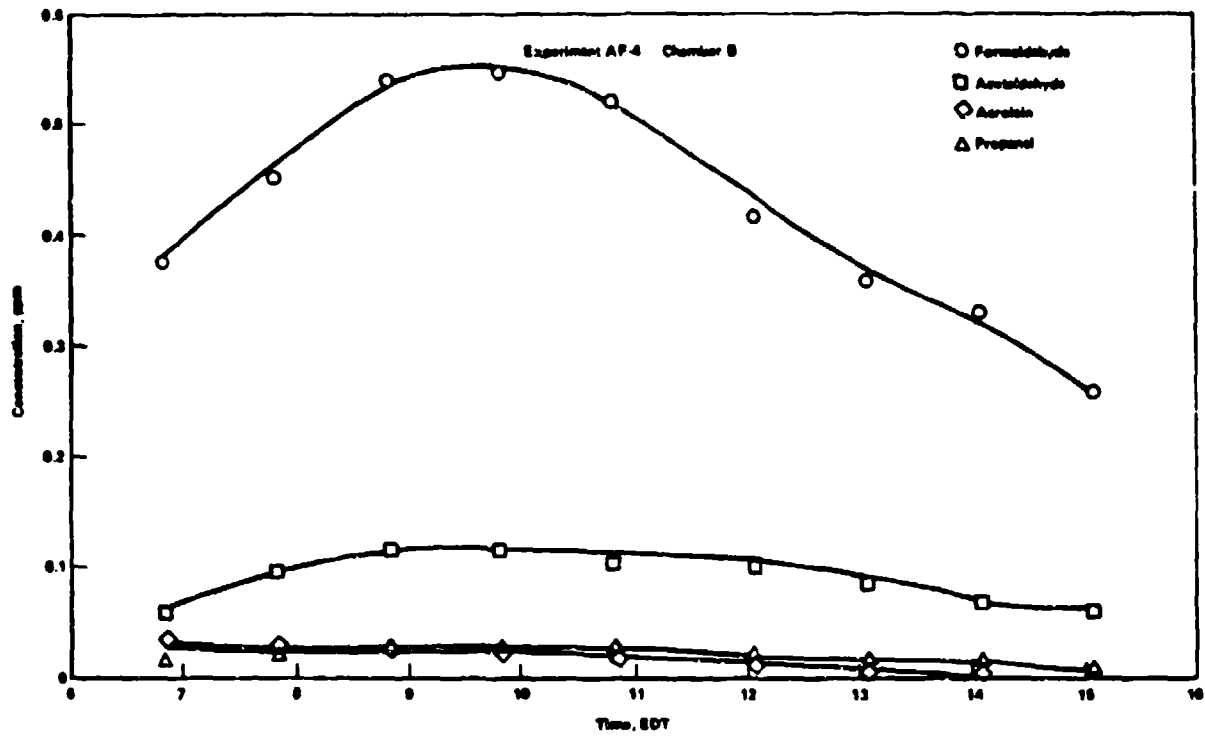
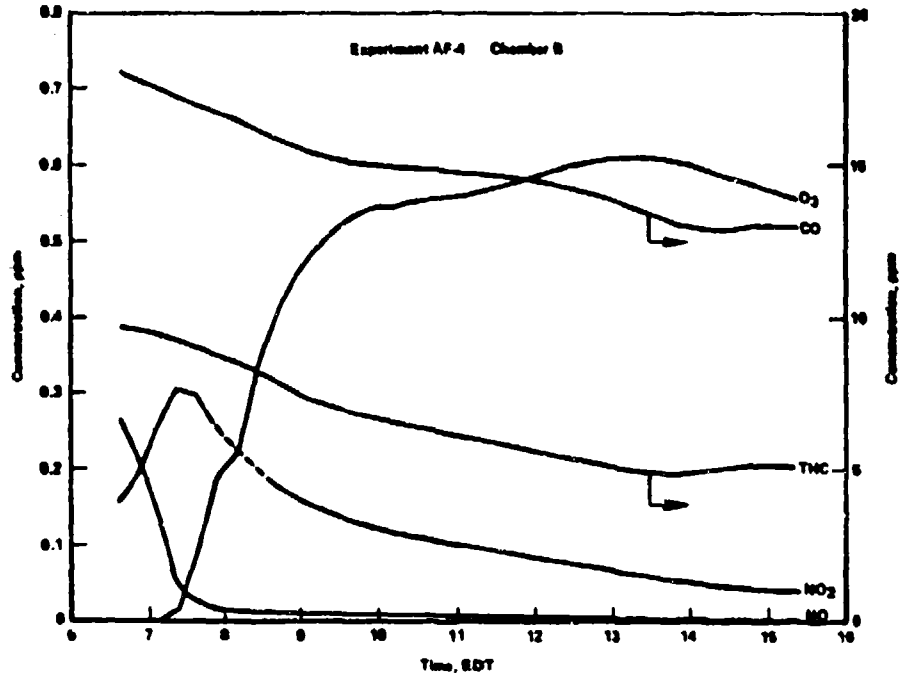


Figure A-9. Smog Chamber Profiles from AF-4 Using TF-39 Engine and JP-4 Fuel (Exhaust Chamber)

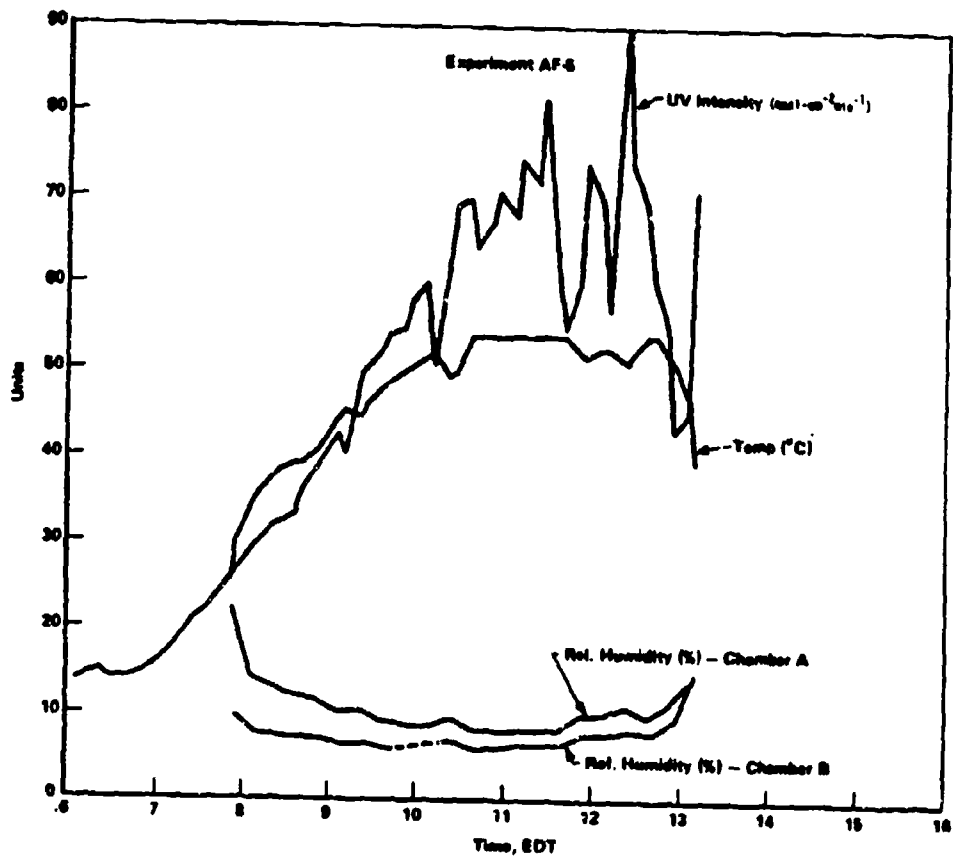


Figure A-10. Smog Chamber Profiles from AF-5 Using TF-39 Engine and JP-8 Shale-Derived Fuel

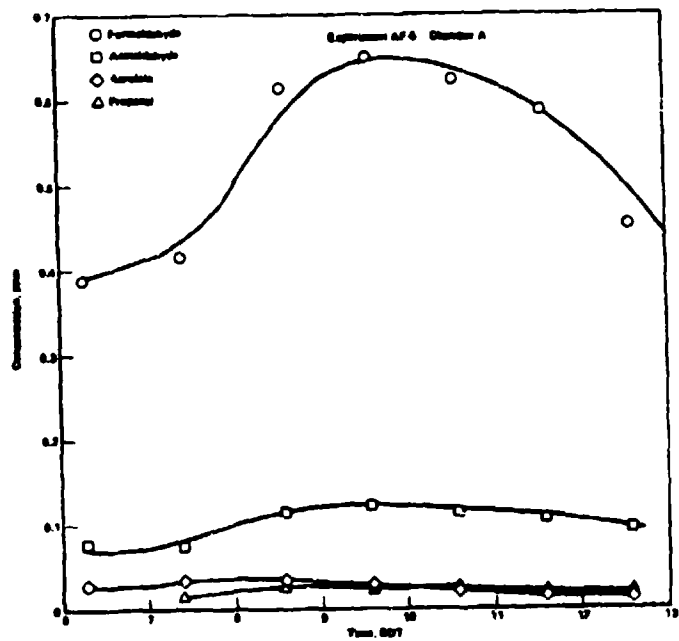
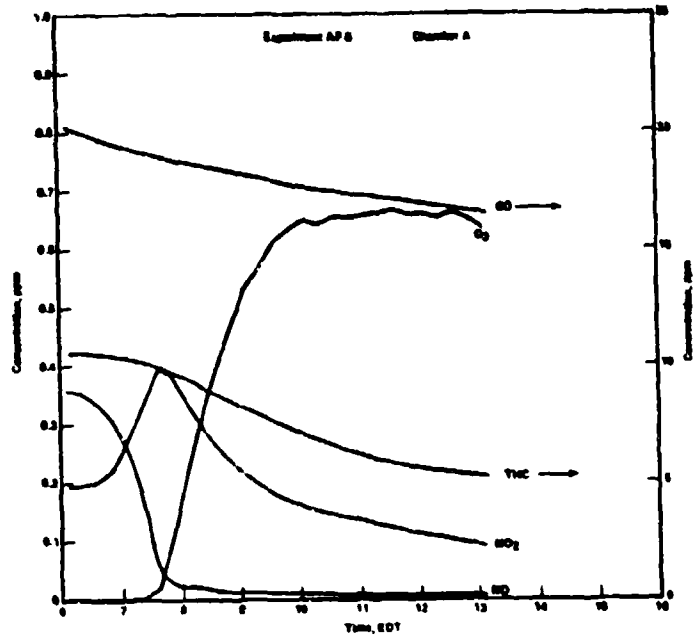


Figure A-11. Smog Chamber Profiles from AF-5 Using TF-39 Engine and JP-8 Shale-Derived Fuel (Exhaust Chamber)

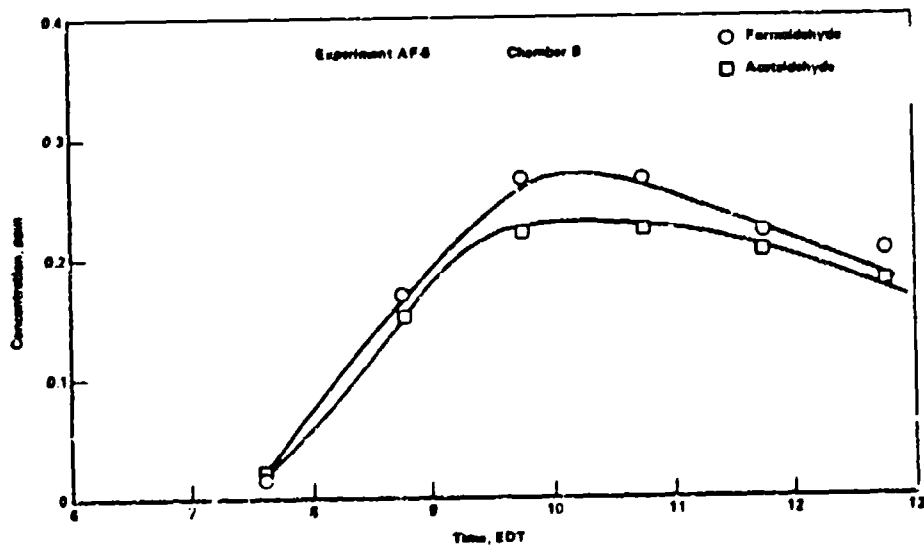
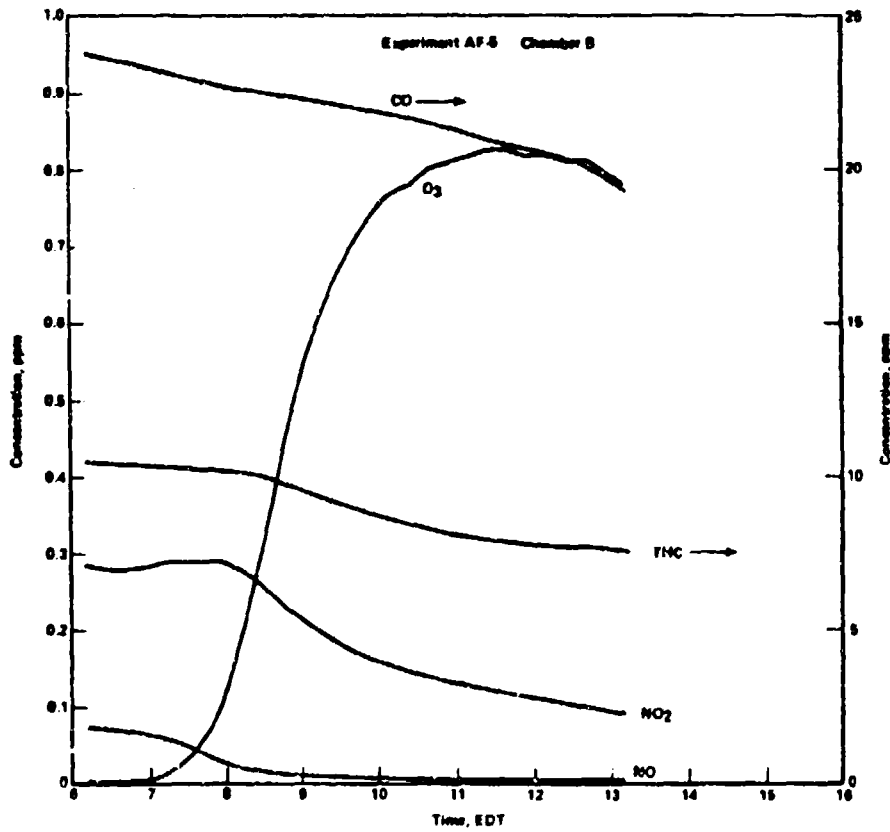


Figure A-12. Smog Chamber Profiles from AF-5 Using TF-39 Engine and JP-8 Shale-Derived Fuel (Reference Chamber)

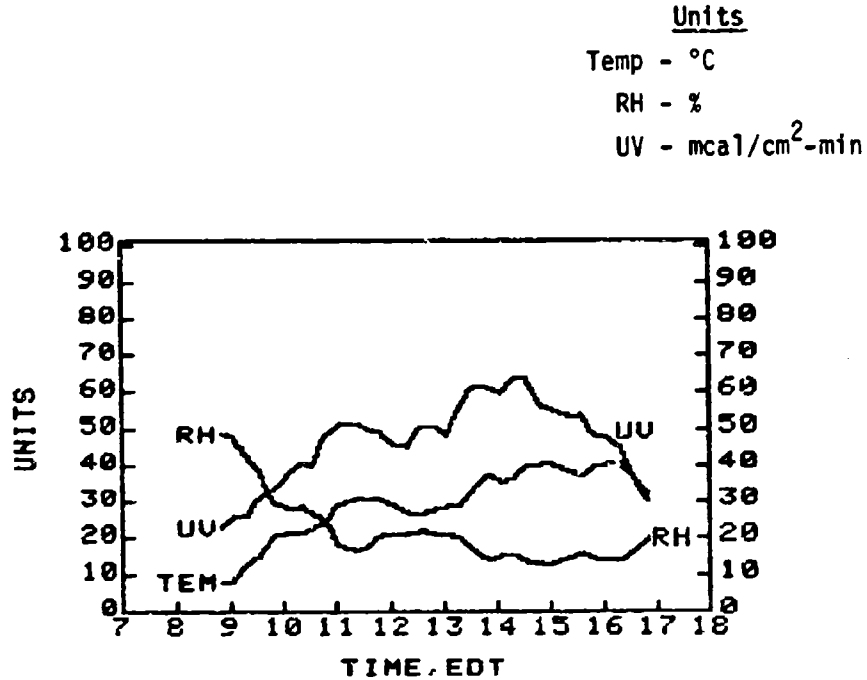
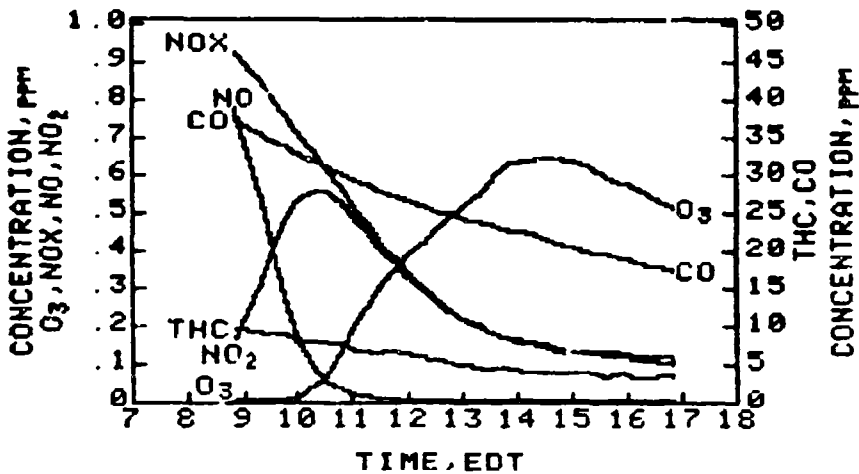
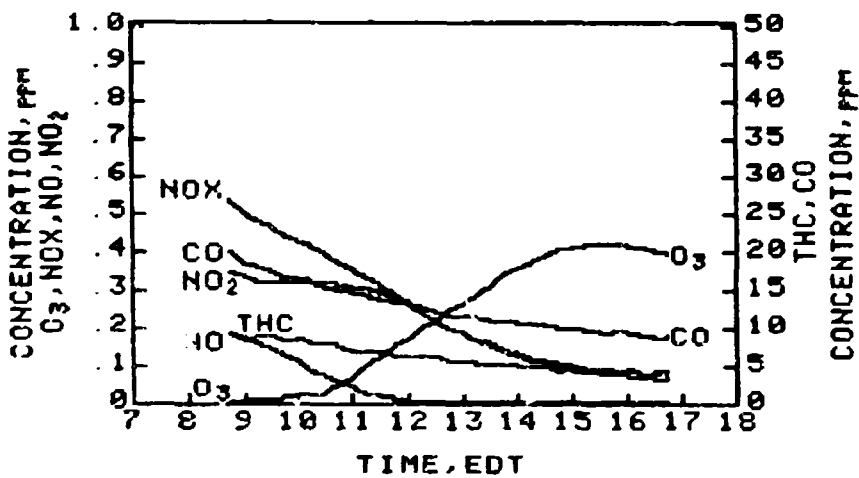


Figure A-13. Profiles from AF-6 Using CFM-56 Engine and JP-5 Fuel, October 19, 1983



PROFILES FROM AF-6 USING CFM-56 ENGINE AND JF-5 FUEL OCT.19 1983



PROFILES FROM AF-6 REFERENCE CHAMBER OCT.19 1983

Figure A-14. Smog Chamber Profiles from AF-6

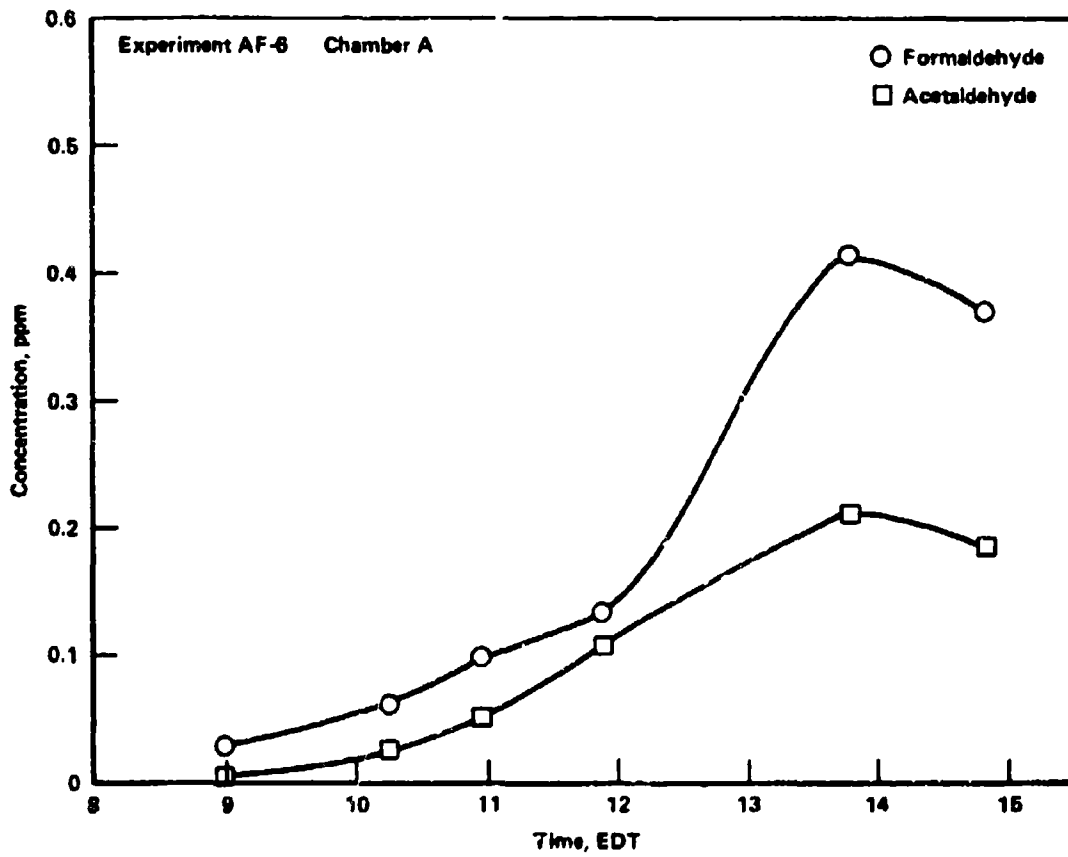


Figure A-15. Smog Chamber Profiles from AF-6
(Reference Chamber)

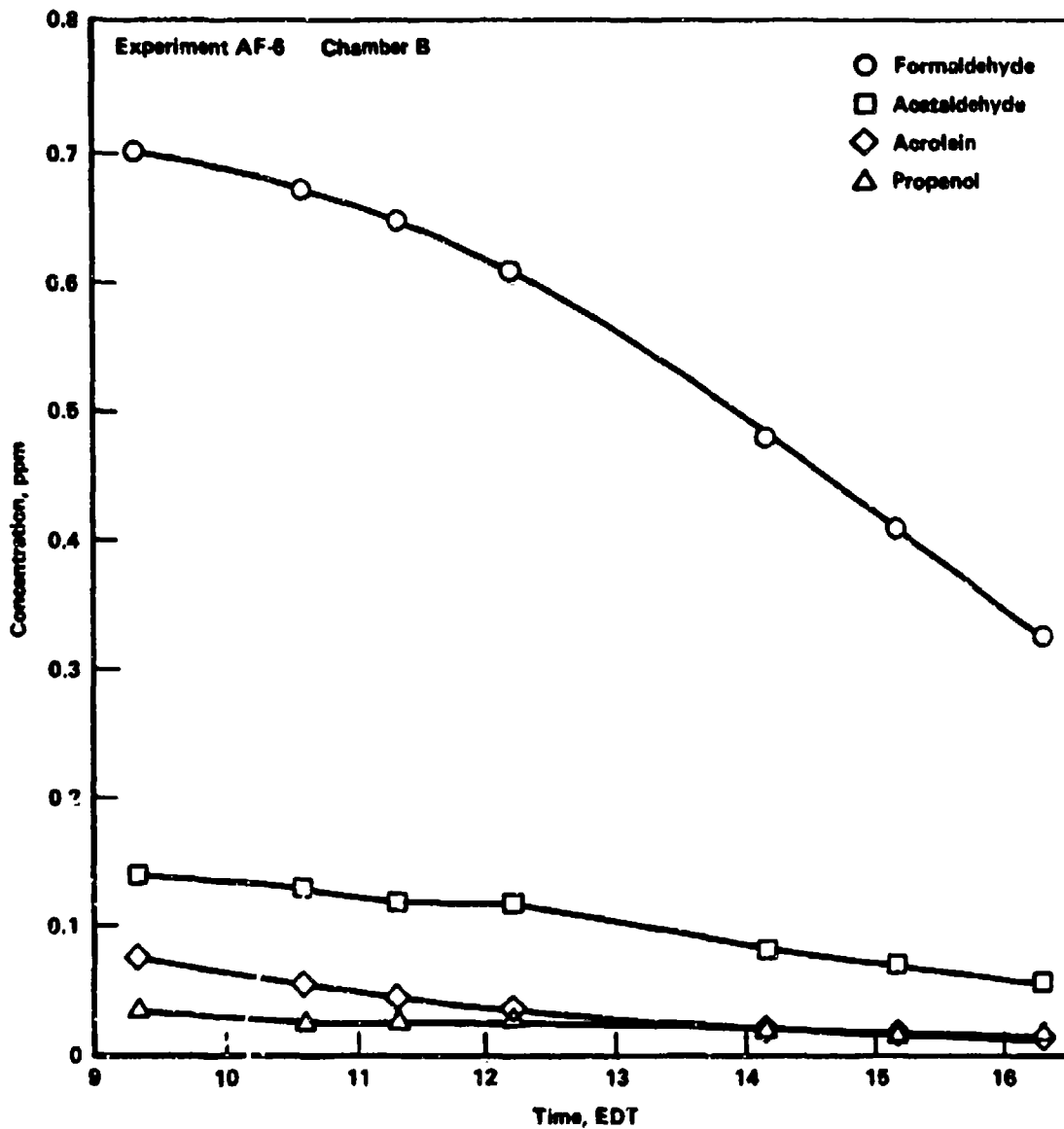


Figure A-16. Smog Chamber Profiles from AF-6 (Exhaust Chamber)

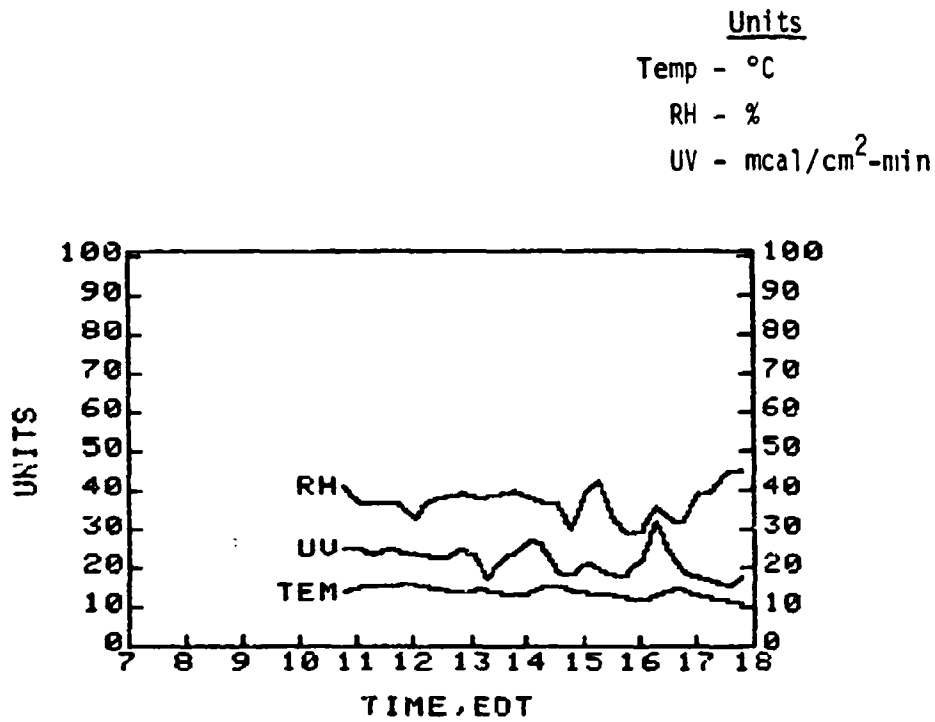
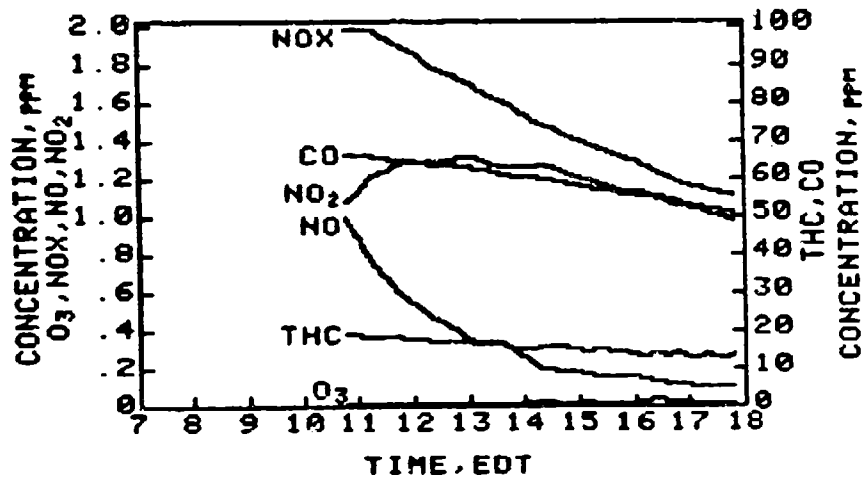
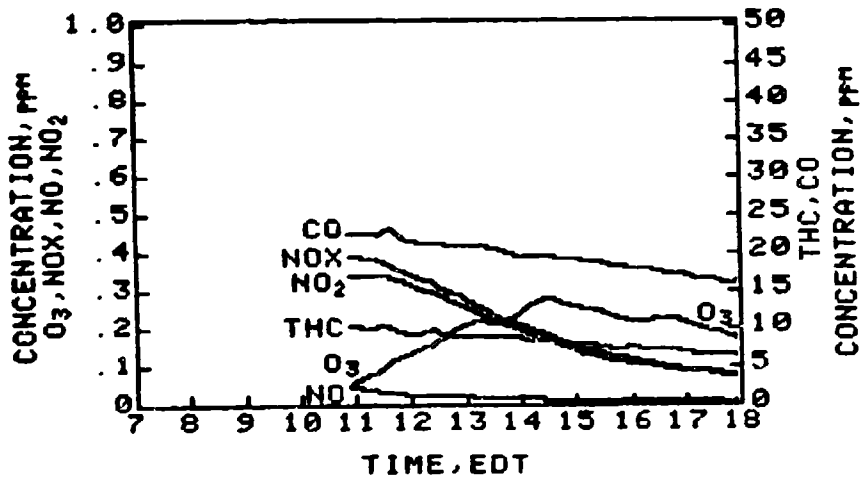


Figure A-17. Profiles from AF-8 Using CFM-56 Engine and JP-4 Fuel, October 25, 1983



PROFILES FROM AF-8 USING CFM-56 ENGINE AND JP-4 FUEL OCT.25 1983



PROFILES FROM AF-8 REFERENCE CHAMBER OCT.25 1983

Figure A-18. Smog Chamber Profiles from AF-8

Units

Temp - °C

RH - %

UV - mcal/cm²-min

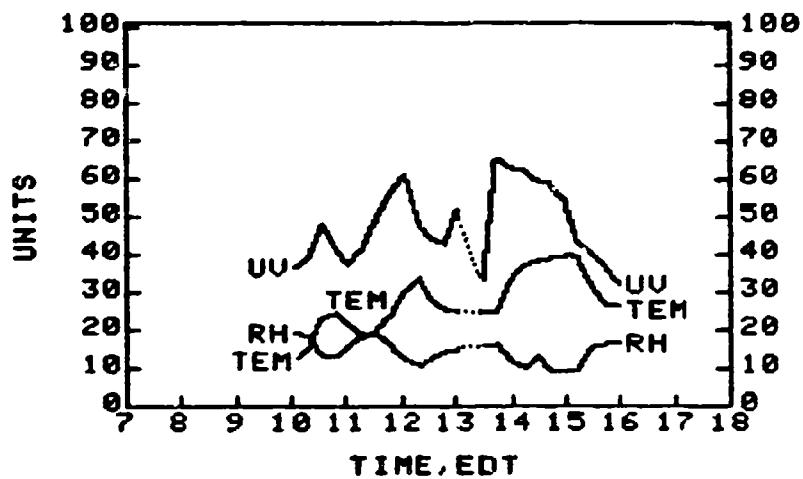


Figure A-19. Profiles from AF-9 Using CFM-56 Engine and JP-4 Fuel, October 26, 1983

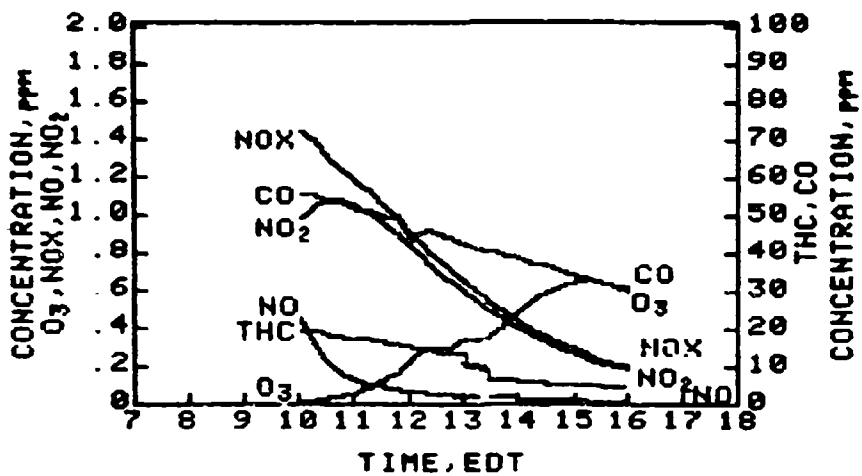


Figure A-19. Profiles from AF-9 Using CFM-56 Engine and JP-4 Fuel, October 26, 1983

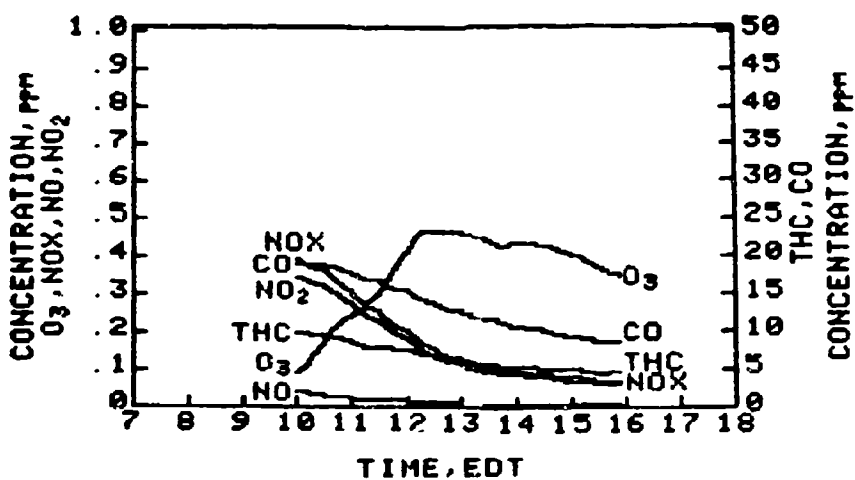


Figure A-20. Profiles from AF-9 Reference Chamber October 26, 1983

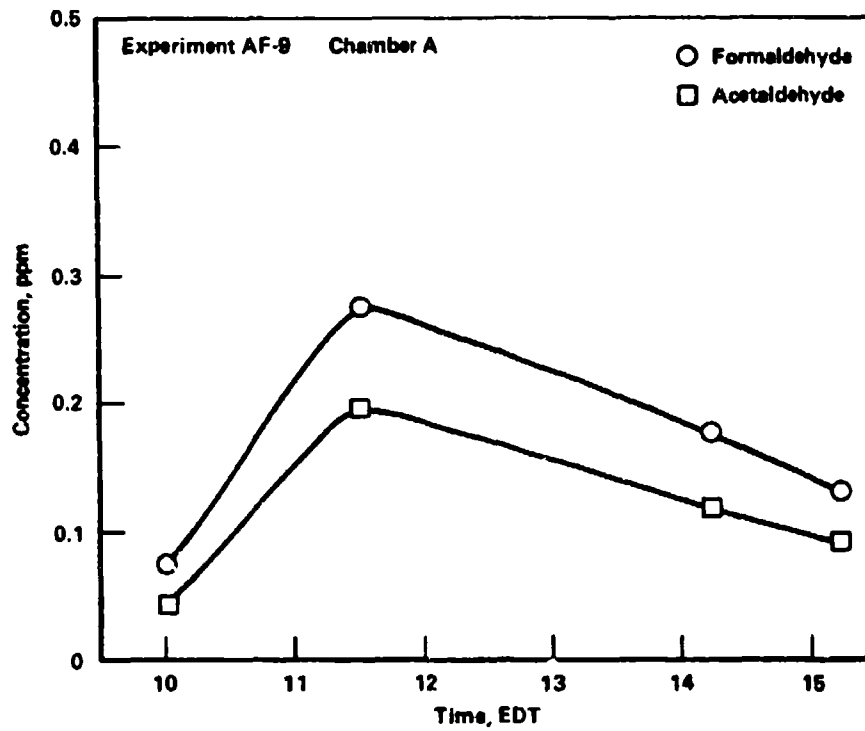


Figure A-21. Smog Chamber Profiles from AF-9
(Reference Chamber)

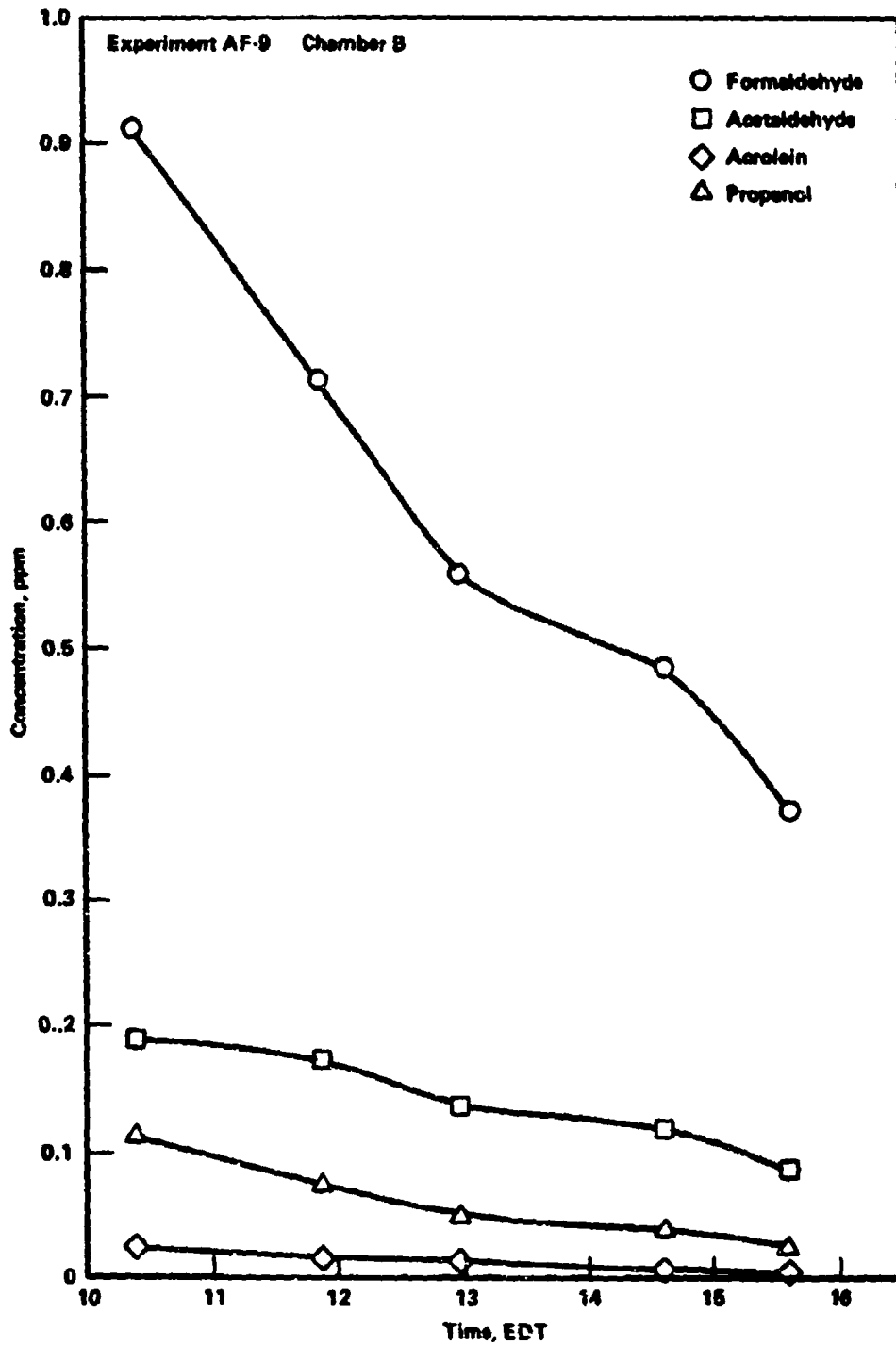


Figure A-22. Smog Chamber Profiles from AF-9 (Exhaust Chamber)

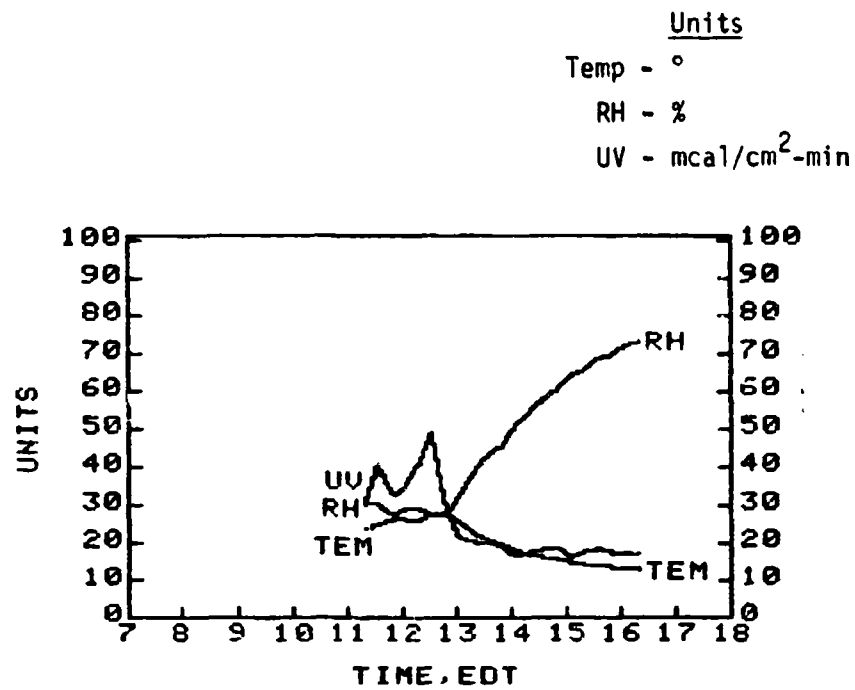
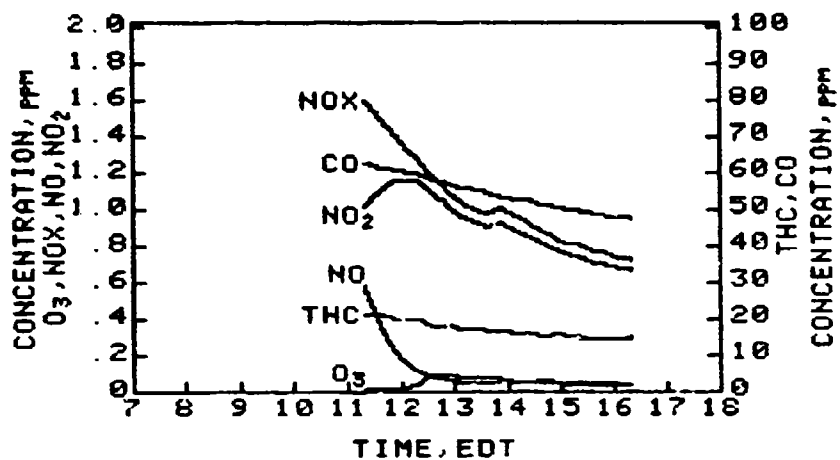
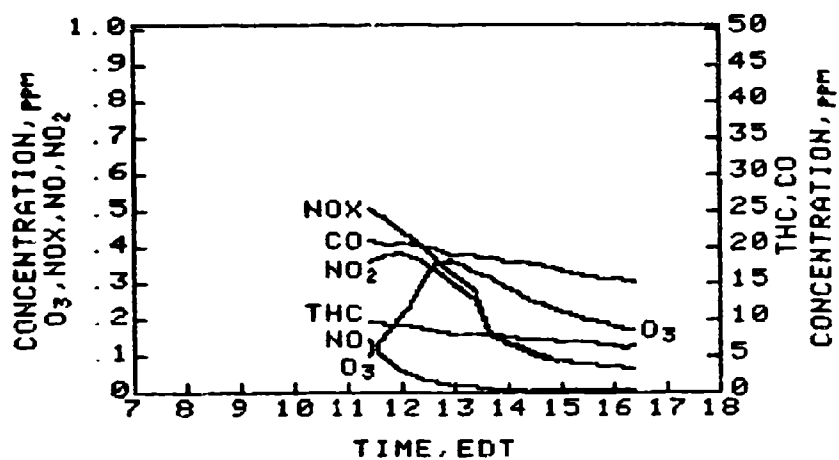


Figure A-23. Profiles from AF-10 Using CFM-56 Engine and JP-5 Fuel, November 3, 1983



PROFILES FROM AF-10 USING CFM-56 ENGINE AND JP-5 FUEL NOV.3 1983



PROFILES FROM AF-10 REFERENCE CHAMBER NOV. 3 1983

Figure A-24. Smog Chamber Profiles from AF-10

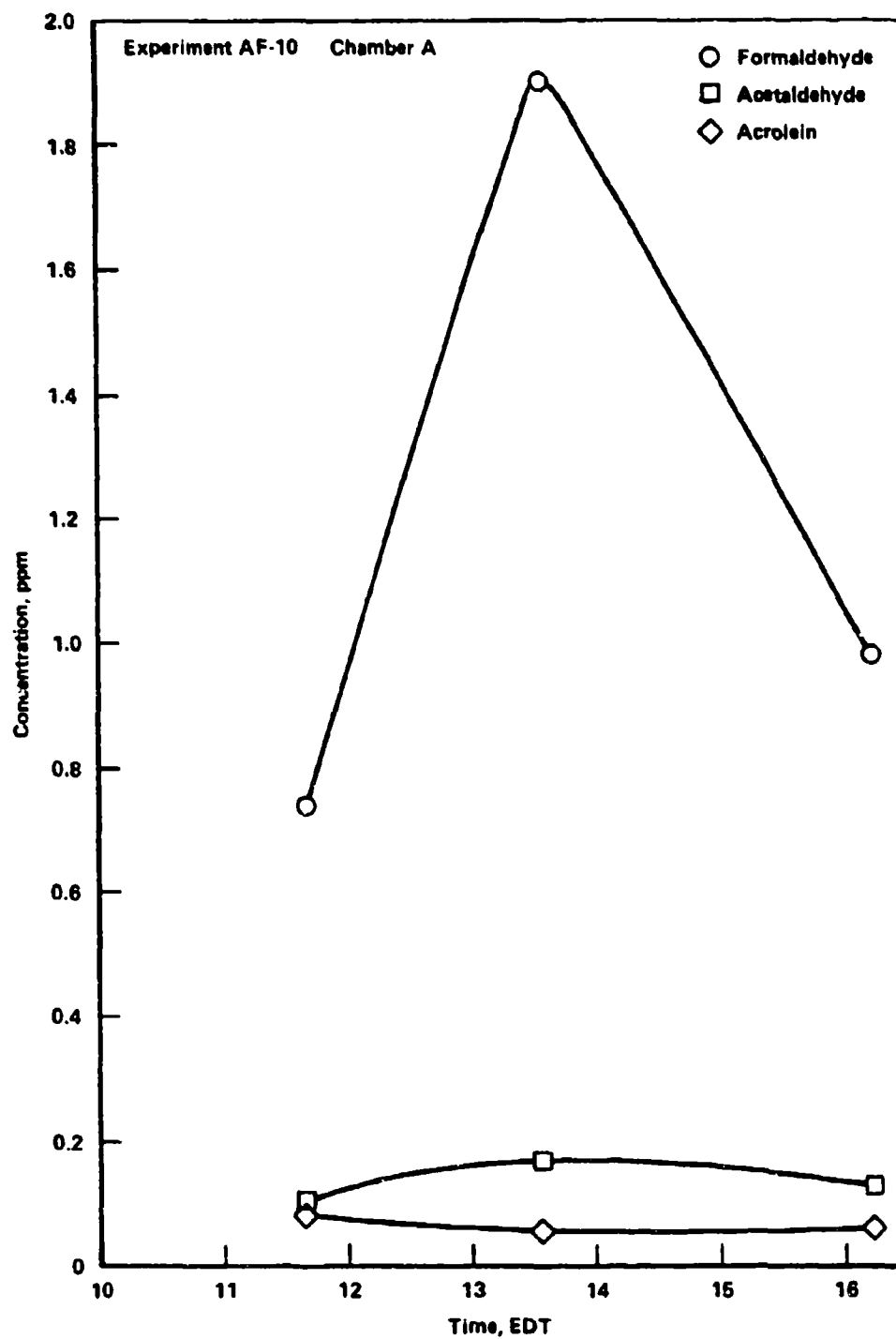


Figure A-25. Smog Chamber Profiles from AF-10 (Exhaust Chamber)

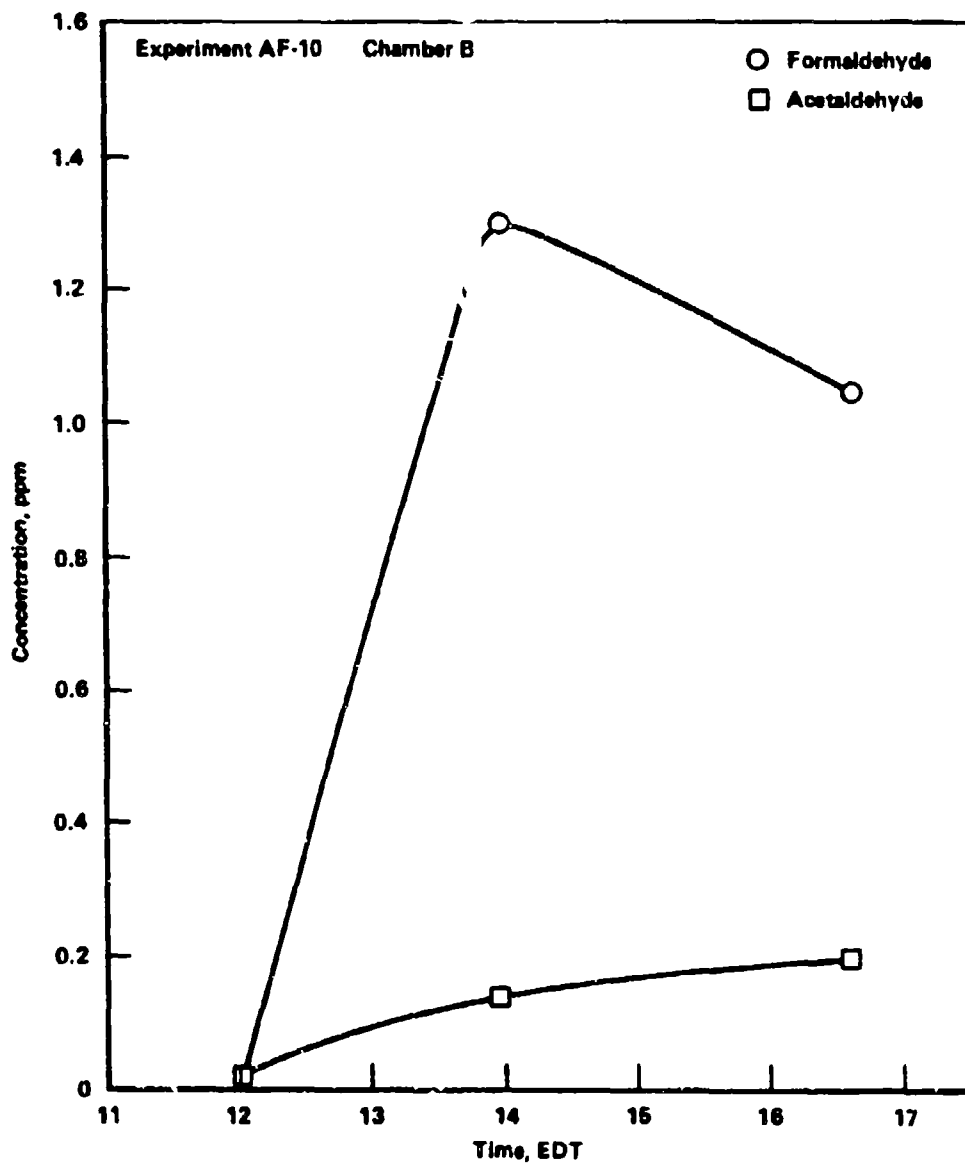


Figure A-26. Smog Chamber Profiles from AF-10 (Reference Chamber)

Units

Temp - °C

RH - %

UV - mcal/cm²-min

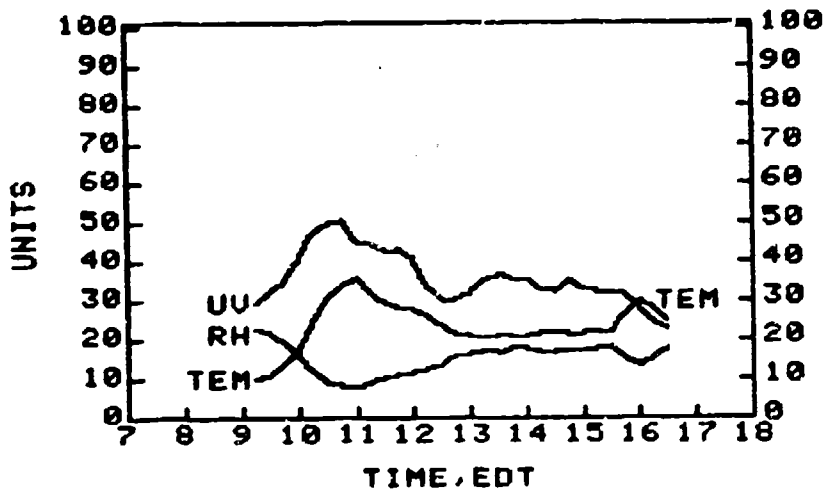
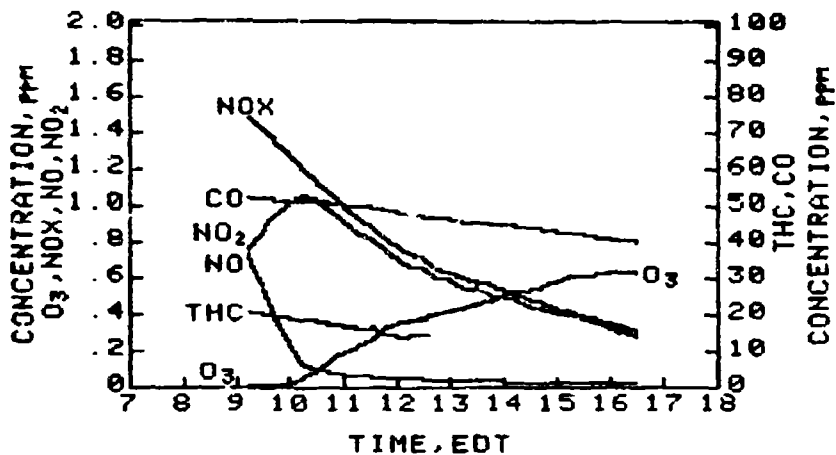
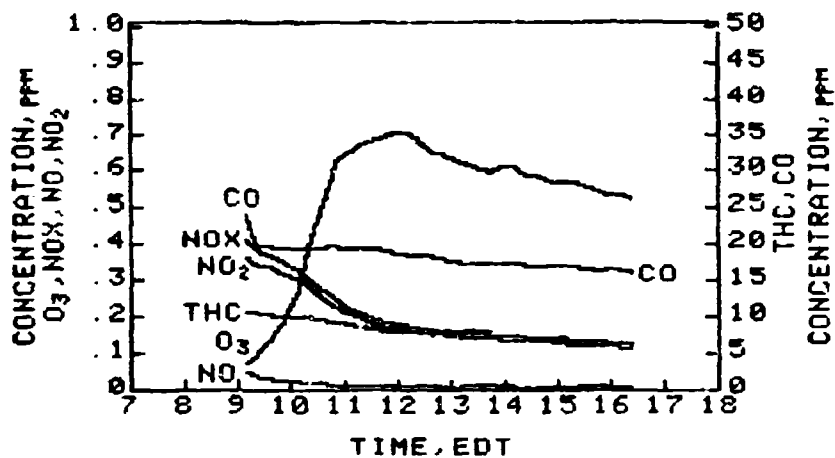


Figure A-27. Profiles from AF-11 Using CFM-56 Engine and JP-8 Fuel. November 7, 1983



PROFILES FROM AF-11 USING CFM-56 ENGINE AND JP-8 FUEL NOV.7 1983



PROFILES FROM AF-11 REFERENCE CHAMBER NOV.7 1983

Figure A-28. Smog Chamber Profiles from AF-11

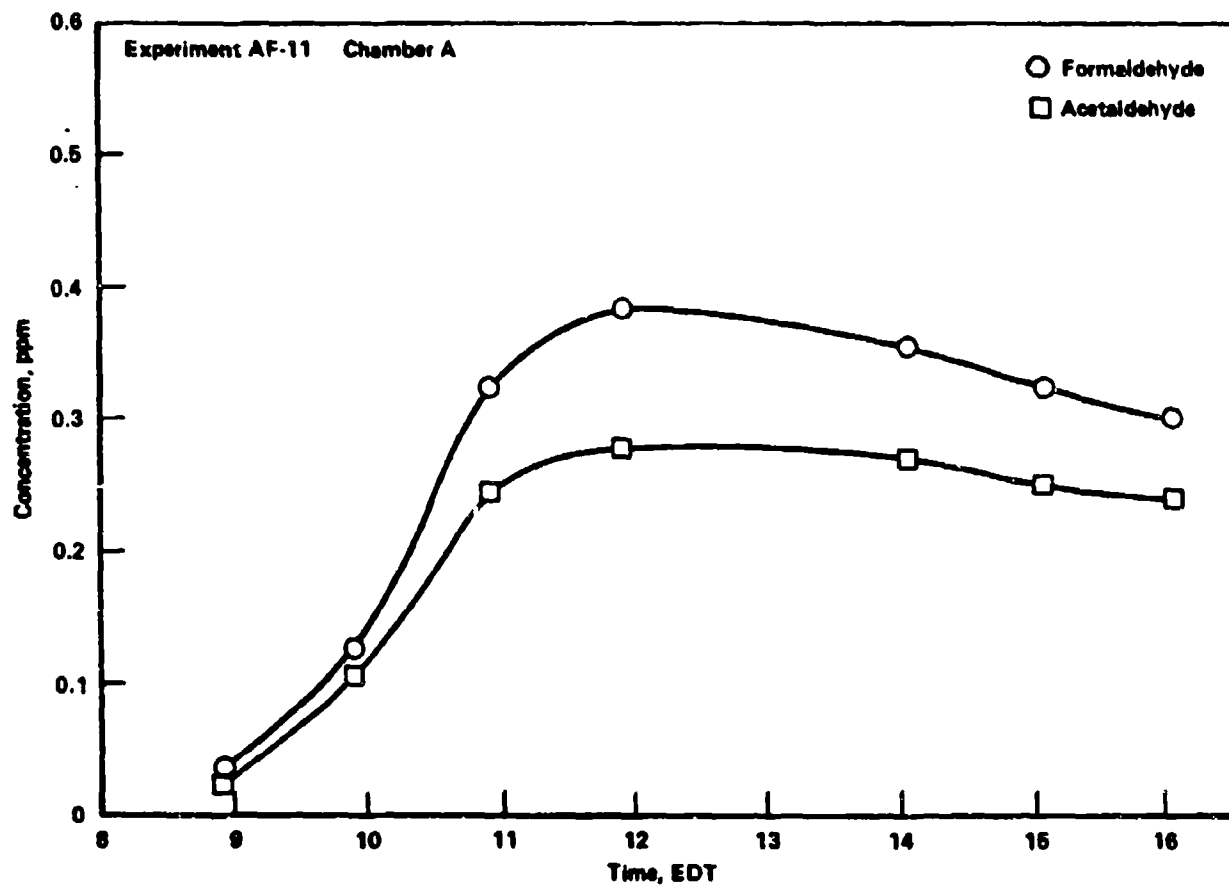


Figure A-29. Smog Chamber Profiles from AF-11 (Reference Chamber)

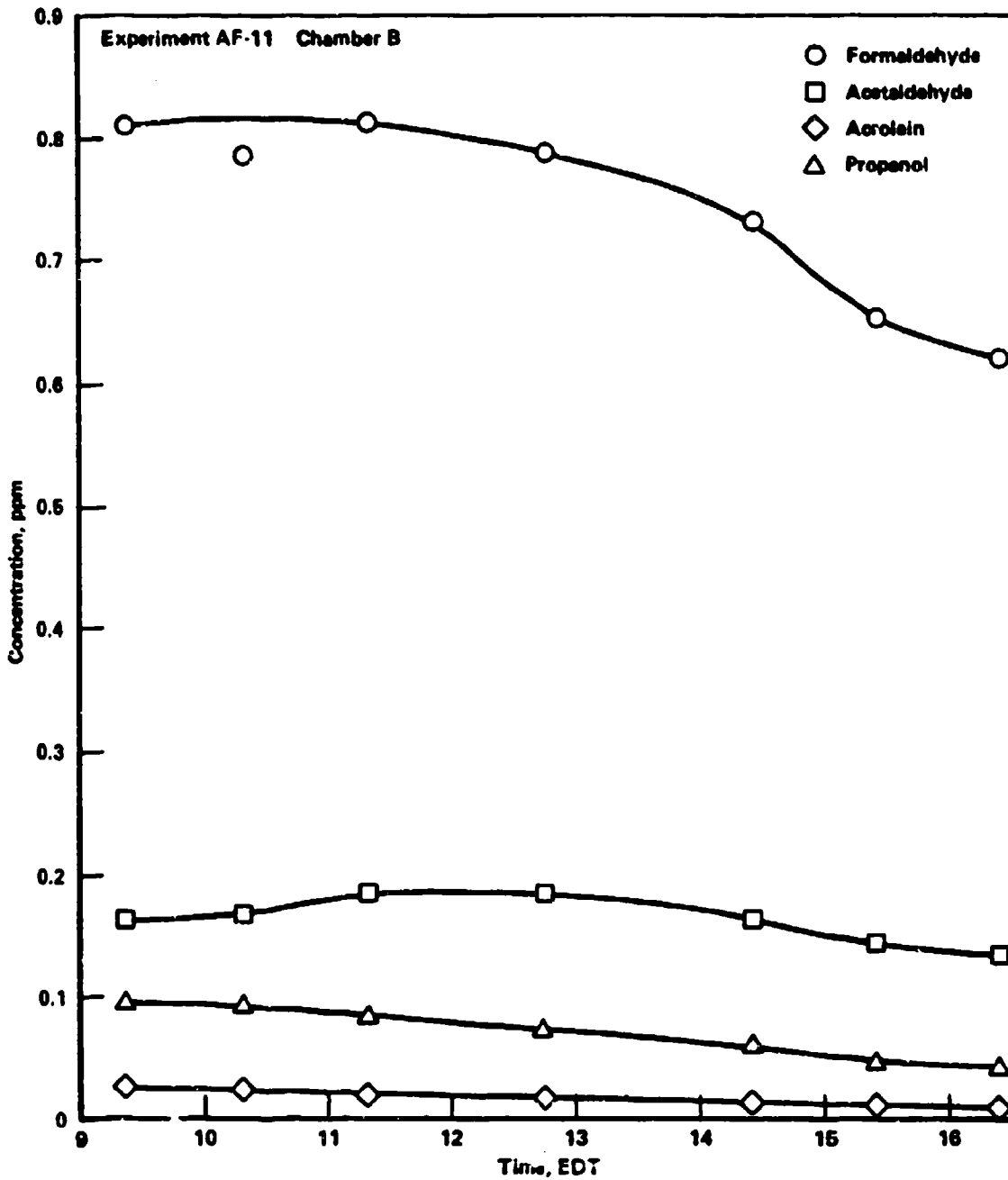


Figure A-30. Smog Chamber Profiles from AF-11 (Exhaust Chamber)